ASSEMBLY OF SUCCINATE DEHYDROGENASE IN MITOCHONDRIA: INTERPLAY BETWEEN IRON-SULFUR COFACTOR INSERTION AND SUBUNIT MATURATION

by

Un Na

A dissertation submitted to the faculty of
The University of Utah
in partial fulfillment of the requirements for the degree of

Doctor of Philosophy

Department of Biochemistry

The University of Utah

December 2015

The University of Utah Graduate School

STATEMENT OF DISSERTATION APPROVAL

The dissertation of **Un Na**

has been approved by the following supervisory committee members:

Dennis R. Winge	, Chair	**10/2/2015** Date Approved
Jared P. Rutter	, Member	**10/2/2015** Date Approved
Michael S. Kay	, Member	**10/2/2015** Date Approved
Markus Babst	, Member	**10/2/2015** Date Approved
Janet M. Shaw	, Member	**10/2/2015** Date Approved

and by **Wesley I. Sundquist & Christopher P. Hill** , Chair/Dean of

the Department/College/School of **Biochemistry**

and by David B. Kieda, Dean of The Graduate School.

ABSTRACT

Succinate dehydrogenase (SDH, also known as complex II) is a protein complex located in the inner mitochondrial membrane. SDH has dual roles as a part of both the citric acid cycle and the electron transport chain required for aerobic respiration in eukaryotes. In the past two decades, the structure of SDH has been extensively studied. The tetrameric complex consists of SDHA, SDHB, SDHC and SDHD (Sdh1, Sdh2, Sdh3 and Sdh4 in yeast) and contains five cofactors: one flavin adenine dinucleotide, three Fe-S clusters and one heme *b*. Mutations in SDH subunit genes are associated with various human diseases. Recently, interest has been refocused on SDH by discovery of SDH assembly factors, SDHAF1 and SDHAF2. However, the mechanism for SDH assembly was still poorly understood. The fact that SDH consists of four subunits and five cofactors supports the idea that maturation of SDH would require several assembly factors, as is the case for other electron transport chain complex I, III and IV. SDH-deficient gastrointestinal stromal tumors and neuroblastomas associated with SDH deficiency without mutations in genes encoding SDH subunits or two aforementioned assembly factors also suggest additional unknown SDH assembly factors.

In this study, we focus on understanding the mechanism for maturation of the Fe-S cluster subunit of SDH, Sdh2. We discovered a novel SDH assembly factor, Sdh7, and characterized its function. We also revealed the molecular function of Sdh6, a yeast ortholog of human SDHAF1, whose mutations were shown to result in SDH deficiency

through an unknown mechanism. We demonstrate that Sdh6 and Sdh7 impart protection for the Fe-S cluster subunit of SDH against reactive oxygen species under oxidative stress conditions during SDH assembly. We also propose that a sequence variant of SDHAF3, a yeast ortholog of Sdh7, could be a pathogenic allele that enhances predisposition to endocrine-related tumors. Lastly, we elucidate the function of Nfu1 in Fe-S cluster delivery to target proteins including Sdh2.

TABLE OF CONTENTS

LIST OF TABLES

LIST OF FIGURES

PREFACE

One of the key biological processes in mitochondria in eukaryotic cells is generating energy for cells. The main metabolic pathway in mitochondria to produce energy in the form of ATP, a major energy currency in cells, consists of the citric acid cycle, the electron transport chain (ETC) and ATP synthase. Mitochondria are subcellular organelles compartmentalized by two double layer membranes. Their compartments consist of the matrix, inner mitochondrial membrane (IMM), intermembrane space (IMS) and outer mitochondrial membrane (OMM) from inside to outside. The citric acid cycle functions in the matrix. It generates ATP and reduces electron carriers in the forms of NADH and $FADH_2$ through oxidation of acetyl-CoA derived from glycolysis, fatty acid oxidation and amino acid metabolism. The ETC is composed of complex I (NADH:ubiquinone oxidoreductase), complex II (succinate dehydrogenase), complex III (ubiquinol-cytochrome *c* reductase) and complex IV (cytochrome *c* oxidase), all of which are embedded in the IMM. The oxidation of NADH and $FADH_2$ is coupled to generating a proton gradient across the IMM by the ETC. ATP synthase subsequently produces ATP using the proton gradient. The key feature of ETC complexes and ATP synthase is that they are membrane-embedded protein complexes composed of multiple subunits and redox cofactors. Therefore, biogenesis of these complexes would be expected to necessitate machineries facilitating assembly of components and ensuring correct topology of complexes.

Mitochondria have their own genome (mitochondrial DNA) encoding 13 proteins, 22 tRNAs and two ribosomal RNAs in humans. Therefore, in order to accommodate ~ 1500 proteins within mitochondria, cells adopted machineries to mediate import of mitochondrial proteins from the cytosol. Nuclear DNA-encoded precursors of mitochondrial proteins are translated in the cytosol, and then translocated into mitochondria through the mitochondrial protein import pathway mainly composed of the translocase of the outer membrane (TOM complex) and the translocase of the inner membrane (TIM complex). Interestingly, complex I, complex III, complex IV and ATP synthase consist of subunits encoded by both mitochondrial DNA and nuclear DNA. Therefore, one could expect a tight regulation that couples translation of subunits encoded by mitochondrial DNA to availability of other subunits imported from the cytosol. The translocation of many precursors is directed by mitochondrial targeting sequences at their N-termini; therefore, the early step of mitochondrial protein maturation in mitochondria often involves peptidases that cleave off mitochondrial targeting sequences, as well as chaperones to stabilize imported precursors prior to their folding.

Protein folding of hydrophobic subunits and insertion into the IMM is another key step for assembly of the ETC complexes. This step often appears to be coupled with the mitochondrial protein import as is the case for concurrent folding of many IMM proteins that are laterally transferred from the translocase of the inner membrane to the IMM. In the case of mitochondrial DNA encoded subunits of complex IV, Cox1, Cox2 and Cox3, a specialized insertase Oxa1 mediates membrane insertion of these proteins from the matrix. It is of particular interest that the Rieske subunit of complex III (Rip1), which has a α-helical transmembrane domain, is folded and matured with a [2Fe-2S] cluster in the

matrix, and then inserted into a complex III assembly intermediate in the IMM. It has been shown that a specialized translocase, Bcs1, is required for insertion of folded and mature Rip1.

Semi-assembled intermediates would be prone to aggregation as many subunits of ETC complexes are hydrophobic. A dedicated chaperone may be required to stabilize assembly intermediates and subunits. It has been shown that Mzm1 is a complex III assembly factor stabilizing mature Rip1 in the matrix prior to its translocation to the IMM via Bcs1.

Redox cofactors such as copper centers, iron-sulfur clusters and hemes are indispensible components for redox chemistry and electron transport within the ETC complexes. These redox cofactors are oxidative damage-prone entities or pro-oxidants when they are exposed to solvent. In addition, assembly intermediates with redox cofactors can generate reactive oxygen species (ROS) as they may not be able to complete their electron transport to physiologically ideal electron carriers. Therefore, specialized factors would be required for shielding redox cofactors during assembly processes and/or preventing assembly intermediate with cofactors from unwanted partial redox reactions.

In the last decade, the mechanism for complex III and complex IV assembly has been extensively studied, especially with respect to the discovery of dedicated assembly factors. In addition, it has been shown that not only mutations in genes encoding subunits, but also mutations in genes encoding assembly factors of complex III and IV are associated with human pathology such as neurodegenerative diseases and cancers. However, little was known about SDH assembly and its implication in human diseases.

Succinate dehydrogenase (SDH, aka complex II) is a tetrameric complex responsible for oxidation of succinate to fumarate in the citric acid cycle. SDH also constitutes a part of the ETC as it catalyzes the reduction of ubiquinone using electrons derived from succinate oxidation. Compared to the other ETC complexes, all four subunits of SDH are encoded in nuclear DNA. However, considering that SDH is a membrane-embedded protein complex composed of multiple subunits and redox cofactors, SDH assembly should also be a process regulated and mediated by assembly factors as is the case for the other ETC complexes. Indeed, interest has been refocused on SDH biogenesis as mutations in two novel SDH assembly factors were linked to infantile leukoencephalopathy and paraganglioma with SDH deficiency.

In this study, I took comprehensive approaches covering proteomics, genetics, biochemistry and molecular biology to understand mechanism of SDH assembly and iron-sulfur cluster delivery in yeast and mammalian cells as model organisms. In addition, the physiological importance of a novel SDH assembly factor SDHAF3 was also examined in a multicellular animal model, fruit flies, and mutations in *SDHAF3* were screened in the context of human endocrine-related tumors. Chapter 1 reviews our current understanding of SDH assembly in great detail, with a summary of up-to-date published studies. Chapter 2 describes a study that further revealed the mechanism of Sdh1 (the flavin adenine dinucleotide subunit of SDH) maturation. In Chapter 3 and 4, function of novel SDH assembly factors and their physiological importance is discussed regarding our novel findings during a course of this study. Lastly, the mechanism for iron-sulfur cluster delivery to target proteins including Sdh2 is proposed in Chapter 5.

CHAPTER 1

INTRODUCTION: PROTEIN-MEDIATED ASSEMBLY OF SUCCINATE DEHYDROGENASE AND ITS COFACTORS

Jonathan G. Van Vranken, Un Na, Dennis R. Winge, Jared Rutter

Reprinted with permission from Critical Reviews in Biochemistry and Molecular Biology

Vol.50, No.2, pp.168-180, March/April 2015

Critical Reviews in Biochemistry and Molecular Biology

http://informahealthcare.com/bmg
ISSN: 1040-9238 (print), 1549-7798 (electronic)
Editor: Michael M. Cox
Crit Rev Biochem Mol Biol, 2015; 50(2): 168–180
 DOI: 10.3109/10409238.2014.990556

informa
healthcare

REVIEW ARTICLE

Protein-mediated assembly of succinate dehydrogenase and its cofactors

Jonathan G. Van Vranken[1], Un Na[1,2], Dennis R. Winge[1,2], and Jared Rutter[1]

[1]Department of Biochemistry and [2]Department of Internal Medicine, University of Utah School of Medicine, Salt Lake City, UT, USA

Abstract

Succinate dehydrogenase (or complex II; SDH) is a heterotetrameric protein complex that links the tribarboxylic acid cycle with the electron transport chain. SDH is composed of four nuclear-encoded subunits that must translocate independently to the mitochondria and assemble into a mature protein complex embedded in the inner mitochondrial membrane. Recently, it has become clear that failure to assemble functional SDH complexes can result in cancer and neurodegenerative syndromes. The effort to thoroughly elucidate the SDH assembly pathway has resulted in the discovery of four subunit-specific assembly factors that aid in the maturation of individual subunits and support the assembly of the intact complex. This review will focus on these assembly factors and assess the contribution of each factor to the assembly of SDH. Finally, we propose a model of the SDH assembly pathway that incorporates all extant data.

Keywords

Assembly factors, redox-active cofactors, respiratory chain, succinate dehydrogenase

History

Received 3 September 2014
Revised 14 November 2014
Accepted 18 November 2014
Published online 9 December 2014

Electron transport chain complex assembly

Mitochondrial ATP synthesis is dependent on the concerted efforts of the electron transport chain (ETC), which couples the generation of an electrochemical gradient to the oxidation of NADH and $FADH_2$ and the reduction of oxygen to water. The ETC is composed of four multimeric complexes and two mobile electron carriers (coenzyme Q and cytochrome *c*), all of which are embedded in or associated with the inner mitochondrial membrane (IMM). Electrons derived from the oxidation of NADH by complex I or succinate from the tricarboxylic acid (TCA) cycle by complex II (succinate dehydrogenase; SDH) are passed along the ETC, coupled with the pumping of protons and establishment of the proton gradient across the IMM. In the end, controlled flow of protons down this electrochemical gradient is utilized by complex V (ATP synthase) to catalyze ATP synthesis.

The assembly of the ETC complexes presents the cell with the problem of coordinating the synthesis and stepwise interactions of individual subunits, transcribed and translated from two distinct genomes in two distinct compartments, into intricate membrane bound complexes. This problem is exacerbated by the nature of the ETC complexes themselves. First, some subunits are embedded in the IMM and, therefore, are hydrophobic and prone to aggregation prior to and during assembly. Furthermore, the complexes contain redox-active cofactors that can perform inappropriate and deleterious reactions when they are not properly secluded within the native complex. As a result, a number of dedicated factors assist the assembly of these complexes by facilitating cofactor insertion, preventing non-productive interactions and stabilizing assembly intermediates (Diaz *et al*., 2011; Fernandez-Vizarra *et al*., 2009). While mammalian ETC complexes I, III and IV contain 44, 11 and 14 subunits, respectively, and include proteins encoded by both mitochondrial and nuclear genomes, complex II or SDH, is the product of just four nuclear-encoded genes. Despite this somewhat simple quaternary structure, it has been made clear recently that SDH, like all ETC complexes, requires assembly factors for its biogenesis.

Succinate dehydrogenase and human disease

The critical role of SDH in mitochondrial metabolism has long been appreciated, however, it has more recently emerged that mutations affecting SDH cause a number of human diseases (Hoekstra & Bayley, 2013; Rutter *et al*., 2010; Table 1). Interestingly, loss of function mutations in SDH core subunits do not cause a single, common pathology, but rather lead to a variety of disease phenotypes that can be grouped into two categories – cancer and neurodegeneration. With respect to SDH-deficient cancers and other tumor syndromes, mutations in the core subunits are most commonly associated with paraganglioma, pheochromocytoma, renal cell carcinoma (RCC) and WT gastrointestinal stromal tumors (WT-GIST). Paragangliomas are neuro-endocrine tumors that occur in cells of the neural crest and tend to be co-localized with oxygen sensing tissues such as the carotid body, while pheochromocytomas represent a related class of tumors that affect the adrenal gland. These two tumors are most

Address for correspondence: Jared Rutter, Department of Biochemistry, University of Utah School of Medicine, Salt Lake City, UT, USA. E-mail: rutter@biochem.utah.edu

DOI: 10.3109/10409238.2014.990556

commonly associated with mutations in *SDHB*, *SDHC* and *SDHD*, however *SDHA* mutations have recently been implicated in rare cases (Astuti *et al*., 2001; Baysal, 2000; Burnichon *et al*., 2010; Peczkowska *et al*., 2008). Mutations in *SDHA*, *SDHB* and *SDHC* have also been associated with WT-GIST, a mesenchymal tumor of the digestive tract (Janeway *et al*., 2011; Pantaleo *et al*., 2011, 2014). Finally, the link between RCC and SDH dysfunction is supported by the discovery of two families with inherited renal cell tumor syndromes resulting from germline mutations in *SDHB* (Vanharanta *et al*., 2004). Taken together, it is clear that normal SDH activity serves to suppress tumors in humans. In addition to the cancers described above, defects in SDH activity also cause a variety of neurodegenerative disorders. In fact, the classical presentation of patients with mutations in *SDHA* is Leigh Syndrome, an early-onset, progressive neurodegenerative disorder (Bourgeron *et al*., 1995). *SDHA* mutations have also been associated with milder forms of atrophy and myopathy (Bourgeron *et al*., 1995; Horváth *et al*., 2006). Although mutations in *SDHC* are rarely, if ever, associated with neurologic disorders, *SDHB* mutations have been shown to cause infantile leukodystrophy (Alston *et al*., 2012) and SDHD mutations have recently been identified in patients with progressive encephalomyopathy (Jackson *et al*., 2014). Therefore, SDH activity not only suppresses tumors but also supports normal neurologic development and function. While it is fascinating that mutations in all four subunits of SDH have been found to cause one of the diseases described above, it is perhaps even more interesting that numerous patients present with disease accompanied by a loss of SDH activity, but have no mutations of any of the core subunits (Jain-Ghai *et al*., 2013). These genetic observations clearly implicate additional auxiliary factors in the maintenance of cellular SDH activity. Furthermore, this supports the notion that a thorough characterization of the SDH assembly pathway will ultimately lead to the discovery of new human disease alleles in the genes that encode SDH assembly factors.

Table 1. SDH associated genes and clinical phenotypes.

Yeast gene	Human ortholog	Disease
SDH1	*SDHA*	Leigh Syndrome Paraganglioma/Pheochromocytoma WT-GIST
SDH2	*SDHB*	Paraganglioma/Pheochromocytoma Renal Cell Carcinoma WT-GIST Infantile Leukodystrophy
SDH3	*SDHC*	Paraganglioma/Pheochromocytoma Renal Cell Carcinoma WT-GIST
SDH4	*SDHD*	Paraganglioma/Pheochromocytoma WT-GIST Progressive Encephalomyopathy
SDH5	*SDHAF2*	Paraganglioma/Pheochromocytoma
SDH6	*SDHAF1*	Infantile Leukodystrophy
SDH7	*SDHAF3*	N/A
SDH8	*SDHAF4*	N/A

Enzymology and structure of succinate dehydrogenase

Eukaryotic SDH is a heterotetrameric complex composed of four nuclear-encoded subunits (Sun *et al*., 2005; Figure 1). SDH is unique amongst eukaryotic ETC complexes in that it functions as part of both the TCA cycle and the ETC and thus couples two of the primary energy-harvesting pathways within the cell. In addition to this distinction, SDH is the only ETC complex that does not pump protons across the IMM nor does it contain any proteins encoded by the mitochondrial genome. In the context of the TCA cycle, SDH catalyzes the oxidation of succinate to fumarate and uses the electrons derived from this oxidation to catalyze the reduction of ubiquinone to ubiquinol. These electrons are passed to Complex III and then Complex IV, thereby contributing to the establishment of the electrochemical gradient across the IMM in support of ATP synthesis. The structure of SDH can be characterized as a hydrophilic head that protrudes into the

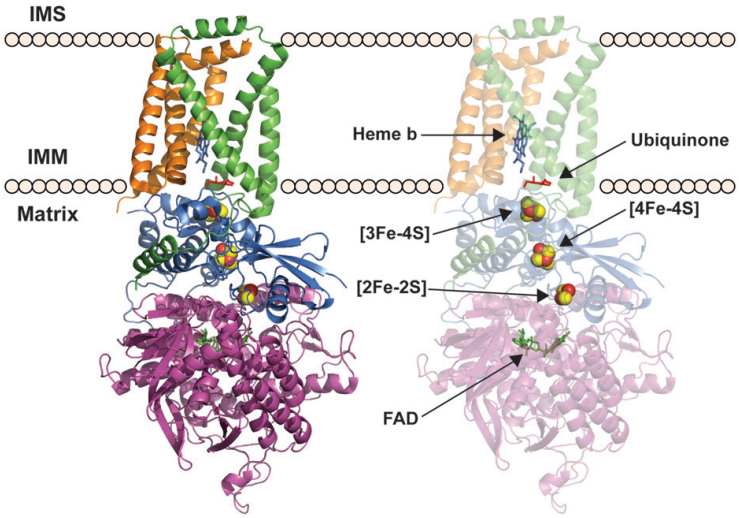

Figure 1. Porcine succinate dehydrogenase (PDB accession number: 1ZOY) embedded in the mitochondrial inner membrane. SdhA (purple ribbon); SdhB (blue ribbon); SdhC (green ribbon); SdhD (brown ribbon); FAD (green stick); FeS centers, [2Fe–2S], [4Fe–4S], [3Fe–4S] from the bottom (red and yellow sphere); Ubiquinone in the Q_P site (red stick); Heme b (blue stick). (see colour version of this figure at www.informahealthcare.com/bmg).

mitochondrial matrix attached to the IMM by a hydrophobic membrane anchor (Sun *et al*., 2005; Yankovskaya *et al*., 2003; Figure 1).

The membrane anchor domain of SDH consists of Sdh3 (SDHC in mammals) and Sdh4 (SDHD; Sun *et al*., 2005; Yankovskaya *et al*., 2003) and serves as the site of ubiquinone binding to connect this hydrophobic mobile electron carrier to the hydrophilic domain of SDH (Figure 1). The hydrophilic domain represents the catalytic core of SDH and is composed of Sdh1 (SDHA in mammals) and Sdh2 (SDHB), each of which contain the redox-active cofactors that facilitate the transfer of electrons from succinate to ubiquinone (Sun *et al*., 2005; Yankovskaya *et al*., 2003; Figure 1). Sdh1 contains a covalently bound FAD cofactor adjacent to the succinate-binding site (Figure 1). Sdh2 harbors the three Fe–S centers that mediate electron transfer from the flavin cofactor to the ubiquinone (Figure 1). The Fe–S clusters of Sdh2, which consist of a 2Fe–2S center adjacent to the FAD site of Sdh1, followed by a 4Fe–4S and finally a 3Fe–4S center proximal to the ubiquinone binding site, serve essentially as a wire used to transfer electrons through the complex (Figure 1). In addition to its important role in the process of electron transfer, Sdh2 also serves as the interface linking the catalytic Sdh1 subunit to the membrane bound Sdh3 and Sdh4 subunits (Sun *et al*., 2005; Yankovskaya *et al*., 2003). Interestingly, recent reports indicate that soluble Sdh1–Sdh2 dimers exist in the absence of one or both of the membrane anchors (Kim *et al*., 2012). This suggests that Sdh1 and Sdh2 are likely to dimerize prior to membrane association, rather than sequentially docking onto the membrane anchor.

The SDH enzymatic reaction begins with the binding of succinate to the open state of Sdh1, which undergoes a conformational change bringing succinate into close proximity with the covalently bound FAD cofactor. Oxidation of succinate is coupled to the two-electron reduction of FAD. Since the Fe–S centers of SDH are single electron carriers, two successive single electron transfer steps are required to re-oxidize $FADH_2$ back to FAD. In the end, the two electrons gained from the oxidation of succinate are used to reduce ubiquinone to ubiquinol, which passes the electrons on to Complex III.

Assembly of SDH

Until recent years, the process of SDH assembly remained highly enigmatic and was primarily focused on the core SDH subunits themselves (Cecchini *et al*., 2002; Lemire & Oyedotun, 2002). Our newfound understanding of this process has been facilitated by the discovery of proteins dedicated to the maturation of individual subunits and the assembly of the holo-complex. Importantly, the discovery of these factors has revealed that SDH assembly is a tightly coordinated process in which the concerted functions of core subunits, dedicated assembly factors and other ancillary factors must coordinate their various activities to achieve the step-wise assembly of this membrane bound complex. Based on the knowledge gained in recent years, it is possible to organize the process of SDH assembly into discrete, subunit-specific events. These events, which include cofactor insertion, stabilization of subcomplex assembly intermediates and prevention of deleterious solvent interactions, result in the maturation of individual subunits and support the complete assembly of SDH. In the subsequent sections, we will review the current understanding of the SDH assembly pathway focusing, in particular, on the factors that facilitate this process (Figure 3).

Sdh1 – the catalytic subunit

Architecture of Sdh1

Sdh1 catalyzes the oxidation of succinate to fumarate. The crystal structure of porcine SDH has revealed that mammalian SDHA assumes a Rossmann-type fold with four distinct domains – an FAD binding domain (residues 52–267 and 355–439; human sequence), a capping domain (residues 268–354), a helical domain (residues 440–537) and a C-terminal domain (residues 548–616). The structure indicates the presence of a covalent bond between FAD and His99 (His90 in yeast) with the FAD being further coordinated by a number of additional residues, which form a well-ordered hydrogen bonding network (Sun *et al*., 2005; Figure 1). In addition to the native SDH, a co-crystal structure of SDH bound to a competitive inhibitor, 3-nitropropionic acid (NPA) was also determined and facilitated the mapping of the putative succinate binding site, which, as expected, is directly adjacent to the FAD. While the precise mechanism for succinate oxidation by Sdh1 has not yet been elucidated, these studies have provided valuable information as to the residues involved in this reaction. The structure demonstrates that the nitryl group of NPA interacts with the FMN group of FAD as well as the main chain of Glu261 and the side chains of Thr260 and His248 while the NPA carboxyl group is anchored by the amide of Glu246, the guanidinium group of Arg403 and the imidazole of His359 (Sun *et al*., 2005).

Biosynthesis and delivery of FAD

FAD is an essential cofactor of Sdh1 and the flavinylation of Sdh1 is dependent on adequate FAD levels in the mitochondrial matrix. Therefore, the synthesis and maintenance of free FAD pools in this compartment plays a vital role in the maturation of Sdh1 (Kim & Winge, 2013). In yeast, the biosynthesis of FAD and its delivery to mitochondria is dependent on the activities of three proteins – riboflavin kinase (Fmn1), FAD synthetase (Fad1) and a putative mitochondrial FAD transporter (Flx1). FAD is derived from dietary riboflavin (vitamin B_2) and its conversion requires the activities of two ATP-dependent enzymes, Fmn1 and Fad1. Fmn1, the riboflavin kinase, phosphorylates the tricyclic isoalloxazine ring yielding flavin mononucleotide (FMN; Santos *et al*., 2000). Although a number of enzymes within the cell use FMN as a cofactor, the majority of FMN is subsequently adenylated and converted to FAD by the FAD synthetase, Fad1 (Wu *et al*., 1995).

Flx1 belongs to the eukaryotic superfamily of IMM carriers and has been described as a putative IMM FAD carrier, but the published literature disagrees as to the exact molecular function of Flx1 (Bafunno *et al*., 2004; Tzagoloff *et al*., 1996). At any rate, cells lacking Flx1 exhibit low matrix FAD concentrations and reduced activity of two matrix flavoproteins, SDH and lipoamide dehydrogenase, due to a defect in

DOI: 10.3109/10409238.2014.990556

flavinylation of these two enzymes (Kim *et al*., 2012; Tzagoloff *et al*., 1996). Therefore, while there is no known direct link between Flx1 and Sdh1, it is clear that Flx1 plays an important role in Sdh1 cofactor insertion as Sdh1 flavinylation is severely compromised in *flx1*Δ cells. This decrease in flavinylation also leads to the destabilization of Sdh1. Interestingly, the *flx1*Δ defect in Sdh1 flavinylation can be suppressed by the overexpression of Fad1 or Sdh5, a dedicated SDH assembly factor that will be discussed in significant detail in the subsequent section (Hao *et al*., 2009).

It is important to note that in mammalian cells, it is not clear whether an Flx1 ortholog is required for SDH maturation. The mammalian ortholog of the *FAD1* gene, *FLAD1*, yields two transcripts encoding two isoforms of FAD synthetase, one of which is cytosolic and the other has a mitochondrial targeting motif (Torchetti *et al*., 2010). Thus, mammalian cells might synthesize FAD within the mitochondrial matrix perhaps making any IMM carrier dispensable.

Sdh1 cofactor insertion

The first known step in the maturation of Sdh1, which is imported into the mitochondrial matrix as an apo-protein, is the insertion and covalent attachment of its FAD cofactor (Robinson *et al*., 1994). Interestingly, succinate appears to be an important allosteric effector of this process as it and several other TCA cycle intermediates stimulate flavinylation significantly *in vitro* (Brandsch & Bichler, 1989). Unlike some bacterial Sdh1 orthologs, eukaryotic Sdh1 is not competent to become flavinylated in the absence of other proteins, which is typically interpreted to mean that the flavinylation of Sdh1 is not autocatalytic (Kounosu, 2014; Robinson & Lemire, 1996). As a result, simply maintaining matrix FAD pools is not sufficient for Sdh1 flavinylation. Early studies focused on this process revealed that there likely exists a protein in the mitochondrial matrix required for flavinylation of Sdh1 as the degree to which Sdh1 can be flavinylated *in vitro* is proportional to the concentration of isolated matrix fraction used in the assay (Robinson & Lemire, 1996). This insight was subsequently validated by the discovery of Sdh5.

Yeast Sdh5 was discovered in the course of studying a collection of uncharacterized mitochondrial proteins with a high degree of conservation throughout eukaryotes (Hao *et al*., 2009). Deletion of *SDH5* in yeast prevented respiratory dependent growth and caused a dramatic reduction in oxygen consumption – two phenotypes indicative of a strong respiratory deficiency. In an attempt to better understand this phenotype, an unbiased tandem affinity purification was performed and it identified Sdh1 as the sole binding partner of Sdh5. This result, consistent with a clear respiratory deficiency, strongly implicated Sdh5 in the maintenance of SDH activity. This connection with SDH was further strengthened by the observation that yeast cells lacking Sdh5 exhibited a complete loss of SDH activity and, in this regard, essentially mirrored an *sdh1*Δ deletion strain. Despite these phenotypic similarities, however, Sdh1 protein was still clearly detectable, albeit at reduced levels, in an *sdh5*Δ mutant strain and, interestingly, the SDH complex remained intact (Hao *et al*., 2009; Kim *et al*., 2012).

Based on the above evidence, it is clear that Sdh5 is required for maintaining SDH activity and that this function is mediated through a direct physical interaction with Sdh1. These data raised the possibility that the primary defect in *sdh5*Δ cells might be failure to covalently flavinylate Sdh1, resulting in a catalytically dead subunit. Indeed, direct interrogation of Sdh1 flavinylation revealed a complete failure to form the covalent bond between Sdh1 His90 and the FAD cofactor. This finding is consistent with related studies that demonstrate flavinylation-deficient Sdh1 His90Ser mutants assemble into a catalytically inactive SDH complex as do *sdh5*Δ mutants (Hao *et al*., 2009; Robinson *et al*., 1994).

It is clear that Sdh5 is required for Sdh1 flavinylation but through what mechanism? The first important clues resulted from further interrogation of the nature of the Sdh1–Sdh5 interaction. BN-PAGE experiments demonstrated that Sdh5 is not a member of the SDH holo-complex but rather migrates to an approximate molecular weight of 90 kDa, consistent with an Sdh1–Sdh5 dimer. Further investigation of this interaction revealed that the formation of this complex is important in maintaining the stability of both proteins. The steady-state levels of Sdh1 are ∼50% reduced in an *sdh5*Δ mutant strain. Conversely, deletion of *SDH1* causes a near complete destabilization of Sdh5, a result that strongly implicates Sdh5 as a dedicated factor whose sole purpose is to act on Sdh1. While Sdh1 protein is required to maintain the stability of Sdh5, this relationship is not dependent on Sdh1 being competent for flavinylation as substitution of Sdh1 His90 with a Ser residue does not lead to destabilization of Sdh5. It is important to note that only a minor fraction of Sdh1 in the matrix is in association with Sdh5 at any given time. Furthermore, deletion of *SDH2* causes the steady-state level of Sdh5 to increase, most likely due to an increase in the fraction of Sdh1 that is bound to Sdh5. As this complex exists independent of all other SDH subunits and accumulates in strains that prevent SDH assembly, it is clear that the actions of Sdh5 and the process of flavinylation are early steps in the SDH assembly pathway (Hao *et al*., 2009; Kim *et al*., 2012).

Further insights into the role of Sdh5 in Sdh1 flavinylation came from structural characterization of yeast Sdh5 by NMR (Eletsky *et al*., 2012). No FAD was detected in purified samples of Sdh5, nor did the addition of FAD to purified Sdh5 cause any perturbation in Sdh5 chemical shifts, suggesting that Sdh5 does not act as a delivery vehicle that brings FAD to apo-Sdh1 (Eletsky *et al*., 2012). The NMR studies revealed that the Sdh5 core assumes a compact 5 α-helical bundle and revealed a concentrated patch of conserved residues on the surface of these α-helices, which is theorized to be the Sdh1 binding site (Eletsky *et al*., 2012)

While it is not yet possible to define the precise mechanism by which Sdh5 supports Sdh1 flavinylation, there is sufficient data to hypothesize as to the role of Sdh5 in this process. Biochemical studies have demonstrated that Sdh5 does not directly bind FAD, thus it seems unlikely that Sdh5 plays a role in physically delivering FAD to Sdh1. While the Sdh1 binding site on Sdh5 has been defined in the above NMR-based study, the region of Sdh1 that binds Sdh5 remains unknown. This information would provide insight into the role of Sdh5 in Sdh1 flavinylation, but for now we are

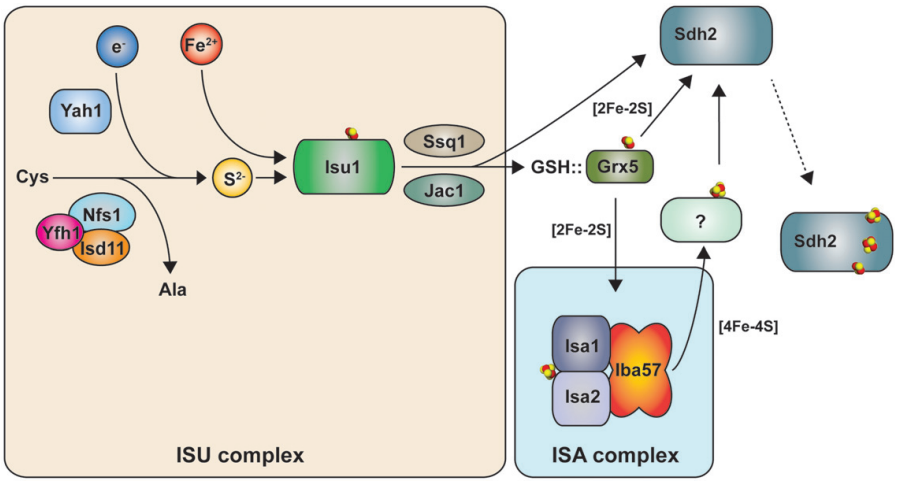

Figure 2. Iron-sulfur cluster synthesis and delivery to Sdh2. The tan box depicts the *de novo* synthesis of 2Fe–2S clusters within the ISU complex. Clusters are formed on the Isu1 scaffold protein with sulfide ions provided by the Nfs1 cysteine desulfurase and Yah1 ferredoxin. It is not clear how ferrous ions are delivered to the ISU complex. The preformed 2Fe–2S cluster is released from the scaffold complex through the actions of Hsp70 (Ssq1) and DnaJ (Jac1) to a transfer complex consisting of GSH-bound Grx5. The GSH–Grx5 delivers 2Fe–2S clusters to the ISA complex for the subsequent 4Fe–4S cluster synthesis depicted in the blue box. However, it is elusive whether the GSH-Grx5 is also required for 2Fe–2S cluster delivery to recipient proteins, in this case, Sdh2. It is also unknown whether the preformed 4Fe–4S clusters are directly delivered to Sdh2 or another factor is in need for this delivery step. All arrows with solid lines indicate transfer of components of Fe–S clusters or pre-formed Fe–S clusters.

forced to theorize as to such details. It seems likely that Sdh5 binds adjacent to the FAD binding site on apo-Sdh1, which could serve one or more of many possible roles. First, it could facilitate the non-covalent insertion of FAD into the pocket, which would enable subsequent autocatalytic covalent flavinylation. Second, Sdh5 could act as a chaperone for unflavinylated apo-Sdh1, thus supporting flavinylation by stabilizing apo-Sdh1 in a flavinylation-competent conformation. Finally, it is possible that Sdh5 might participate directly in the covalent flavinylation reaction by providing catalytic residues to this active site. Regardless of the precise mechanism, it is clear that Sdh5 specifically binds to apo-Sdh1 and is required for its covalent flavinylation (Figure 3).

Sdh8 is a chaperone for flavinylated Sdh1

Following Sdh5-dependent covalent flavinylation, Sdh1 is destined to form a soluble dimer with Sdh2; however, there remains a population of Sdh1 that exists in an unbound state free from any other core subunits in the mitochondrial matrix. It is likely that Sdh1 is present in excess to other core SDH subunits within the mitochondrial matrix as deletion of Sdh1 destabilizes the remaining core subunits, Sdh2, Sdh3 and Sdh4, while Sdh1 protein levels are maintained, albeit at a reduced level, upon deletion of any of the other core subunits. This free, flavinylated Sdh1 appears to be maintained in a soluble, assembly-competent state by a newly discovered, subunit-specific chaperone, Sdh8 (Figure 3).

SDH8 is conserved throughout eukaryotes and encodes a small protein that is localized to the mitochondrial matrix (Van Vranken *et al*., 2014). Yeast cells lacking Sdh8 exhibit slow growth on non-fermentable carbon sources but are still respiratory competent. The first observation that suggested a role for Sdh8 in SDH assembly or activity was its metabolomics phenotype. Yeast cells and *Drosophila* mutants lacking Sdh8 (or its ortholog) exhibit a significant but subtle block in the TCA cycle centered at SDH (i.e. an accumulation of succinate and a depletion of fumarate and malate, the two TCA cycle intermediates downstream of SDH). It is important to note that the magnitude of succinate accumulation is much less than a mutant lacking one of the four core subunits or Sdh5, which exhibits a complete loss of SDH activity. Consistent with this finding, *sdh8*Δ mutant yeast maintain approximately 40% of wild-type SDH activity and abundance of SDH holo-complexes. Interestingly, deletion of the *Drosophila* ortholog, *dSdhaf4*, causes a much more severe phenotype. These mutants accumulate significantly more succinate and have a ∼90% decrease in SDH activity, while assembled SDH complexes are nearly undetectable. Thus, while Sdh8 clearly supports SDH biogenesis, it does not appear to be absolutely required for assembling functional SDH complexes as some level of SDH activity is maintained in organisms lacking Sdh8 or its orthologs (Van Vranken *et al*., 2014).

While metabolomics clearly implicated Sdh8 in enabling SDH activity, the first evidence as to its particular function came when Sdh1 was discovered to be its primary binding partner. Further interrogation of the specificity of this interaction revealed that Sdh8 bound to Sdh1 independent of any other SDH core subunits and importantly, Sdh5. In addition, it was determined that the Sdh1–Sdh8 interaction depends on covalent flavinylation of Sdh1, as Sdh8 fails to interact with Sdh1 in an *sdh5*Δ background and also fails to interact with two covalent flavinylation-deficient Sdh1 mutants (H90S and H90A). BN-PAGE analysis further confirmed that Sdh8 is not associated with the SDH

DOI: 10.3109/10409238.2014.990556

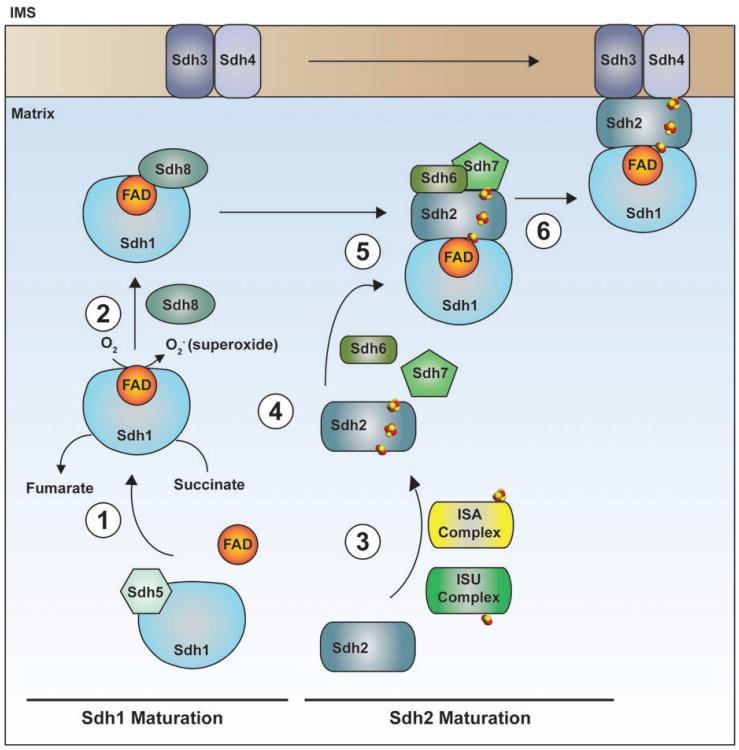

Figure 3. Model of the SDH assembly pathway. Each SDH core subunit is translated in the cytosol and must be subsequently translocated to the mitochondria. (1) Upon mitochondrial import, apo-Sdh1 is rapidly bound by the subunit-specific chaperone, Sdh5, forming a dimeric complex that supports covalent attachment of the FAD cofactor. (2) Following covalent flavinylation, the Sdh1–Sdh5 dimer disintegrates resulting in a pool of flavinylated Sdh1 that is unbound by any other core subunits. This leads to the formation of a complex comprised of Sdh1 and Sdh8, another subunit-specific chaperone. (3) The formation of this complex supports the formation of the subsequent Sdh1–Sdh2 soluble dimer and also prevents the spurious production of superoxide by flavinylated Sdh1. Meanwhile, apo-Sdh2 must also mature into a complex-competent subunit. This process involves the insertion of three Fe–S clusters generated by the ISU and ISA complexes. (4) Following maturation of Sdh2, it interacts with Sdh6 and Sdh7, which serve to protect exposed Fe–S clusters during the assembly process and (5) further associates with a mature Sdh1 subunit forming a heterotetrameric assembly intermediate. (6) Finally, the Sdh1–Sdh2 hydrophillic head docks to the IMM via interactions with the Sdh3–Sdh4 membrane anchor domain, which may or may not pre-assemble at the IMM. In the end, the concerted efforts of core subunits, dedicated assembly factors and other ancillary factors facilitate the stepwise assembly of SDH. (see colour version of this figure at www.informahealthcare.com/bmg).

holo-complex, but forms a stable subcomplex with Sdh1, which hyper-accumulates in *sdh2*Δ and *sdh4*Δ backgrounds. Consistent with this finding, Sdh8 steady-state protein levels also increase in these conditions, presumably to occupy the augmented pool of unbound and flavinylated Sdh1. Furthermore, deletion of Sdh1 causes significant destabilization of Sdh8, indicating that the stability of Sdh8 depends upon its ability to form a complex with Sdh1. Taken together, these data indicate that Sdh8 is a subunit-specific chaperone that occupies flavinylated Sdh1 prior to the formation of the Sdh1–Sdh2-soluble dimer (Van Vranken *et al*., 2014; Figure 3).

Why exactly does unbound Sdh1 require such a chaperone? The first evidence came from assessing the steady-state levels of SDH core subunits in the *sdh8*Δ mutant. While there was little or no destabilization of Sdh1, the primary binding partner of Sdh8, there was a marked decrease in the steady-state abundance of Sdh2. This was accompanied by, and probably a result of, a decrease in the Sdh1–Sdh2 soluble dimer as assessed by co-immunoprecipitation. Although this result is somewhat difficult to interpret, it suggests that the interaction between Sdh1 and Sdh8 facilitates the formation of the Sdh1–Sdh2 dimer by maintaining Sdh1 in a state that is competent for Sdh2 binding. Therefore, in the absence of Sdh8, Sdh1 does not interact as efficiently with Sdh2, which is unstable on its own. Interestingly, studies focused on *Drosophila dSdhaf4* demonstrate that this assembly factor is required for maintaining the stability of SdhA. Therefore, it is possible that in higher eukaryotes Sdh8 orthologs support the formation of the hydrophilic head by maintaining subunit stability. Overall, this data suggests that the chaperone activity of Sdh8 promotes SDH assembly by stabilizing Sdh1 and maintaining it in an assembly-competent state prior to interaction with Sdh2 (Van Vranken *et al*., 2014).

In addition to promoting formation of the Sdh1–Sdh2 dimer, Sdh8 might also function to prevent potentially deleterious interactions of free and flavinylated Sdh1 with the solvent. Indeed, studies focused on SDH have demonstrated that impaired electron transport at the level of the FAD can generate significant quantities of superoxide (Ishii *et al*., 2005; Messner & Imlay, 2002; Yankovskaya *et al*., 2003). Furthermore, previous studies in mammalian cells demonstrate that silencing of SDHB (Sdh2 ortholog), but not SDHA (Sdh1 ortholog) causes an increase in ROS levels (Guzy *et al*., 2008; Ishii *et al*., 2005). This increase in oxidative stress mediated by Sdh1 is thought to be dependent on the ability of the exposed FAD cofactor to interact with the surrounding solvent. In a phenomenon referred to as auto-oxidation, free Sdh1 oxidizes succinate to fumarate independent of the SDH holo-complex. This oxidation causes a reduction of the FAD cofactor, which then reduces molecular oxygen to form superoxide (Messner & Imlay, 2002). If Sdh8 functions to prevent Sdh1 auto-oxidation then overexpression of Sdh1 should be toxic to *sdh8*Δ mutant cells. In fact, Sdh1 overexpression proved toxic to both WT and *sdh8*Δ mutant cells; however, cells lacking Sdh8 were particularly sensitive

to this stress. Furthermore, overexpression of Sdh8 was capable of partially rescuing the toxicity associated with overexpressed Sdh1. Additional studies demonstrated that *sdh8*Δ mutant cells exhibited higher levels of oxidative stress and that the growth phenotype associated with *sdh8*Δ mutant cells was predominantly the result of oxidative stress rather than respiratory deficiency. Indeed, while overexpression of YAP1, a transcription factor involved in mediating oxidative stress, is capable of rescuing the *sdh8*Δ growth phenotype it fails to have any impact on the SDH deficiency of these cells (Van Vranken *et al*., 2014). Therefore, Sdh8 might have two important functions related to Sdh1. It appears to facilitate assembly with Sdh2 and may also function to seclude the FAD cofactor from the solvent, thus preventing spurious oxidation (Van Vranken *et al*., 2014).

Sdh2 – the electron wire

Architecture of Sdh2

Sdh2 (SDHB in mammals) is the Fe–S cluster-containing subunit of SDH. The crystal structure of porcine heart SDH demonstrates that SDHB contains two distinct domains (Sun *et al*., 2005; Figure 1). The N-terminal domain (residues 37–142; human sequence) consists of a single small α-helix and a five-strand β-sheet. This domain harbors the FAD-proximal 2Fe–2S center, which is ligated by Cys93, Cys98, Cys101 and Cys113. The C-terminal domain (residues 142–280) consists of six α-helices and harbors the 4Fe–4S and 3Fe–4S centers, which are coordinated by Cys186, Cys189, Cys192 and Cys253 and Cys196, Cys243 and Cys249, respectively. These three Fe–S centers essentially act as a wire that carries electrons from FAD to ubiquinone. SDHB also serves to connect the catalytic subunit, SDHA, with the hydrophobic anchor domain. Both the N-terminal domain and the C-terminal domain mediate the interaction with SDHA. Meanwhile, the C-terminal domain is mainly responsible for the interaction with the hydrophobic anchor domain. Importantly, SDHB contributes several residues to the ubiquinone-binding site, which otherwise is mediated by the hydrophobic anchor domain. In this way, the terminal 3Fe–4S center is poised adjacent to the ubiquinone to enable the final electron transfer (Sun *et al*., 2005).

Iron–sulfur cluster biogenesis

The aforementioned Fe–S clusters are key cofactors required for electron transfer from FAD to the Q_P site. Fe–S clusters are preformed in the mitochondrial matrix on a scaffold complex (ISU) consisting of four proteins, Nfs1, Isd11, Yfh1 and Isu1 (or Isu2; yeast nomenclature) (Lill *et al*., 2012; Schmucker *et al*., 2011; Tsai & Barondeau, 2010). The sulfide ions necessary for cluster biogenesis are provided by the Nfs1 cysteine desulfurase, along with its effector proteins Isd11 and Yfh1 (Pandey *et al*., 2012, 2013) and the Yah1 ferredoxin reductant (Sheftel *et al*., 2010). Fe(II) and sulfide ions form 2Fe–2S clusters on the Isu1 (or Isu2) scaffold proteins prior to transfer to client proteins. The preformed cluster is transferred to the monothiol Grx5, an Fe–S shuttle protein, through the binding of the DnaJ protein Jac1 to Isu1, which dissociates the ISU complex (Majewska *et al*., 2013) and the recruitment of the Hsp70 enzyme Ssq1. The cluster is released from Isu1 by the ATPase activity of Ssq1 (Ciesielski *et al*., 2012; Majewska *et al*., 2013; Uzarska *et al*., 2013). Grx5, which is pre-associated with Ssq1, transiently binds the 2Fe–2S cluster together with glutathione (GSH) for subsequent transfer steps (Banci *et al*., 2014; Johansson *et al*., 2011; Uzarska *et al*., 2013). The human ortholog of Jac1 was shown to also bind Fe–S client proteins, so Grx5-mediated cluster transfer may occur in pre-bound complexes with client proteins (Maio *et al*., 2014). Clusters consisting of 4Fe–4S and perhaps 3Fe–4S stoichiometries are matured on a downstream ISA scaffold complex consisting of Isa1, Isa2 and Iba57 (Gelling *et al*., 2008; Muhlenhoff *et al*., 2011; Sheftel *et al*., 2012) and perhaps Nfu1 (Cameron *et al*., 2011; Lill *et al*., 2012; Navarro-Sastre *et al*., 2011). Nfu1 is likely a targeting factor to Fe–S client proteins in bacteria (Py *et al*., 2012). Yeast depleted of ISU components or the Fe–S targeting factors Grx5, ISA components and Nfu1 are impaired in SDH activity (Jensen & Culotta, 2000; Muhlenhoff *et al*., 2011; Rodriguez-Manzaneque *et al*., 2002). Mutations in human orthologs of Isd11, Isu1, Iba57 or Nfu1 (Ajit Bolar *et al*., 2013; Cameron *et al*., 2011; Crooks *et al*., 2012; Ferrer-Cortes *et al*., 2013; Hall *et al*., 1993; Lim *et al*., 2013; Navarro-Sastre *et al*., 2011) or RNAi depletion of Isa1, or Isa2 lead to compromised SDH function (Sheftel *et al*., 2012; Figure 2).

Recently, mutations in a novel mitochondrial protein BolA3 were shown to result in defects in similar respiratory complexes and 2-oxoacid dehydrogenases as mutations in Nfu1 (Baker *et al*., 2014; Cameron *et al*., 2011), suggesting that BolA3 may likewise function in late stages of mitochondrial Fe–S biogenesis or transfer. BolA proteins typically function with glutaredoxins (Li & Outten, 2012), therefore, one prediction is that BolA3 has a role in conjunction with Grx5.

Sdh2 cofactor insertion

The architecture of Sdh2 raises several questions regarding cofactor insertion and maturation. Analogous to Sdh1, which receives its FAD cofactor within the mitochondrial matrix, Sdh2 receives its three Fe–S clusters in the matrix after import (Figure 3). Based on the Fe–S biogenesis pathway outlined above, one prediction is that the 2Fe–2S center in the N-terminal domain of Sdh2 is received from the Grx5:GSH complex, whereas the clusters in the C-terminal domain may be populated by the late-stage targeting factors ISA and Nfu1. Recently, Maio *et al*. (2014) reported that the mammalian Jac1 ortholog HSC20, the Ssq1 ortholog HSPA9 and the Isu1 scaffold, ISCU, form a complex with SDHB. This SDHB assembly intermediate was visualized on BN-PAGE after co-immunoprecipitation of SDHB. SDH activity appeared to be attenuated upon depletion of HSC20 or HSPA9 using siRNA knock down. Therefore, the study suggested that cluster transfer to SDHB occurs within this complex. *In vitro* synthesized SDHB is readily imported into isolated mitochondria. Co-immunoprecipitation of the imported SDHB at different time points revealed that the interaction of SDHA with SDHB comes later than the formation of the HSC20/HSPA9/ISCU/SDHB complex, indicating that cluster transfer

DOI: 10.3109/10409238.2014.990556

may precede binding of SDHB to SDHA. However, the ISA components and Nfu1 failed to be co-adsorbed with the HSC20 pulldown. These results may imply that only the 2Fe–2S center is transferred within the HSC20/HSPA9/ISCU/SDHB complex and a subsequent transfer step mediates insertion of the C-terminal SDHB clusters. This process could be either a zip-up from 2Fe–2S through 3Fe–4S or a zip-down from 3Fe–4S through 2Fe–2S. Alternatively, SDHB may remain associated with HSC20 during the insertion of the 4Fe–4S and 3Fe–4S centers, although the targeting factors may not stably associate with the HSC20/HSPA9/ISCU/SDHB complex (Maio *et al*., 2014).

It should be noted that reduced Cys thiolates are required for Fe–S clusters to be assembled into Sdh2 as oxidized Cys ligands cannot coordinate Fe–S clusters. However, it is unknown whether cells depend on the thioredoxin/thioredoxin reductase, glutathione/glutathione reductase or peroxiredoxin to ensure the presence of thiolates for Fe–S coordination. It is also intriguing how meta-stable Sdh2 intermediates are protected specially from ROS after Fe–S cluster insertion. It has been well known that Fe–S clusters are extremely susceptible for damage upon exposure to oxygen (Imlay, 2006). Since 2Fe–2S and 3Fe–4S clusters are exposed to solvent in Sdh2 prior to association with Sdh1 and the membrane anchor domain, it is possible that specialized chaperones are required to sequester these Fe–S clusters from oxidative stressors present in the solvent.

In the following section, we discuss two recently reported SDH assembly factors required for the maturation of Sdh2.

Sdh6 and Sdh7 are chaperone required for Sdh2 maturation

Sdh6 (SDHAF1 in human) is the first SDH assembly factor reported. Mutations in human SDHAF1 compromise the stable assembly of SDH, which leads to SDH deficiency associated with infantile leukoencephalophaty (Ghezzi *et al*., 2009, Ohlenbusch *et al*., 2012). Sdh6 is a small mitochondrial matrix protein that belongs to the LYR motif protein family, which is defined by the presence of a short LX(L/A)YRXX(L/I)(R/K) motif. Previous studies showed that the functions of several other LYR motif proteins are related to Fe–S cluster metabolism. Ghezzi *et al*. reported that yeast or human cells lacking wild-type Sdh6 (or its ortholog) exhibited significantly reduced SDH activity, accompanied by attenuation of SDH assembly (Ghezzi *et al*., 2009). They suggested the possibility that Sdh6 is an assembly factor required for the Fe–S containing subunit, Sdh2, based on the fact that Sdh6 is an LYR motif protein. While prescient, this hypothesis remained unproven as the biochemical data supporting it were not yet available. We recently reported that Sdh6 is indeed an assembly factor required for stable Sdh2 maturation during SDH assembly (Na *et al*., 2014). In yeast cells lacking Sdh6, Sdh2 steady-state levels were significantly diminished, but Sdh1 steady-state levels and covalent flavinylation remained unaffected. Moreover, Sdh6 appeared to accumulate in *sdh3*Δ or *sdh4*Δ cells lacking the SDH membrane anchor domain where an Sdh1/Sdh2 subcomplex accumulated. Furthermore, immunoprecipitation of Sdh6 in mitochondrial lysates from cells lacking Sdh4 resulted in co-precipitation of Sdh1 and Sdh2, but immunoprecipitation of Sdh6 in WT or *sdh2*Δ mutants failed to yield Sdh1 or Sdh2. Thus, these results suggested that Sdh6 interacts with an Sdh1/Sdh2 complex and the interface for the interaction resides within Sdh2 (Figure 3). Indeed, Sdh6 overexpression in *sdh1*Δ mutants, in which Sdh2 is extremely labile, increased Sdh2 accumulation, thus, corroborating the postulate that Sdh6 acts on Sdh2 during SDH assembly.

Why does Sdh2 require the function of Sdh6 during the process of SDH assembly? One possibility is that Sdh6 is a chaperone stabilizing Sdh2 prior to Sdh1 association. However, Sdh2 overexpression failed to restore SDH activity in *sdh6*Δ mutants. Thus, Sdh6 likely exerts its function on Sdh2 maturation rather simply maintaining an apo-Sdh2 pool. Unbiased high-copy genetic suppressor screening provided a hint regarding Sdh6 function (Na *et al*., 2014). Yap1, a transcription factor that increases expression of a repertoire of genes required for oxidative stress tolerance was recovered from this screen. Yap1 overexpression enhanced the respiratory growth of *sdh6*Δ mutants and restored SDH activity. Conversely, artificially increased superoxide generation in the presence of paraquat severely impaired the respiratory growth of *sdh6*Δ cells. Moreover, Sdh2 protein levels under this condition were dramatically decreased. Given that ROS levels were not increased in *sdh6*Δ mutants, this exacerbated phenotype with paraquat suggests that Sdh6 is important for protecting Sdh2 from ROS-induced damage.

In the meantime, a genetic interaction between Sdh6 and Acn9 (renamed Sdh7), another protein in the LYR motif protein family, was observed. Sdh7 is also a small mitochondrial matrix protein, required for normal respiratory growth. Overexpression of Sdh6 in *sdh7*Δ mutants slightly rescued the respiratory growth defect although overexpression of Sdh7 in *sdh6*Δ mutants failed to do so. Metabolite profiling suggested an SDH deficiency in *sdh7*Δ mutant cells as succinate accumulated in the mutants. BN-PAGE analysis and SDH activity assay confirmed SDH deficiency with reduced SDH complex levels in *sdh7*Δ mutants. Biochemical analysis of *sdh7*Δ mutants suggested that Sdh7 function is similar to that of Sdh6 (Na *et al*., 2014). Among the SDH structural subunits, the steady-state levels of Sdh2 were the most impaired in *sdh7*Δ mutants. Sdh7 exhibited increased abundance and interaction with the Sdh1/Sdh2 subcomplex in cells lacking the SDH membrane anchor. In addition, Yap1 overexpression restored SDH activity and paraquat supplement markedly attenuated Sdh2 steady-state levels in *sdh7*Δ cells. However, Sdh2 overexpression failed to restore SDH activity in *sdh7*Δ cells. Thus, these results suggested that Sdh7 is another assembly factor for protecting Sdh2 from ROS damage. Deletion of the *Drosophila melanogaster SDH7* ortholog, *dSdhaf3*, caused a dramatic SDH deficiency with muscular and neuronal defects that are reminiscent of neurodegeneration observed in humans with mutations in *SDHAF1* (Na *et al*., 2014).

It is clear that Sdh6 and Sdh7 support the assembly of SDH under normal physiological conditions, although their deficiencies do not result in total ablation of SDH biogenesis. This might be due to a theoretical bypass pathway that can substitute for Sdh6 and Sdh7 functions. Otherwise, the importance of these two assembly factors is limited with

passive roles for Sdh2 maturation under certain circumstances. Our study shows that iron salt supplementation enhances the respiratory growth of *sdh6*Δ cells and *sdh7*Δ cells. It has been shown that ROS-inactivated aconitase under aerobic conditions regains activity following iron salt supplementation (Kennedy *et al*., 1983). The active site of aconitase harbors a 4Fe–4S cluster, which loses one Fe atom upon exposure to superoxide, resulting in inactivation. Increased concentration of iron salts facilitates re-insertion of Fe(II) ion back into the damaged 3Fe–4S center, leading to reactivation of aconitase. Therefore, it is possible that Sdh6 and Sdh7 are involved in shielding the aforementioned solvent-exposed Fe–S centers from ROS until an Sdh1/Sdh2 complex is fully assembled with Sdh3 and Sdh4. A recent study on Fe–S cluster insertion to SDHB has revealed that SdhB (Sdh2) can be expressed as two separate domains *in vivo* and SDHAF1 (Sdh6) interacts with the C-terminal domain of SdhB, but not with the N-terminal domain (Maio *et al*., 2014). The C-terminal domain harbors 4Fe–4S and 3Fe–4S centers (Sun *et al*., 2005). Therefore, it is possible that Sdh6 is required for protecting the solvent-exposed 3Fe–4S center from ROS damage. However, there is no data suggesting how Sdh7 would exert its protection on Sdh2.

The origin of the damaging ROS is unclear, but a likely source is either the 2-oxoacid dehydrogenases including 2-oxoglutarate dehydrogenase and pyruvate dehydrogenase or the respiratory complexes (Quinlan *et al*., 2014). However, it is also possible that ROS generated intrinsically within an Sdh1/Sdh2 subcomplex might play a role. Like flavinylated monomeric Sdh1, an Sdh1/Sdh2 subcomplex is also competent to catalyze succinate oxidation (Lemire & Oyedotun, 2002; Nihei *et al*., 2001). It is expected that the electrons extracted from succinate oxidation can travel to Fe–S centers. Once the electrons reach the solvent-exposed surface via Fe–S centers, the electrons can react with oxygen to generate local ROS that can damage Fe–S centers in the vicinity. Therefore, one alternative role of Sdh6 and Sdh7 might be that they interact with an Sdh1/Sdh2 complex to inhibit the electron transfer to Fe–S centers within the subcomplex.

It has also been suggested that Sdh6 may be directly involved in the process for Fe–S insertion into Sdh2 based on the observation that the SDH assembly factor SDHAF1 (Sdh6) was recovered in the immunoadsorption of HSC20 (Maio *et al*., 2014). It remains unclear, however, whether SDHAF1 is a dedicated Fe–S targeting factor for SDHB since no additional evidence is available to show that Sdh6 has an active role in Fe–S cluster formation.

Sdh3 and Sdh4 – the hydrophobic anchor

Architecture of the hydrophobic anchor

The SDH membrane anchor consists of an Sdh3–Sdh4 heterodimer and an intercalated heme b moiety. The structure of mammalian SDH demonstrates that SDHC contains four total helices while SDHD contains five (Sun *et al*., 2005; Figure 1). The N-terminal helix of SDHD is localized to the mitochondrial matrix and interacts with SDHB to promote membrane localization of the hydrophilic dimer. Each subunit contributes two transmembrane helices to the formation of a four-helix bundle, which comprises the core of the membrane anchor, while the remaining transmembrane helix from each subunit flanks the core. The remaining helices from each subunit protrude from the membrane and arrange in antiparallel fashion in the IMS essentially capping the transmembrane core. In addition to the helical arrangement of this domain, the structure reveals that SDHC and SDHD coordinate a heme b cofactor at the interface of the core four-helix bundle, which interacts with the porphyrin ring. Each subunit contributes a conserved histidine residue that coordinates the heme iron while two arginine residues, one from SDHC and one from SDHD, as well as another histidine residue from SDHC interact with the heme propionate groups (Sun *et al*., 2005).

The membrane anchor domain contains the site of ubiquinone binding and reduction, which ultimately facilitates electron transfer from succinate to subsequent ETC complexes (Sun *et al*., 2005). In fact, this domain contains two ubiquinone binding sites that are distinguished by their disparate affinities for ubiquinone (Oyedotun & Lemire, 2001; Silkin *et al*., 2007). The high-affinity site (Q_P-proximal) lies on the matrix-proximal side of the IMM and is the dominant ubiquinone binding site (Figure 1). The Q_P site is composed of residues from SDHC, SDHD and SDHB including the terminal 3Fe–4S cluster of SDHB (Sun *et al*., 2005). The second binding site (Q_D-distal) lies closer to the IMS side of the IMM and is a lower affinity site. This site is composed entirely of residues from SDHD (Sun *et al*., 2005). Ubiquinone reduction occurs in two stepwise single electron transfers, in contrast to the two-electron reduction of FAD. Importantly, the Q_P site stabilizes the partially reduced semiquinone intermediate and facilitates full reduction of ubiquinone to ubiquinol, thereby preventing the generation of reactive oxygen species (ROS; Yankovskaya *et al*., 2003).

Assembly of the hydrophobic anchor

With respect to assembly of the hydrophobic anchor, there remain more questions than answers. Sdh3 and Sdh4 are translated in the cytosol and imported to mitochondria through the TOM complex. They may then be transferred to the TIM23 complex in the IMM and laterally released to the final destination like other α-helical transmembrane IMM proteins (Dudek *et al*., 2013). Unfortunately, membrane insertion represents the bulk of our knowledge regarding assembly of this dimer and thus many questions remain. Do Sdh3 and Sdh4 folding and subsequent dimer formation require a chaperone? How is the Sdh3–Sdh4 assembly intermediate stabilized prior to formation of the holocomplex? Although little is known about this process, it is intriguing that stable Sdh3/Sdh4 dimerization requires the hydrophilic domain as deletion of either Sdh1 or Sdh2 causes near complete loss of both Sdh3 and Sdh4 (Kim *et al*., 2012; Na *et al*., 2014). Thus, it appears that biogenesis of the hydrophobic anchor is in some manner connected to the rest of the assembly process.

Perhaps the most intriguing question regarding the hydrophobic anchor relates to the heme b cofactor. In fact, it is unclear whether heme b is actually required for the electron transfer from FAD to ubiquinone in the Q_P site. The heme b lies further away from the 3Fe–4S (13.3 Å) than the Q_P site

DOI: 10.3109/10409238.2014.990556

does (7.6 Å; Sun *et al*., 2005; Yankovskaya *et al*., 2003). Moreover, the redox potential of heme b (−185 mV) is much lower than the 3Fe–4S (+60 mV) in SDH (Hägerhäll, 1997). Therefore, these two barriers would make the electron transfer from 3Fe–4S to heme b thermodynamically unfavorable compared to the direct electron transfer to ubiquinone (+113 mV). In fact, SDH complexes lacking heme b (from yeast cells expressing Sdh3 H106A and Sdh4 C78A heme-ligand mutants) appeared to be able to catalyze succinate-dependent quinone reduction (Oyedotun *et al*., 2007). It should be noted, however, that the heme b is important for the structural integrity of the membrane anchor domain in mammalian cells. SDH and SDHD steady-state levels were decreased in cells expressing SDHC His-ligand mutants (H127A or H127Y) in the absence of wild-type SDHC (Lemarie *et al*., 2011).

Regardless of its precise function, the heme b cofactor is present in SDH across all species, suggesting its importance in either electron transfer or complex stability. However, it is not yet known how Sdh3 and Sdh4 are assembled with heme b in the IMM. Does an assembly factor deliver and/or insert the heme b into a pre-existing Sdh3/Sdh4 dimer? It has been shown that several assembly factors, including Coa1, Coa2 and Shy1, are required for proper heme insertion into the complex IV subunit Cox1 in the IMM (Atkinson *et al*., 2010; Mashkevich *et al*., 1997; Pierrel *et al*., 2007, 2008). Therefore, one might expect that an assembly factor is required for SDH hemylation. Overall, studies addressing the assembly of this domain represent an important next step in understanding SDH biogenesis.

Conclusion

Prior to the discovery of the assembly factors reviewed herein, it was difficult to fully appreciate the complexity of the SDH assembly pathway. This is perhaps best illustrated by the fact that at least four and quite possible more, dedicated assembly factors are required for the maturation of the two soluble subunits alone. This does not even consider the process of assembling the Sdh3–Sdh4 hydrophobic domain. In the end, the assembly of SDH does not happen spontaneously, but is rather the result of a highly intricate and stepwise process facilitated by the concerted efforts of a number of accessory assembly factors.

These discoveries have dramatically increased our understanding of the assembly process and allow us to propose a more complete model of the SDH assembly pathway (Ghezzi *et al*., 2009; Hao *et al*., 2009; Na *et al*., 2014; Van Vranken *et al*., 2014; Figure 3). Following cytosolic translation, Sdh1 and Sdh2 are imported into the mitochondrial matrix as apo-proteins. Each of these subunits must subsequently mature in a process that is facilitated by subunit-specific assembly factors. Upon import, Sdh1 must be flavinylated and is bound by Sdh5, which enables this process. Although the precise mechanism remains poorly defined, Sdh5 most likely maintains apo-Sdh1 in a confirmation that facilitates insertion and covalent binding of FAD. Once Sdh1 has been covalently flavinylated, Sdh5 is released and holo-Sdh1 binds another subunit-specific chaperone, Sdh8. Sdh8 appears to serve dual roles in the process of assembly. First, Sdh8 prevents the generation of superoxide by Sdh1 through limiting the spurious reduction of oxygen. In addition to this, Sdh8 also appears to facilitate the formation of the Sdh1–Sdh2 soluble dimer. Like Sdh1, apo-Sdh2 must also mature prior to complex formation. The initial step in the maturation of this subunit is the insertion of the three Fe–S clusters generated by the ISU and ISA complexes. At this point, both Sdh1 and Sdh2 have matured into holo-proteins and can proceed through the assembly process. Sdh2 comes into association with two additional chaperones, Sdh6 and Sdh7 as it forms a soluble complex with Sdh1, thereby displacing Sdh8 and generating a heterotetrameric assembly intermediate. This intermediate, which is facilitated by Sdh6 and Sdh7, serves to protect surface-exposed Fe–S clusters and possibly prevents the spurious generation of superoxide by the redox active Sdh1–Sdh2 dimer. Finally, the Sdh1–Sdh2 dimer is bound by the Sdh3–Sdh4 hydrophobic domain, which may or may not be pre-assembled in the IMM, bringing the hydrophilic head in close association with the IMM and forming the active holo-complex (Figure 3).

In general, the contribution of subunit-specific assembly factors to the process of SDH assembly can be organized into three distinct functions. First, they mediate the insertion of essential cofactors. All ETC complexes utilize cofactors to perform the redox chemistry necessary to oxidize and reduce substrates and transfer electrons. Therefore, the maturation of individual subunits and subsequent assembly of active complexes is dependent on the post-translational insertion of essential redox-active cofactors. This is highlighted by the fact that eukaryotic genomes have maintained a specific Sdh1/SDHA flavinylation factor, which is absolutely required for the covalent attachment of FAD to this subunit. It remains to be determined whether Sdh6 or Sdh7 also has an active role in the insertion of one or more of the Fe–S clusters in Sdh2.

Second, assembly factors act as subunit-specific chaperones that stabilize individual subunits and assembly intermediates. The process of SDH, and more generally, ETC assembly, relies on the step-wise assembly of potentially dozens of individual subunits translated from two different genomes to form a single intricately constructed complex. As the structures of individual subunits are optimized to exist and function in the context of fully assembled complexes, it is not surprising that individual subunits and sub-complexes require chaperones to maintain stability during assembly. In terms of SDH assembly, this has been validated by discovery of specific factors that mediate the stability of both individual subunits and multimeric assembly intermediates. Indeed, work in *Drosophila* has demonstrated that the fly ortholog of Sdh8 is required for stabilization of holo-SdhA. Furthermore, the requirement for stabilizing holo-assembly intermediates is more manifested in the case of assembly intermediates containing oxidatively labile cofactors such as Fe–S centers. Sdh6 and Sdh7 appear to specifically bind and stabilize the Sdh1–Sdh2 soluble dimer prior to membrane association via Sdh3/Sdh4.

Third, assembly factors serve to prevent spurious and potentially deleterious interactions between individual redox-active subunits and the surrounding solvent. As a result of the unique chemistry enabled by their cofactors, individual ETC complex subunits are potentially toxic when not secluded

within a fully assembled complex. Indeed, the cell contains numerous protein complexes that need to be assembled in an organized fashion; however, dedicated assembly factors are much more common for those complexes in which individual subunits contain redox-active cofactors. This is highlighted by the role of Sdh8 as a chaperone for covalently flavinylated Sdh1. In isolation, flavinylated Sdh1 is capable of oxidizing succinate, which results in the spurious generation of superoxide upon reduction of molecular oxygen. By occupying free Sdh1, Sdh8 serves to minimize these deleterious chemical reactions, thus protecting the matrix from ROS. Sdh6 and Sdh7, which specifically bind the potentially redox-active Sdh1–Sdh2 dimer, could potentially mediate similar protection as Sdh8.

In addition to providing valuable insights into the SDH assembly pathway the recent discovery of SDH assembly factors has also facilitated a greater understanding of SDH-deficient pathologies (Table 1). The literature has many reports of patients with SDH deficiencies; however, it is clear that only a subset of these cases can be explained by mutations in the genes encoding the four core subunits. With the discovery of a number of proteins intimately involved in the SDH assembly pathway, this disparity may now start to be resolved. Indeed, it is now clear that loss of function mutations in SDH assembly factors are capable of causing the same pathologies as the core subunits themselves. Analogous to mutations in *SDHA*, mutations in *SDHAF1*, the human ortholog of *SDH6*, were discovered as a cause of leukoencephalopathy, a neurodegenerative disorder similar to Leigh Syndrome (Ghezzi *et al*., 2009). Furthermore, mutations in *SDHAF2*, the human ortholog of *SDH5*, were shown to be the causative lesion in at least two families with familial paraganglioma syndrome, mirroring the physiological consequences of core subunit mutations (Hao *et al*., 2009). Currently, there are no published reports describing human mutations in *SDHAF3* (*SDH7*) or *SDHAF4* (*SDH8*); however, these genes have only recently been implicated in the SDH assembly pathway. We suspect that, in time, mutations in these genes will ultimately be discovered in patients with SDH-deficient pathologies, thus further clarifying the connection between succinate dehydrogenase and human disease.

Declaration of interest

The authors report no declaration of interest.

References

Ajit Bolar N, Vanlander AV, Wilbrecht C, *et al*. (2013). Mutation of the iron-sulfur cluster assembly gene IBA57 causes severe myopathy and encephalopathy. Hum Mol Genet 22:2590–602.

Alston CL, Davison JE, Meloni F, *et al*. (2012). Recessive germline SDHA and SDHB mutations causing leukodystrophy and isolated mitochondrial complex II deficiency. J Med Gen 49:569–77.

Astuti D, Latif F, Dallol A, *et al*. (2001). Gene mutations in the succinate dehydrogenase subunit SDHB cause susceptibility to familial pheochromocytoma and to familial paraganglioma. Am J Hum Genet 69:49–54.

Atkinson A, Khalimonchuk O, Smith P, *et al*. (2010). Mzm1 influences a labile pool of mitochondrial zinc important for respiratory function. J Biol Chem 285:19450–9.

Bafunno V, Giancaspero TA, Brizio C, *et al*. (2004). Riboflavin uptake and FAD synthesis in *Saccharomyces cerevisiae* mitochondria: involvement of the Flx1p carrier in FAD export. J Biol Chem 279: 95–102.

Baker II PR,, Friederich MW, Swanson MA, *et al*. (2014). Variant non ketotic hyperglycinemia is caused by mutations in LIAS, BOLA3 and the novel gene GLRX5. Brain 137:366–79.

Banci L, Brancaccio D, Ciofi-Baffoni S, *et al*. (2014). [2Fe-2S] cluster transfer in iron-sulfur protein biogenesis. Proc Natl Acad Sci USA 111:6203–8.

Baysal BE. (2000). Mutations in SDHD, a mitochondrial complex II gene, in hereditary paraganglioma. Science 287:848–51.

Bourgeron T, Rustin P, Chretien D, *et al*. (1995). Mutation of a nuclear succinate dehydrogenase gene results in mitochondrial respiratory chain deficiency. Nat Genet 11:144–9.

Brandsch R, Bichler V. (1989). Covalent cofactor binding to flavoenzymes requires specific effectors. Eur J Biochem 182:125–8.

Burnichon N, Briere JJ, Libe R, *et al*. (2010). SDHA is a tumor suppressor gene causing paraganglioma. Hum Mol Genet 19: 3011–20.

Cameron JM, Janer A, Levandovskiy V, *et al*. (2011). Mutations in iron-sulfur cluster scaffold genes NFU1 and BOLA3 cause a fatal deficiency of multiple respiratory chain and 2-oxoacid dehydrogenase enzymes. Am J Hum Genet 89:486–95.

Cecchini G, Schroder I, Gunsalus RP, Maklashina E. (2002). Succinate dehydrogenase and fumarate reductase from *Escherichia coli*. Biochim Biophys Acta 1553:140–57.

Ciesielski SJ, Schilke BA, Osipiuk J, *et al*. (2012). Interaction of J-protein co-chaperone Jac1 with Fe-S scaffold Isu is indispensable in vivo and conserved in evolution. J Mol Biol 417:1–12.

Crooks DR, Jeong SY, Tong WH, *et al*. (2012). Tissue specificity of a human mitochondrial disease: differentiation-enhanced mis-splicing of the Fe-S scaffold gene ISCU renders patient cells more sensitive to oxidative stress in ISCU myopathy. J Biol Chem 287:40119–30.

Diaz F, Kotarsky H, Fellman V, Moraes CT. (2011). Mitochondrial disorders caused by mutations in respiratory chain assembly factors. Semin Fetal Neonatal Med 16:197–204.

Dudek J, Rehling P, van der Laan M. (2013). Mitochondrial protein import: common principles and physiological networks. BBA-Mol Cell Res 1833:274–85.

Eletsky A, Jeong M-Y, Kim H, *et al*. (2012). Solution NMR structure of yeast succinate dehydrogenase flavinylation factor Sdh5 reveals a putative Sdh1 binding site. Biochemistry 51:8475–7.

Fernandez-Vizarra E, Tiranti V, Zeviani M. (2009). Assembly of the oxidative phosphorylation system in humans: what we have learned by studying its defects. Biochim Biophys Acta 1793:200–11.

Ferrer-Cortes X, Font A, Bujan N, *et al*. (2013). Protein expression profiles in patients carrying NFU1 mutations. Contribution to the pathophysiology of the disease. J Inherit Metab Dis 36:841–7.

Gelling C, Dawes IW, Richhardt N, *et al*. (2008). Mitochondrial Iba57p is required for Fe/S cluster formation on aconitase and activation of radical SAM enzymes. Mol Cell Biol 28:1851–61.

Ghezzi D, Goffrini P, Uziel G, *et al*. (2009). SDHAF1, encoding a LYR complex-II specific assembly factor, is mutated in SDH-defective infantile leukoencephalopathy. Nat Genet 41:654–6.

Guzy RD, Sharma B, Bell E, *et al*. (2008). Loss of the SdhB, but Not the SdhA, subunit of complex II triggers reactive oxygen species-dependent hypoxia-inducible factor activation and tumorigenesis. Mol Cell Biol 28:718–31.

Hägerhäll C. (1997). Succinate:quinone oxidoreductases. variations on a censerved theme. Biochim Biophys Acta 1320:107–41.

Hall RE, Henriksson KG, Lewis SF, *et al*. (1993). Mitochondrial myopathy with succinate dehydrogenase and aconitase deficiency. Abnormalities of several iron-sulfur proteins. J Clin Invest 92:2660–6.

Hao HX, Khalimonchuk O, Schraders M, *et al*. (2009). SDH5, a gene required for flavination of succinate dehydrogenase, is mutated in paraganglioma. Science 325:1139–42.

Hoekstra AS, Bayley J-P. (2013). The role of complex II in disease. Biochim Biophys Acta Bioenergetics 1827:543–51.

Horváth R, Abicht A, Holinski-Feder E, *et al*. (2006). Leigh syndrome caused by mutations in the flavoprotein (Fp) subunit of succinate dehydrogenase (SDHA). J Neurol Neurosurg Psychiatry 77:74–6.

Imlay JA. (2006). Iron-sulphur clusters and the problem with oxygen. Mol Microbiol 59:1073–82.

Ishii T, Yasuda K, Akatsuka A, *et al*. (2005). A mutation in the SDHC gene of complex II increases oxidative stress, resulting in apoptosis and tumorigenesis. Cancer Res 65:203–9.

DOI: 10.3109/10409238.2014.990556

Jackson CB, Nuoffer J-M, Hahn D, *et al*. (2014). Mutations in SDHD lead to autosomal recessive encephalomyopathy and isolated mitochondrial complex II deficiency. J Med Genet 51:170–5.

Jain-Ghai S, Cameron JM, Al Maawali A, *et al*. (2013). Complex II deficiency – a case report and review of the literature. Am J Med Genet A 161A:285–94.

Janeway KA, Kim SY, Lodish M, *et al*. (2011). Defects in succinate dehydrogenase in gastrointestinal stromal tumors lacking KIT and PDGFRA mutations. Proc Natl Acad Sci USA 108:314–18.

Jensen LT, Culotta VC. (2000). Role of *Saccharomyces cerevisiae* ISA1and ISA2 in iron homeostasis. Mol Cell Biol 20:3918–27.

Johansson C, Roos AK, Montano SJ, *et al*. (2011). The crystal structure of human GLRX5: iron-sulfur cluster co-ordination, tetrameric assembly and monomer activity. Biochem J 433:303–11.

Kennedy MC, Emptage MH, Dreyer JL, Beinert H. (1983). The role of iron in the activation-inactivation of aconitase. J Biol Chem 258: 11098–105.

Kim HJ, Jeong MY, Na U, Winge DR. (2012). Flavinylation and assembly of succinate dehydrogenase are dependent on the C-terminal tail of the flavoprotein subunit. J Biol Chem 287:40670–9.

Kim HJ, Winge DR. (2013). Emerging concepts in the flavinylation of succinate dehydrogenase. Biochim Biophys Acta 1827:627–36.

Kounosu A. (2014). Analysis of covalent flavinylation using thermostable succinate dehydrogenase from *Thermus thermophilus* and *Sulfolobus tokodaii* lacking SdhE homologs. FEBS Lett 588:1058–63.

Lemarie A, Huc L, Pazarentzos E, *et al*. (2011). Specific disintegration of complex II succinate: ubiquinone oxidoreductase links pH changes to oxidative stress for apoptosis induction. Cell Death Differ 18: 338–49.

Lemire BD, Oyedotun KS. (2002). The *Saccharomyces cerevisiae* mitochondrial succinate: ubiquinone oxidoreductase. Biochim Biophys Acta 1553:102–16.

Li H, Outten CE. (2012). Monothiol CGFS glutaredoxins and BolA-like proteins: [2Fe-2S] binding partners in iron homeostasis. Biochemistry 51:4377–89.

Lill R, Hoffmann B, Molik S, *et al*. (2012). The role of mitochondria in cellular iron-sulfur protein biogenesis and iron metabolism. Biochim Biophys Acta 1823:1491–508.

Lim SC, Friemel M, Marum JE, *et al*. (2013). Mutations in LYRM4, encoding iron-sulfur cluster biogenesis factor ISD11, cause deficiency of multiple respiratory chain complexes. Hum Mol Genet 22:4460–73.

Maio N, Singh A, Uhrigshardt H, *et al*. (2014). Cochaperone binding to LYR motifs confers specificity of iron sulfur cluster delivery. Cell Metab 19:445–57.

Majewska J, Ciesielski SJ, Schilke B, *et al*. (2013). Binding of the chaperone Jac1 protein and cysteine desulfurase Nfs1 to the iron-sulfur cluster scaffold Isu protein is mutually exclusive. J Biol Chem 288:29134–42.

Mashkevich G, Repetto B, Glerum DM, *et al*. (1997). SHY1, the yeast homolog of the mammalian SURF-1 gene, encodes a mitochondrial protein required for respiration. J Biol Chem 272:14356–64.

Messner KR, Imlay JA. (2002). Mechanism of superoxide and hydrogen peroxide formation by fumarate reductase, succinate dehydrogenase, and aspartate oxidase. J Biol Chem 277:42563–71.

Muhlenhoff U, Richter N, Pines O, *et al*. (2011). Specialized function of yeast Isa1 and Isa2 proteins in the maturation of mitochondrial [4Fe-4S] proteins. J Biol Chem 286:41205–16.

Na U, Yu W, Cox JE, *et al*. (2014). The LYR factors SDHAF1 and SDHAF3 mediate maturation of the iron-sulfur subunit of succinate dehydrogenase. Cell Metab 20:253–66.

Navarro-Sastre A, Tort F, Stehling O, *et al*. (2011). A fatal mitochondrial disease is associated with defective NFU1 function in the maturation of a subset of mitochondrial Fe-S proteins. Am J Hum Genet 89: 656–67.

Nihei C, Nakayashiki T, Nakamura K, *et al*. (2001). Abortive assembly of succinate-ubiquinone reductase (complex II) in a ferrochelatase-deficient mutant of *Escherichia coli*. Mol Genet Genomics 265: 394–404.

Ohlenbusch A, Edvardson S, Skorpen J, *et al*. (2012). Leukoencephalopathy with accumulated succinate is indicative of SDHAF1 related complex II deficiency. Orphanet J Rare Dis 7:69.

Oyedotun KS, Lemire BD. (2001). The Quinone-binding sites of the *Saccharomyces cerevisiae* succinate-ubiquinone oxidoreductase. J Biol Chem 276:16936–43.

Oyedotun KS, Sit CS, Lemire BD. (2007). The *Saccharomyces cerevisiae* succinate dehydrogenase does not require heme for ubiquinone reduction. Biochim Biophys Acta 1767:1436–45.

Pandey A, Golla R, Yoon H, *et al*. (2012). Persulfide formation on mitochondrial cysteine desulfurase: enzyme activation by a eukaryote-specific interacting protein and Fe-S cluster synthesis. Biochem J 448: 171–87.

Pandey A, Gordon DM, Pain J, *et al*. (2013). Frataxin directly stimulates mitochondrial cysteine desulfurase by exposing substrate-binding sites, and a mutant Fe-S cluster scaffold protein with frataxin-bypassing ability acts similarly. J Biol Chem 288:36773–86.

Pantaleo MA, Astolfi A, Indio V. (2011). SDHA loss-of-function mutations in KIT-PDGFRA wild-type gastrointestinal stromal tumors identified by massively parallel sequencing. J Natl Cancer Inst 103: 983–7.

Pantaleo MA, Astolfi A, Urbini M, *et al*. (2014). Analysis of all subunits, SDHA, SDHB, SDHC, SDHD, of the succinate dehydrogenase complex in KIT/PDGFRA wild-type GIST. Eur J Hum Genet 22:32–9.

Peczkowska M, Cascon A, Prejbisz A, *et al*. (2008). Extra-adrenal and adrenal pheochromocytomas associated with a germline SDHC mutation. Nat Clin Pract End Met 4:111–15.

Pierrel F, Bestwick ML, Cobine PA, *et al*. (2007). Coa1 links the Mss51 post-translational function to Cox1 cofactor insertion in cytochrome c oxidase assembly. EMBO J 26:4335–46.

Pierrel F, Khalimonchuk O, Cobine PA, *et al*. (2008). Coa2 is an assembly factor for yeast cytochrome c oxidase biogenesis that facilitates the maturation of Cox1. Mol Cell Biol 28:4927–39.

Py B, Gerez C, Angelini S, *et al*. (2012). Molecular organization, biochemical function, cellular role and evolution of NfuA, an atypical Fe-S carrier. Mol Microbiol 86:155–71.

Quinlan CL, Goncalves RL, Hey-Mogensen M, *et al*. (2014). The 2-oxoacid dehydrogenase complexes in mitochondria can produce superoxide/hydrogen peroxide at much higher rates than complex I. J Biol Chem 289:8312–25.

Robinson KM, Lemire BD. (1996). Covalent attachment of FAD to the yeast succinate dehydrogenase flavoprotein requires import into mitochondria, presequence removal, and folding. J Biol Chem 271: 4055–60.

Robinson KM, Rothery RA, Weiner JH, Lemire BD. (1994). The covalent attachment of FAD to the flavoprotein of *Saccharomyces cerevisiae* succinate dehydrogenase is not necessary for import and assembly into mitochondria. Eur J Biochem 222:983–90.

Rodriguez-Manzaneque MAT, Tamarit J, Bellí G, *et al*. (2002). Grx5 is a mitochondrial glutaredoxin required for the activity of iron/sulfur enzymes. Mol Biol Cell 13:1109–21.

Rutter J, Winge DR, Schiffman JD. (2010). Succinate dehydrogenase – assembly, regulation and role in human disease. Mitochondrion 10: 393–401.

Santos MAA, Jiménez A, Revuelta J. (2000). Molecular characterization of FMN1, the structural gene for the monofunctional flavokinase of *Saccharomyces cerevisiae*. J Biol Chem 275:28618–24.

Schmucker S, Martelli A, Colin F, *et al*. (2011). Mammalian frataxin: an essential function for cellular viability through an interaction with a preformed ISCU/NFS1/ISD11 iron-sulfur assembly complex. PLoS One 6:e16199.

Sheftel AD, Stehling O, Pierik AJ, *et al*. (2010). Humans possess two mitochondrial ferredoxins, Fdx1 and Fdx2, with distinct roles in steroidogenesis, heme, and Fe/S cluster biosynthesis. Proc Natl Acad Sci USA 107:11775–80.

Sheftel AD, Wilbrecht C, Stehling O, *et al*. (2012). The human mitochondrial ISCA1, ISCA2, and IBA57 proteins are required for [4Fe-4S] protein maturation. Mol Biol Cell 23:1157–66.

Silkin Y, Oyedotun KS, Lemire BD. (2007). The role of Sdh4p Tyr-89 in ubiquinone reduction by the Saccharomyces cerevisiae succinate dehydrogenase. Biochim Biophys Acta 1767:143–50.

Sun F, Huo X, Zhai Y, *et al*. (2005). Crystal structure of mitochondrial respiratory membrane protein complex II. Cell 121:1043–57.

Torchetti EM, Brizio C, Colella M, *et al*. (2010). Mitochondrial localization of human FAD synthetase isoform 1. Mitochondrion 10: 263–73.

Tsai CL, Barondeau DP. (2010). Human frataxin is an allosteric switch that activates the Fe-S cluster biosynthetic complex. Biochemistry 49: 9132–9.

Tzagoloff A, Jang J, Glerum DM, Wu M. (1996). FLX1 codes for a carrier protein involved in maintaining a proper balance of flavin nucleotides in yeast mitochondria. J Biol Chem 271:7392–7.

Uzarska MA, Dutkiewicz R, Freibert SA, *et al*. (2013). The mitochondrial Hsp70 chaperone Ssq1 facilitates Fe/S cluster transfer from Isu1 to Grx5 by complex formation. Mol Biol Cell 24: 1830–41.

Van Vranken JG, Bricker DK, Dephoure N, *et al*. (2014). SDHAF4 promotes mitochondrial succinate dehydrogenase activity and prevents neurodegeneration. Cell Metab 20:241–52.

Vanharanta S, Buchta M, Mcwhinney SR, *et al*. (2004). Early-onset renal cell carcinoma as a novel extraparaganglial component of SDHB-associated heritable paraganglioma. Am J Hum Genet 74:153–9.

Wu M, Repetto B, Glerum DM, Tzagoloff A. (1995). Cloning and characterization of FAD1, the structural gene for flavin adenine dinucleotide synthetase of *Saccharomyces cerevisiae*. Mol Cell Biol 15:264–71.

Yankovskaya V, Horsefield R, Tornroth S, *et al*. (2003). Architecture of succinate dehydrogenase and reactive oxygen species generation. Science 299:700–4.

CHAPTER 2

FLAVINYLATION AND ASSEMBLY OF SUCCINATE DEHYDROGENASE ARE DEPENDENT ON THE C-TERMINAL TAIL OF THE FLAVOPROTEIN SUBUNIT

Hyung J. Kim, Mi-Young Jeong, Un Na, Dennis R. Winge

Reprinted with permission from The Journal of Biological Chemistry

Vol.287, No.48, pp.40670-40679, November 23, 2012

THE JOURNAL OF BIOLOGICAL CHEMISTRY VOL. 287, NO. 48, pp. 40670–40679, November 23, 2012

Flavinylation and Assembly of Succinate Dehydrogenase Are Dependent on the C-terminal Tail of the Flavoprotein Subunit*

Received for publication, July 27, 2012, and in revised form, October 4, 2012 Published, JBC Papers in Press, October 7, 2012, DOI 10.1074/jbc.M112.405704

Hyung J. Kim[1,2], **Mi-Young Jeong**[1], **Un Na, and Dennis R. Winge**[3]

From the Departments of Medicine and Biochemistry, University of Utah Health Sciences Center, Salt Lake City, Utah 84132

Background: Succinate dehydrogenase (SDH) requires a covalent addition of FAD for catalytic function.
Results: Mutational analyses of Sdh1 implicate C-terminal region Arg residues involvement in covalent flavinylation and SDH assembly.
Conclusion: SDH assembly is dependent on FAD binding to Sdh1 but not covalent binding.
Significance: These results document the basis for the SDH deficiency and pathology seen with mutations in human Sdh1.

The enzymatic function of succinate dehydrogenase (SDH) is dependent on covalent attachment of FAD on the ~70-kDa flavoprotein subunit Sdh1. We show presently that flavinylation of the Sdh1 subunit of succinate dehydrogenase is dependent on a set of two spatially close C-terminal arginine residues that are distant from the FAD binding site. Mutation of Arg^{582} in yeast Sdh1 precludes flavinylation as well as assembly of the tetrameric enzyme complex. Mutation of Arg^{638} compromises SDH function only when present in combination with a Cys^{630} substitution. Mutations of either Arg^{582} or Arg^{638}/Cys^{630} do not markedly destabilize the Sdh1 polypeptide; however, the steady-state level of Sdh5 is markedly attenuated in the Sdh1 mutant cells. With each mutant Sdh1, second-site Sdh1 suppressor mutations were recovered in Sdh1 permitting flavinylation, stabilization of Sdh5 and SDH tetramer assembly. SDH assembly appears to require FAD binding but not necessarily covalent FAD attachment. The Arg residues may be important not only for Sdh5 association but also in the recruitment and/or guidance of FAD and or succinate to the substrate site for the flavinylation reaction. The impaired assembly of SDH with the C-terminal Sdh1 mutants suggests that FAD binding is important to stabilize the Sdh1 conformation enabling association with Sdh2 and the membrane anchor subunits.

Succinate dehydrogenase (SDH),[4] also known as succinate: quinone oxidoreductase, is a citric acid cycle enzyme that links directly to the aerobic respiratory chain. The enzyme catalyzes the FAD-dependent oxidation of succinate to fumarate coupled with the reduction of ubiquinone to ubiquinol. SDH is a heterotetrameric integral membrane protein complex. The eukaryotic enzyme is embedded within the mitochondrial inner membrane by a hydrophobic module associated with the catalytic module protruding into the mitochondrial matrix (1). The hydrophilic catalytic module consists of Sdh1 and Sdh2 subunits and the electron transfer cofactors. Succinate oxidation occurs in the FAD-containing Sdh1 with the abstracted electrons from the reaction shuttled via three iron-sulfur centers in Sdh2 to the ubiquinone reduction site (Q_P -proximal) at the interface of Sdh2 and the membrane anchor (1–4). The Sdh3/Sdh4 membrane domain contains a bound heme *b* moiety at the subunit interface of Sdh3 and Sdh4 with each providing one of the two axial His ligands, although the role of the heme in eukaryotic SDH is unresolved (5).

The FAD of Sdh1 is covalently attached at an active site His residue (2). This covalent bond increases the FAD redox potential by ~60 mV to permit succinate oxidation (6). SDH is the major mitochondrial protein containing a covalent bound flavin (7). Sdh1 containing a H90S substitution is enzymatically inactive in succinate oxidation but assembles into a tetrameric complex that exhibits fumarate reductase activity (8). Fumarate reductase activity in SDH does not require covalent flavinylation. SDH is related to the bacterial fumarate reductase and both enzymes can catalyze succinate oxidation and fumarate reduction with different efficiencies (9). Flavinylation of Sdh1 was found to occur after import into the matrix and to be influenced by the presence of the iron/sulfur cluster subunit Sdh2 but largely independent of the membrane anchor (10). The presence of citric acid intermediates stimulated the flavinylation process (10).

The covalent addition of FAD was proposed to be autocatalytic (7), but recently, a dedicated assembly factor Sdh5 was identified that is required for covalent flavinylation (11). The role of Sdh5 in Sdh1 flavinylation was discovered by the interaction of the two proteins and the demonstration that *sdh5*Δ yeasts were devoid of SDH activity and lacked flavinylated Sdh1. The direct role of Sdh5 in Sdh1 flavinylation was shown by the enhanced covalent addition of FAD to recombinant Sdh1 expressed in bacteria in the presence of Sdh5. However, the

* This work was supported by Grant ES03817 from the NIEHS, National Institutes of Health (to D. R. W.), funding from the Huntsman Cancer Institute (P30 CA042014), and support from the National Institutes of Health (R24DK092784-01).
[1] Both authors contributed equally to this work.
[2] Supported by Training Grant T32 DK007115 from the National Institutes of Health.
[3] To whom correspondence should be addressed. Tel.: 801-585-5103; Fax: 801-585-3432; E-mail: dennis.winge@hsc.utah.edu.
[4] The abbreviations used are: SDH, succinate dehydrogenase; BN-PAGE, blue native PAGE; FAD, flavin adenine dinucleotide; DDm, n-dodecyl-β-D-maltoside.

mechanism by which the 22-kDa Sdh5 protein mediates flavinylation of Sdh1 remains unresolved.

The human Sdh5 ortholog, SDHAF2, was shown to have a corresponding role in covalent flavinylation in human cells (11). Mutations in SDHAF2 are associated with a neuroendrocrine tumor designated as paraganglioma. Mutations in the SDH structural genes are also detected in a range of tumors, including paraganglioma, pheochromocytomas, gastrointestinal stromal tumors, and renal cell carcinoma (12). Recently, the bacterial ortholog of Sdh5 was identified in the bacterium *Serratia*. The factor designated SdhE was shown to interact with the flavoprotein (SdhA) and independently associate with FAD (13). This is the first suggestion that the assembly factor may mediate Sdh1 flavinylation by presenting bound FAD. Whereas *sdh5*Δ cells exhibited a specific defect in SDH, the bacterial *sdh*E mutant showed a more pleiotropic defect, suggesting SdhE may flavinylate other flavoproteins (13).

SDH is one of many flavoproteins with a covalently bound cofactor. SDH has an 8α-N^3-histidyl-FAD linkage, but other flavoproteins use cysteinyl-FAD or tyrosyl-FAD linkages (14). Two large families of covalent flavoproteins are the glucose oxidase/methanol oxidase family and the vanillyl-alcohol oxidase family. Within the vanillyl-alcohol oxidase family, FAD linkages to histidine, cysteine, and tyrosine are known, although no ancillary enzyme is known to catalyze the covalent addition. Covalent flavinylation with FAD is known to proceed nonenzymatically, albeit slowly.

In the present study, we identify essential arginines in the C-terminal tail in yeast Sdh1 that are required for flavinylation and SDH assembly. The impaired assembly of the tetrameric enzyme with these Sdh1 mutants correlates with the lack of FAD binding.

MATERIALS AND METHODS

Yeast Strains and Vectors—All *Saccharomyces cerevisiae* strains used in this study were derivatives of Trp^{303} (Mat**a** *ura3-1 ade2-1 trp1-1 his3-11,15 leu2-3 112*). Deletion strains *sdh1*Δ, *sdh2*Δ, *sdh3*Δ, and *sdh4*Δ, in addition to plasmid pRS414 Sdh2-His_6Myc_2, were kindly provided by Dr. Jared Rutter at the University of Utah. Additional deletion strains (*flx*Δ, *sdh5*Δ, *sdh3*Δ*sdh4*Δ double) were constructed by homologous recombination using either the *KanMX4* or the *HIS3MX6* disruption cassettes (15). The C-terminal mutants of *SDH1* along with *SDH1* WT under the control of its own promoter and *CYC1* terminator were expressed in *sdh1*Δ strain or subcloned into integrating pRS405 vectors for chromosomal expression. The integrating constructs were further digested with AflII and integrated at the *leu2-3,112* locus of *sdh1*Δ to be able to express wild type and mutants *SDH1* chromosomally. All integrated strains were confirmed by PCR analysis of the locus. The C-terminal point mutations were introduced by QuikChange mutagenesis PCR system (Agilent Technology). All mutations were confirmed by DNA sequencing. Yeast strains were transformed using lithium acetate. Strains were grown in synthetic complete medium lacking the amino acid(s) to maintain plasmid selection with either 2% galactose or 2% glycerol/lactate as the carbon source.

For carbon swap cultures overnight, 50-ml glucose-grown cultures were used to inoculate 1 liter of medium containing 2% galactose as the carbon source. Cells were grown to an $A_{600\ nm}$ ~ 0.4 to 0.5 and harvested in a sterile manner. The cell pellet was resuspended in fresh medium containing 2% glycerol/lactate as the carbon source and grown for ~10 h (~3–4 doublings) before harvesting.

Mitochondria Isolation—Intact mitochondria were isolated using previously described methods of Glick and Pon (16) and Diekert *et al.* (17). For HPLC experiments, isolated mitochondria were further purified using ultracentrifugation through a Histodenz (Sigma Aldrich) step gradient (14 and 22%). Total mitochondrial protein was quantified using either the Bradford (18) or the bicinchoninic acid assays (19).

Immunoblotting and Blue-native PAGE—Steady-state levels of mitochondrial proteins were analyzed using the NuPAGE Bis-Tris gel system (Invitrogen) using MES as the buffer system. Proteins were subsequently transferred to nitrocellulose membrane and probed using the indicated primary antibodies and visualized using enhanced chemiluminescence (ECL) reagents with horseradish peroxidase-conjugated secondary antibodies. Primary antibodies were obtained from the following: anti-Sdh1, Sdh2, Sdh3, and Sdh5 were generated in this study (21st Century Biochemicals). Anti-HA, anti-Myc, and anti-porin were purchased from Rockland, Roche Applied Science, and Molecular Probes, respectively. Anti-F1 ATP synthase was a generous gift from Alex Tzagoloff.

Analysis of yeast mitochondrial native membrane complexes was performed using the native PAGE gel system (Invitrogen) that is based on the blue-native polyacrylamide gel electrophoresis (BN-PAGE) technique developed by Schägger and von Jagow (20). Solubilized mitochondria (1% digitonin for 20–40 μg of mitochondrial protein) were separated on either 3–12% or 4–16% Bis-Tris native gels, transferred to PVDF membrane, and analyzed by immunoblotting.

Hemin-agarose Pulldown Assays and Immunoprecipitation—Purified mitochondria (0.75 to 1 mg of total protein) were solubilized using either 0.1% DDM or 1% digitonin in PBS buffer and clarified at 20,000 × *g* for 5 min. For hemin-agarose pulldown assay, the clarified lysates were incubated with 20 to 40 μl of hemin-agarose beads (Sigma), which had been prereduced using DTT. Binding was performed for 2 h or overnight at 4 °C. Beads were subsequently washed (15 min × 4) with PBS buffer, 0.1% DDM or 1% digitonin, ± DTT, and eluted with 2× SDS-PAGE loading buffer. For immunoprecipitation, the clarified lysates were incubated with anti-HA or anti-Myc beads for 2 h or overnight at 4 °C, washed four times with PBS buffer + 0.1% DDM or 1% digitonin, and eluted with 2× SDS-PAGE loading buffer. The clarified lysate, final wash, and eluate fraction were analyzed by SDS-PAGE and immunoblotting. Bands from Coomassie-stained SDS-PAGE gel from hemin-agarose pulldown assay were also excised for identification using MS analysis of the tryptic digests.

SDH Activity Assay—SDH activities in isolated yeast mitochondria were measured spectrophotometrically at 22 °C following the succinate-dependent, phenazine methosulfate-mediated reduction of either 2,6-dichlorophenolindophenol or

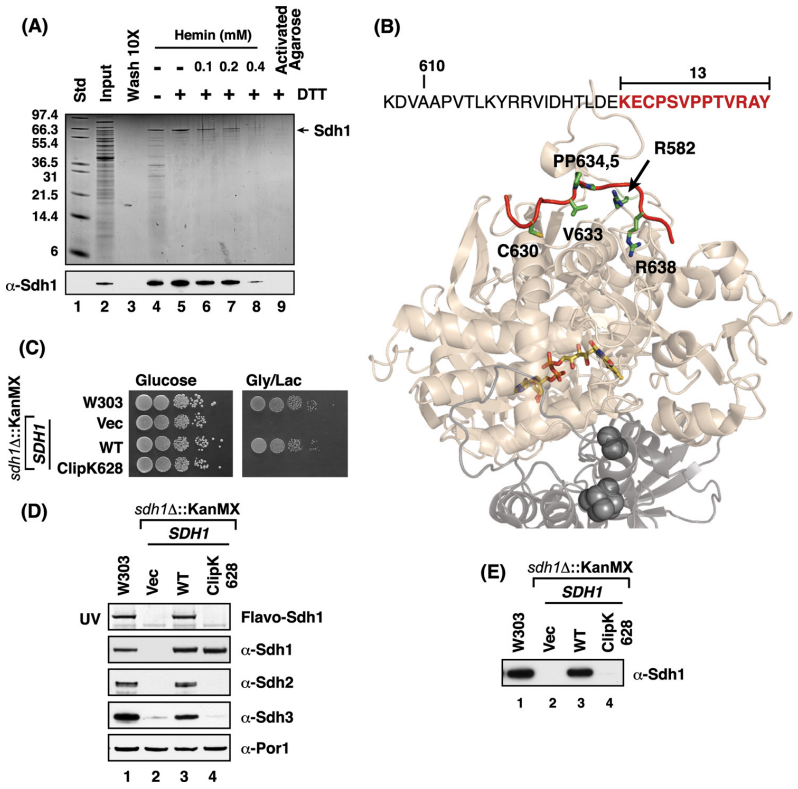

FIGURE 1. **Subunit 1 of SDH (Sdh1) binds hemin *in vitro*, and truncation of its last 13 residues abrogates this heme binding and renders the cells respiratory defective.** *A*, Coomassie-stained SDS-PAGE gel of hemin-agarose purified Sdh1 from DDM-solubilized mitochondria ± DTT (*lane 4 versus 5*) and in the presence of increasing concentrations of free hemin as a competitor to the hemin-agarose beads (*lanes 6–8*). Activated agarose beads conjugated to a six-carbon linker (minus hemin) failed to capture Sdh1 (*lane 9*) *std*, protein standards; *wash*, final wash of the resin concentrated 10-fold. *B*, the last 13 residues of Sdh1 is a featureless strand (highlighted in *red*) located on the surface of the protein and away from the buried FAD cofactor (*colored sticks*). Sdh1 is shown in *light beige*, Sdh2 is shown in *light gray*, and its iron-sulfur clusters are shown as *dark gray spheres*. PyMOL was used to generate the figure from Protein Data Bank code 2H88 (avian). *C*, WT and *sdh1*Δ strains transformed with vectors (*Vec*) encoding full-length and truncated Sdh1 were spotted on fermentable (glucose) and non-fermentable (glycerol/lactate) medium with serial dilution and incubated at 30 °C. Cells with truncation of the last 13 residues in Sdh1 (Clip K628) failed to grow on respiratory medium. *D*, SDS-PAGE and immunoblot analysis of mitochondria isolated from strains in *B*. Covalent flavinylation of Sdh1 is lost in cells with truncation of the last 13 residues in Sdh1 (Clip K629) as analyzed by UV illumination of SDS-PAGE gel. Immunoblots show that steady-state levels of Sdh2 and Sdh3 are also affected by C-terminal truncation. *E*, immunoblot analysis of hemin-agarose purification of Sdh1 using mitochondria isolated from strains indicated in *B* shows that heme binding is lost in the Sdh1 C-terminal truncate (Clip K629). *Flavo*, flavoprotein. *KanMX* is the deletion cassette.

cytochrome *c* as the terminal electron acceptor described for intact mitochondria (21).

Analysis of Sdh1-bound FAD and Total Mitochondrial FAD Levels—Levels of covalently attached FAD to Sdh1 were analyzed as described previously (11, 22). Mitochondrial proteins were resolved on SDS-PAGE, and the gel was placed in a 10% acetic acid solution for 20 min to oxidize flavin. The FAD band was visualized upon exposure to UV light using a Bio-Rad Gel Doc transilluminator.

Freely soluble mitochondrial FAD levels were analyzed as described previously (23). Purified mitochondria (500 μg) were pelleted at 20,000 × *g* for 10 min and resuspended in 500 μl of deionized water and boiled at 105 °C for 10–15 min to precipitate proteins. The resulting yellowish supernatant was clarified at 20,000 × *g* for 5 min and analyzed on a Waters Sunfire C_{18} HPLC column (5 μm 4.6 × 150 mm) equilibrated with 15% MeOH in 10 mM ammonium acetate, pH 6.4. Flavin was eluted using a linear MeOH gradient to 75% in 10 mM ammonium acetate, pH 6.4, for 25 min and monitored at 450 nm. Elution times were compared with FAD and FMN flavin mononucleotide standards (Sigma). The concentration of FAD for the peak area was determined using an extinction coefficient of 11,300 M^{-1} cm^{-1} at 450 nm (9).

RESULTS

Adsorption of Sdh1 on Heme Agarose—The focus on SDH flavinylation initiated from a goal to isolate heme-binding proteins within the mitochondria using affinity purification with a heme-agarose matrix. Detergent-solubilized mitochondrial lysates were chromatographed on heme-agarose affinity beads either in the oxidized (Fe^{3+}; hemin) or reduced (Fe^{2+}; heme) state (Fig. 1*A*). Proteins adsorbed on the heme matrix were eluted by SDS treatment and analyzed by SDS-PAGE. With reduced heme-agarose, a single major band was apparent with Coomassie staining that was identified as Sdh1 by mass spectrometry. The 67-kDa band was further verified to be Sdh1 by

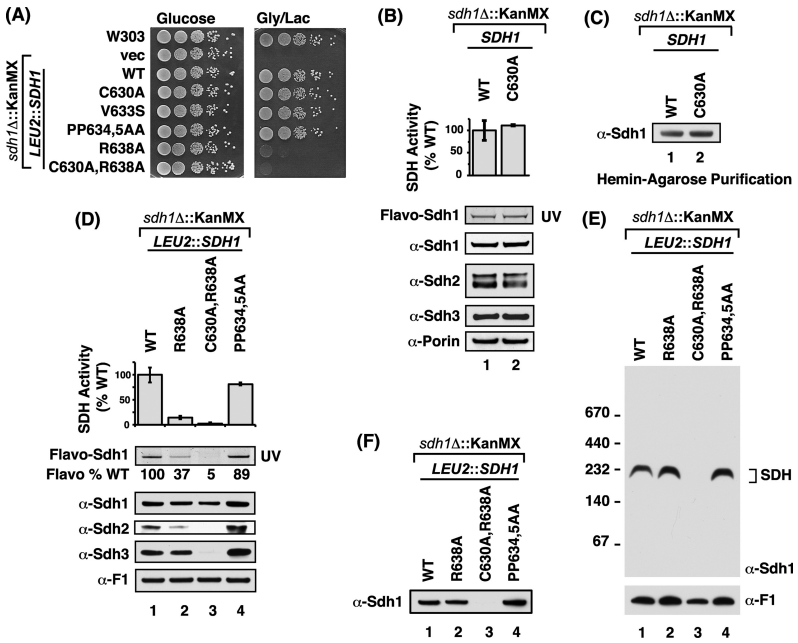

FIGURE 2. **Double mutation of C630A and R638A residues leads to loss of respiratory growth and assembly of the SDH complex and loss of heme binding to Sdh1.** *A*, growth test of strains with chromosomally integrated *SDH1* C-terminal point mutants. Cells possessing R638A substitutions showed growth impairment on fermentable medium with the double C630A,R638A mutant showing the greatest growth defect. *B*, *upper panel*: SDH activities of isolated mitochondria from *sdh1*Δ strains transformed with vectors (*vec*) encoding WT and C630A Sdh1 mutant. Activities expressed as a percentage of WT ($n \geq 3 \pm$ S.D.). *Lower panels*, corresponding immunoblot analysis of mitochondria isolated from above strains showing steady-state levels of covalent flavinylation (UV illumination) and SDH subunits. *C*, immunoblot analysis of hemin-agarose purification of Sdh1 using mitochondria isolated from strains indicated in *B*. *D*, *upper panel*: SDH activities of isolated mitochondria from strains expressing chromosomally integrated *SDH1* C-terminal point mutants expressed as a percentage of WT ($n \geq 3 \pm$ S.D.). *Lower panel*: steady-state of flavinylated-Sdh1 and SDH complex subunits in corresponding mitochondria of *upper panel*. The flavoprotein (*Flavo*) % WT is a relative comparison to WT based on band density as quantified by ImageJ software. *E*, BN-PAGE immunoblots of isolated mitochondria from *B*. 20 μg of isolated mitochondria were solubilized in 1% digitonin and separated on 3–12% native PAGE. Native protein complexes were transferred onto PVDF membrane and probed with antibodies to Sdh1 and F1 (loading control). *F*, immunoblot analysis of hemin-agarose purification of Sdh1. DDM-solubilized mitochondria lysates in *B* shows that heme binding is lost in the double C630A,R638A mutant.

immunoblotting using Sdh1 antisera. Subunits Sdh2 and Sdh3 were also detected with their respective antiseras but in less abundance compared with Sdh1 (data not shown). The adsorption of Sdh1 on heme-agarose was competed by preincubation of the lysate with free heme, and no Sdh1 was retained on activated agarose beads lacking the heme moiety.

The retention of Sdh1 on heme-agarose suggested Sdh1 may possess a heme-binding motif. Inspection of the yeast Sdh1 protein sequence showed a single CP motif in the C-terminal tail found in a subset of heme-binding proteins (Fig. 1*B*). This C-terminal tail strand lies on the surface of Sdh1 and is located far from the buried FAD cofactor. Deletion of a C-terminal 13-residue segment in Sdh1 generated a truncate (designated ClipK628) that was stably expressed, although cells harboring this truncate failed to propagate on non-fermentable carbon sources (Fig. 1*C*). The presence of the Sdh1 truncate abrogated assembly of the tetrameric SDH enzyme and steady-state levels of Sdh2 and Sdh3 were markedly attenuated (Fig. 1*D*). The truncated Sdh1 was not flavinylated as shown by the lack of a FAD fluorescence band after SDS-PAGE (10). Chromatography of detergent lysates on the mutant cells on heme-agarose did not result in any retention of the Sdh1 truncate on the column (Fig. 1*E*).

C-terminal Segment of Sdh1 Is Critical for Flavinylation—Site-directed mutagenesis was carried out to map the residues responsible for flavinylation and heme-agarose binding. C630A, V633S, or a double P634A,P635A mutation in Sdh1 had no effect of glycerol/lactate growth (Fig. 2*A*). Furthermore, the C630A mutant in the CP motif did not attenuate SDH activity or compromise steady-state protein levels (Fig. 2*B*). Heme-agarose binding was also unaffected (Fig. 2*C*). However, cells harboring a mutant allele of Sdh1 with a R638A substitution were compromised in glycerol/lactate growth (Fig. 2*A*) and SDH activity (Fig. 2*D*). Flavinylation of the mutant Sdh1 was attenuated by ~60% relative to the WT subunit. Assembly of the mutant Sdh1 into the tetrameric complex was not impaired as seen by BN-PAGE (Fig. 2*E*). The R638A mutant Sdh1 retained the ability to associate with the heme-agarose matrix (Fig. 2*F*).

A double C630A,R638A mutant revealed a more impaired phenotype than the single R638A mutant. The double mutant in Sdh1 failed to support SDH assembly of the tetrameric complex (Fig. 2*E*), resulting in a marked drop in steady-state levels of Sdh2 and Sdh3 (Fig. 2*D*). The mutant Sdh1 exhibited no flavinylation, although the mutant Sdh1 was stably expressed. Furthermore, the double mutant failed to associate with the heme-agarose matrix (Fig. 2*F*).

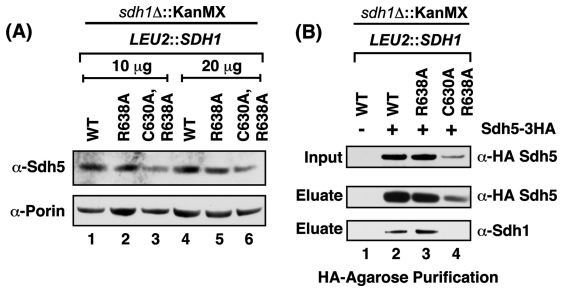

FIGURE 3. **The steady-state level of Sdh5 is diminished in the C630A,R638A double mutant.** *A*, steady-state immunoblot analysis of endogenous Sdh5 from isolated mitochondria from strains expressing chromosomally integrated *SDH1* C-terminal mutants. *B*, immunoprecipitation of HA-tagged Sdh5. Isolated mitochondria from cells expressing exogenous HA-tagged Sdh5 on top of the strains in *A* were solubilized in digitonin and subject to IP. The Sdh1-Sdh5 interaction was analyzed by SDS-PAGE immunoblot analysis of the HA-agarose purification eluate and probed with antibodies to HA (Sdh5) and Sdh1.

Sdh1-Sdh5 Interaction in the Sdh1 C-terminal Mutants—The diminished flavinylation in the C-terminal Sdh1 mutants raised the possibility that the mutations attenuated the known interaction of Sdh1 and Sdh5 that is important in Sdh1 flavinylation. The cellular level of Sdh5 has been observed to be dependent on Sdh1 (11) (*i.e.* Sdh5 is destabilized in cells lacking Sdh1). Steady-state levels of Sdh5 were tested in *sdh1*Δ cells expressing Sdh1 mutant alleles (Fig. 3*A*). A significant diminution in Sdh5 levels was apparent in cells with the double C630A,R638A Sdh1 mutant.

The interaction of Sdh1 and Sdh5 is apparent by co-immunoprecipitation. Mitochondria from cells containing HA-tagged Sdh5 and wild-type Sdh1 were solubilized with digitonin and incubated with anti-HA beads. The immunoprecipitation of Sdh5 led to the co-purification of Sdh1 in the WT as expected (Fig. 3*B*). This was also true with Sdh1 containing the single R638A mutation. Attempts to test binding of Sdh5 to the double C630A,R638A Sdh1 mutant were compromised by the attenuated steady-state levels of Sdh5 in the Sdh1 mutant cells. Although the IP of Sdh5-HA failed to show any Sdh1, the reduction in input Sdh5 makes the absence of Sdh1 in the co-immunoprecipitate difficult to interpret.

We evaluated whether the impaired SDH function observed in *sdh1*Δ cells expressing Sdh1 mutant alleles was suppressed by overexpressing *SDH5* (Fig. 4*A*). Expression of *SDH5* from a low-copy vector in the Sdh1 mutant cells did not significantly increase total Sdh5 levels as measured by immunoblotting with antisera to Sdh5 (data not shown). However, the expression of *SDH5* gave a modest improvement in respiratory growth (Fig. 4*A*) as well as SDH activity (Fig. 4*B*) in cells harboring the R638A mutant Sdh1. Sdh1 flavinylation was also partially elevated by overexpression of Sdh5. The respiratory growth enhancement was not further increased by overexpression of *SDH5* using a high-copy vector (data not shown). In contrast, no rescue was observed in growth or SDH activity of cells containing the double C630A,R638A Sdh1 mutant. The effect of overexpression of Sdh5 in cells with the Sdh1 double mutant actually led to a diminution in SDH activity rather than any restoration.

Isolation of Intragenic SDH1 Suppressors—In the absence of a more marked rescue of the respiratory defect of R638A Sdh1 mutant cells by overexpression of *SDH5*, we isolated genetic suppressors in the mutant cells to gain possible insight into the mechanism underlying the point mutants. In addition to focusing on the R638A mutant, we analyzed a Sdh1 mutant in a second conserved arginine residue (Arg^{582}) that is spatially adjacent to Arg^{638}. The corresponding residue in human SDHA is Arg^{589} and a R589W mutation was reported in a patient afflicted with paraganglioma (24). We generated R582W and R582A mutations in yeast Sdh1 and observed that both substitutions resulted in lack respiratory growth (Fig. 5*A*).

Plating *sdh1*Δ cells expressing either R638A, R589A, or R589W Sdh1 from high-copy plasmids at high density on glycerol/lactate medium resulted in the appearance of papillae that contained mutants proficient in respiratory growth. The suppressors failed to respire in each case when the plasmid expressing the Sdh1 point mutation was shed, suggesting intragenic suppression. Rescue of the plasmid in *Escherichia coli* and retransformation in parent *sdh1*Δ cells resulted in glycerol/lactate growth.

DNA sequencing of the R638A mutant *SDH1* gene revealed a second-site mutation resulting in a G70V substitution. The respiratory competency of the G70V,R638A Sdh1 mutant is shown in Fig. 5*A*. Gly^{70} is located 35 Å from Arg^{638} but is close to the FAD. It is also on the opposite face from the His^{90} that forms the covalent bond (Fig. 5*B*). SDH activity was restored in these second-site mutant cells (Fig. 6*A*).

The cultures used for the studies in Fig. 6 were propagated using a carbon swap protocol in which cultures initially grown in glucose to an $A_{600\ nm} \sim 0.5$ were switched to glycerol/lactate for the last 10 h of the experiment. Under these conditions, even the *sdh1*Δ cells maintained viability during the last phase of growth. Propagation of *sdh1*Δ cells with the R638A Sdh1 mutant on galactose medium rather than the carbon swap protocol resulted in markedly reduced SDH activity as seen in Figs. 2*D* and 4*B*; however, the presence of the G70V,R638A Sdh1 suppressor mutant did not exhibit enhanced SDH activity. The abundance of wild-type and mutant SDH complexes is markedly enhanced in glycerol/lactate medium relative to galactose medium (data not shown).

The genetic suppressor screen carried out with the R582A Sdh1 mutant cells resulted in the recovery of a second site suppressor with a M599R Sdh1 substitution in addition to the original R582A mutation (Fig. 5*A*). Met^{599} is spatially close to Arg^{582} and Arg^{638} (Fig. 5, *C* and *D*). The double R582A,M599R Sdh1 mutant was catalytically active unlike the R582A single mutant (Fig. 6*A*). Steady-state levels of Sdh1, Sdh2, and Sdh3 were restored. The suppressor was able to partially assemble, unlike the $R^{582}A$ single mutant, into a tetrameric SDH complex that could be visualized upon extended exposure of the blue-native immunoblot (Fig. 6*B*). In addition, the double mutant was competent to bind the heme-agarose matrix (Fig. 6*D*). The suppressor mutation resulted in a stabilized Sdh5 polypeptide.

A second site suppressor was also found for the non-functional R582W Sdh1 mutant (Fig. 5*A*). The suppressor mutant consisted of a conversion of the Trp to a Cys residue (Fig. 5*A*).

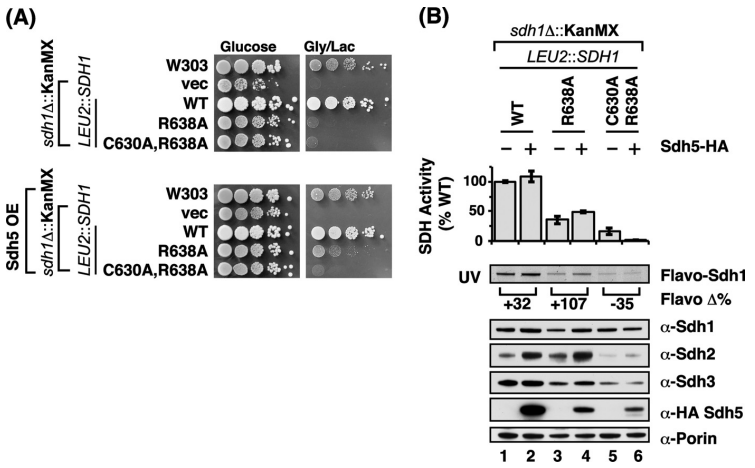

FIGURE 4. **Overexpression of Sdh5 partially restores growth of the single R638A mutant; the double C630A,R638A is unaffected.** Similar effects are observed for steady-state covalent flavinylation and protein levels. *A*, growth test of strains with chromosomally integrated *SDH1* C-terminal point mutants minus (*top panel*) or plus (*bottom panel*) low-copy vector (*vec*) expressing Sdh5. Cells were grown on glucose (fermentable) and glycerol/lactate (non-fermentable) media at 30 °C. *B*, *upper panel*: SDH activities of isolated mitochondria from strains in *A* expressed as a percentage of WT ($n \geq 3 \pm$ S.D.). *Lower panels*: corresponding immunoblot analysis of mitochondria isolated from above strains showing steady-state levels of covalent flavinylation levels (UV illumination) and SDH subunit. The flavoprotein (*Flavo*) Δ% is a relative band density (quantified using ImageJ software) comparison of the Sdh5 overexpressing strain to that of the non-overexpressing strain.

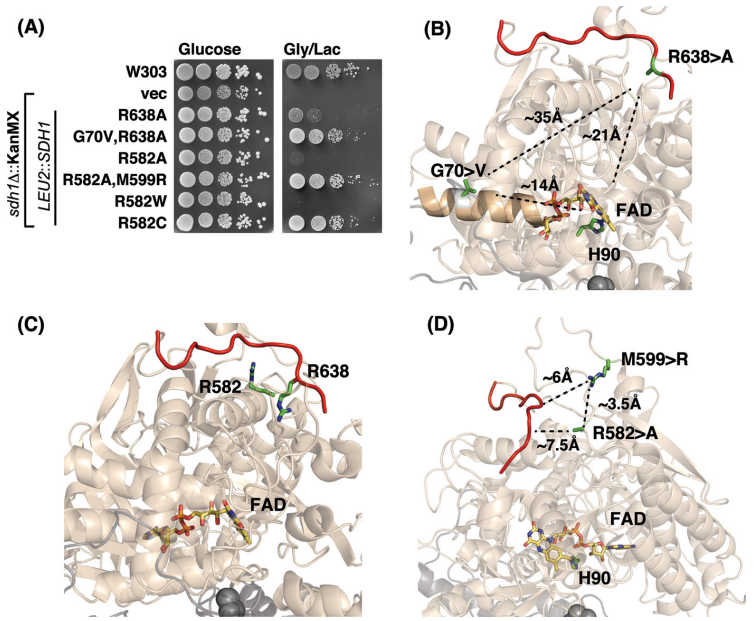

FIGURE 5. **Spontaneous intragenic second-site suppressors of the Sdh1 flavinylation defect shows restoration of growth.** *A*, growth test of intragenic second-site spontaneous suppressors to Sdh1 Arg mutants. The plasmid-borne *SDH1* second site mutations were integrated chromosomally into *sdh1*Δ strains at *LEU2* locus along with the original Arg mutation and tested for growth on fermentable (glucose) and non-fermentable (glycerol/lactate) medium at 30 °C. *B*, PyMOL-generated representation of avian SDH (Protein Data Bank code 2H88) showing the two critical Arg residues that are located on (Arg^{638}) or near (Arg^{582}) the C terminus (*red strand*) that when mutated causes a covalent flavinylation defect. *C*, the second-site mutation G70V that restores the growth defect of the R638A mutation lies on a helix that makes contact with the phosphate group of FAD but lies 35 Å away from the Arg^{638} and 14 Å away from FAD. PyMOL generated representation of avian SDH (Protein Data Bank code 2H88). *D*, the second-site mutation M599R is spatially close to the C-terminal tail (~6 Å) of Sdh1 and to the original R582A (~3.5 Å) mutation. In eukaryotes, the residue corresponding to Met^{599} in yeast has already been replaced to Arg. PyMOL generated figure using avian SDH (Protein Data Bank code 2H88). *vec*, vector.

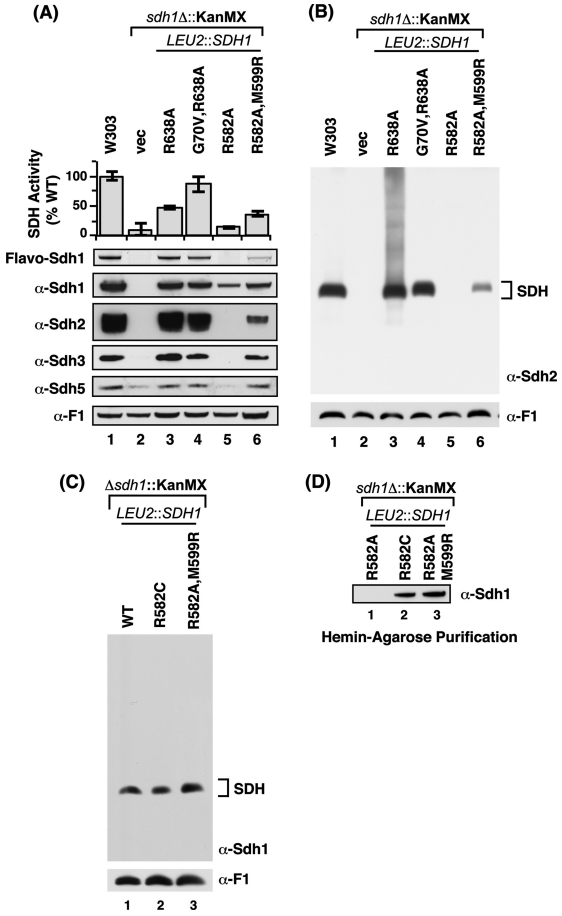

FIGURE 6. **Spontaneous intragenic second-site suppressors of the Sdh1 flavinylation defect restores SDH activity, SDH assembly, and heme binding to Sdh1.** *A*, *upper panel*: SDH activities of isolated mitochondria from strains in Fig. 5*A* expressed as a percentage of WT ($n \geq 3 \pm$ S.D.) when cells were grown initially on 2% glucose and swapped to 2% glycerol/lactate (carbon swap; see "Material and Methods"). *Lower panels*: corresponding immunoblot analysis of mitochondria isolated from above strains showing steady-state levels of covalent flavinylation levels (UV illumination) and SDH subunit. *B*, corresponding blue native immunoblot analysis of mitochondria isolated from strains in *A*. The streaking in *lane 3* (R638A) is likely a result of fractional amounts of soluble aggregates of Sdh2 formed in this mutant background. *C*, BN-PAGE immunoblot analysis of mitochondria isolated from selected strains in *A* but cultured in 2% glycerol/lactate showing the full restoration of complex assembly under respiratory condition for the two spontaneous suppressors (R582C and the double R582A,M599R). *D*, hemin-agarose purification of Sdh1 from isolated mitochondria from selected strains in *C* showing the restored heme-binding to Sdh1 in the spontaneous suppressors (R582C and the double R582A,M599R) but not in the original point mutant (R582A). *Flavo*, flavoprotein; *vec*, vector.

The R582C Sdh1 mutant is active and assembles into the tetrameric complex (Fig. 6*C*) and is capable of adsorption on heme-agarose beads (Fig. 6*D*). Thus, Sdh1 with either an Arg or Cys at sequence position 582 is functional.

Role of FAD in SDH Complex Assembly—The lack of assembly in the R582A and the double C630A,R638A mutant Sdh1 and the lack of Sdh1 flavinylation in those mutants raised the question of whether SDH assembly is dependent on flavinylation. Yeast lacking Sdh5 were reported to be impaired in SDH assembly (11), but cells containing a mutant H90S Sdh1 mutant with a replacement of the histidyl residue forming the covalent FAD adduct was able to assemble into the tetrameric complex (8). We confirmed the latter result; the H90S Sdh1 yeast lacked any observable covalent FAD (Fig. 7*A*), yet it exhibited a tetrameric complex on BN-PAGE (Fig. 7*B*). Although no covalent FAD was seen, Robinson *et al.* (8) reported that FAD was still associated non-covalently with the enzyme. Sdh5 levels were normal in cells containing the H90S mutant Sdh1 (Fig. 7*A*).

In the case of *sdh5*Δ cells, despite no covalent flavinylation (Fig. 7*A*), we observed varying degrees of SDH assembly in multiple independent experiments with three different *sdh5*Δ strains (Fig. 7*C*). This variability occurs within a given deletion strain. The variable assembly states seen by BN-PAGE may imply that the SDH complex is unstable and dissociates under the Coomassie gel conditions. In these mitochondrial lysates, we quantified steady-state Sdh2 and Sdh3 levels to assess the *in vivo* stability of the SDH complex (Fig. 7*D*). The level of Sdh2 correlated with the abundance of the assembled SDH complex. Thus, it appears likely that the complex is destabilized *in vivo* and that an equilibrium exists between assembly and disassembly in which some mutants are more prone to the latter step.

A correlation between SDH assembly and Sdh1 flavinylation is also seen in *flx1*Δ cells. Flx1 is a mitochondrial carrier protein implicated in FAD utilization (23, 25, 26). Sdh1 flavinylation is impaired in yeast lacking the mitochondrial carrier Flx1 (23, 25, 26). Although some uncertainty exists on whether Flx1 functions to import or export FAD from mitochondria, a careful quantitation of matrix FAD levels in *flx1*Δ cells showed a marked diminution (Fig. 7*E*) as was reported previously (23). Steady-state levels of Sdh1 and Sdh2 were markedly attenuated in the *flx1*Δ cells, yet Sdh5 levels were normal (Fig. 7*F*). As expected from the reduced Sdh1 and Sdh2 levels, no assembled SDH was observed on BN-PAGE (data not shown).

Role of Other SDH Subunits in Sdh1 Flavinylation—In the pioneering work of Bernard Lemire on SDH assembly and flavinylation, Sdh1 flavinylation was shown to occur upon mitochondrial import and proteolytic processing of Sdh1. In a pulse-chase study, the flavinylation of Sdh1 was assessed (10) in strains lacking one of the other SDH subunits to assess the dependence of Sdh1 flavinylation on the presence of other subunits (10). Robinson and Lemire (10) reported that Sdh1 flavinylation is independent of the membrane anchor subunits Sdh3 and Sdh4 and partially attenuated in cells lacking Sdh2. We extended their observations and found that steady-state Sdh1 levels were normal in cells lacking Sdh2 and the membrane anchor Sdh3 (Fig. 8*A*). Cells lacking Sdh4, or Sdh3 and Sdh4 double, possess a similar phenotype as cells lacking Sdh3 only (data not shown). Sdh2 steady-state levels were near normal in cells lacking Sdh3, but Sdh2 levels were absent in cells lacking Sdh1. Sdh1 flavinylation was partially depressed in *sdh2*Δ cells. However, flavinylation of Sdh1 occurred normally in *sdh3*Δ (Fig. 8*A*). The Sdh1 and Sdh2 subunits persisting in double *sdh3*Δ,*sdh4*Δ mutant formed a complex as indicated by affinity purification (Fig. 8*B*). Thus, flavinylation of Sdh1 occurs to a limited extent in the absence of other SDH subunits, but Sdh2 is

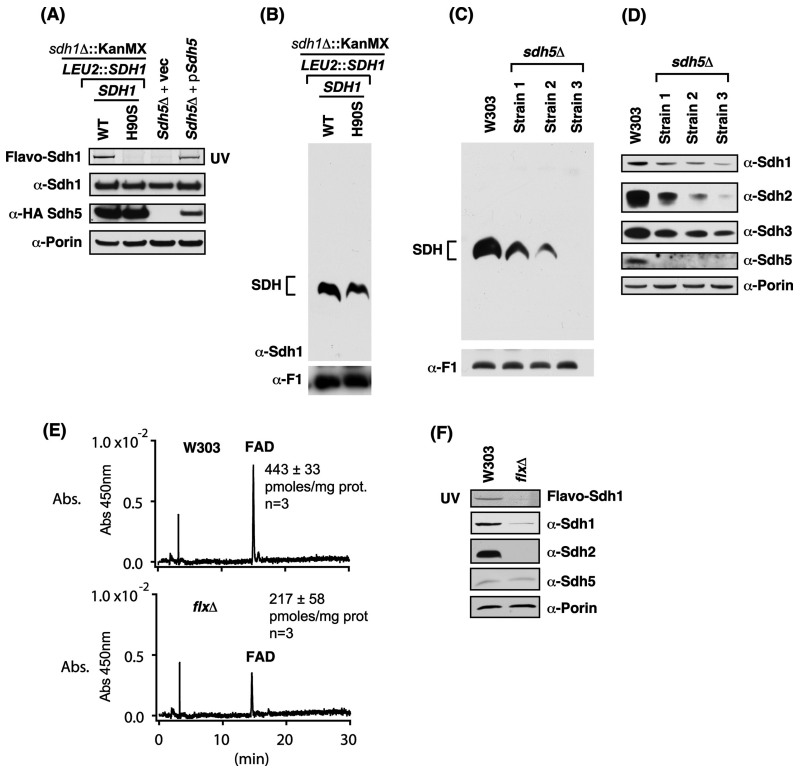

FIGURE 7. **Covalent flavinylation of Sdh1 is not required for assembly of SDH as indicated by *sdh5*Δ and H90S Sdh1 mutants.** However, Sdh1-FAD binding is likely required for stability of Sdh1 and SDH assembly. *A*, steady-state immunoblot analysis of isolated mitochondria from *sdh1*Δ strains expressing either wild type Sdh1 or H90S substitution (*lanes 1* and *2*) and *sdh5*Δ cells transformed with the indicated vectors (*vec*; *lanes 3* and *4*). *B*, corresponding BN-PAGE immunoblot analysis of mitochondria from *A* showing the assembly of SDH even in the absence of covalent flavinylation. *C*, BN-PAGE immunoblot analysis of mitochondria from WT and three different *sdh5*Δ cells showing the assembly of SDH even in the absence of covalent flavinylation. *D*, steady-state immunoblot analysis of isolated mitochondria from *C*. *E*, HPLC analysis of FAD levels in purified mitochondria from WT and *flx*Δ strains showing the ~50% decrease in FAD levels in the *flx*Δ strain. *F*, steady-state SDS-PAGE UV and immunoblot analysis of isolated mitochondria from strains in *E*. Note the dramatic decrease in Sdh1 and the absence of Sdh2 in the *flx*Δ strain likely resulting from the decrease in mitochondrial FAD levels. *Abs.*, absorbance. *prot*, total mitochondrial protein.

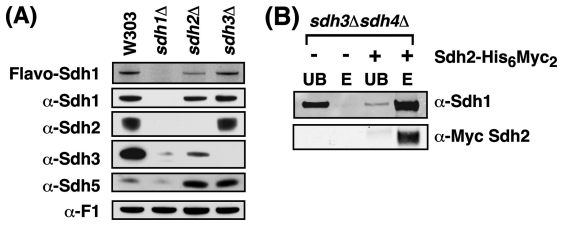

FIGURE 8. **Sdh1 is flavinylated in the absence of the membrane anchor subunits and forms a stable dimeric complex with Sdh2.** *A*, steady-state immunoblot and Sdh1 flavinylation analysis (UV illumination). *B*, nickel-nitrilotriacetic acid purification of Sdh2-His_6Myc_2 in mitochondria isolated from *sdh3*Δ*sdh4*Δ cells. *UB*, unbound; *E*, eluate; *Flavo*, flavoprotein.

important for efficient covalent FAD binding. Interestingly, the Sdh5 steady-state levels were elevated in *sdh2*Δ or *sdh3*Δ cells (Fig. 8*A*).

DISCUSSION

We show presently that flavinylation of the Sdh1 subunit of succinate dehydrogenase is dependent on a set of two spatially close Arg residues near the C terminus, which are distant (>20 Å) from the FAD binding site but are critical in flavinylation. These residues are also important for the assembly of Sdh1 into the tetrameric enzyme complex. Mutant Sdh1 proteins with either a R582A or double C630A,R638A substitution are neither flavinylated nor assembled into the SDH complex (Table 1).

With each mutant Sdh1, second-site Sdh1 suppressor mutations were recovered in Sdh1 permitting both flavinylation and SDH assembly. In the case of the single R638A mutation, the second site suppressor was a G70V substitution, whereas the R582A second site suppressor was a M599R substitution. The presence of the Arg at residue 599 restores a positively charged residue in proximity to residue position 582. It is of interest that the corresponding residue to Met^{599} in humans and metazoans is Arg.

In the human SDHA (Sdh1 equivalent), the Arg residue corresponding to yeast Arg^{582} is Arg^{589}. Substitution of this Arg^{589} to a Trp (R589W) has been reported in a patient afflicted with paraganglioma (24). Yeast harboring a corresponding R582W mutant Sdh1 are compromised in SDH assembly and flavinylation, but a reversion mutant of R582C restores both Sdh1 flavinylation and SDH assembly.

TABLE 1

Molecular properties of strains with mutations or deletions that result in the loss of covalent flavinylation in Sdh1

The double C630A,R638A and the single R582W mutations at or near the C terminus lead to loss of SDH assembly as well as binding to heme-agarose beads. However, mutations or deletions that maintain heme-agarose binding also maintain SDH assembly. ND, not determined.

Strain	Heme binding	SDH assembly	Sdh2 steady-state	Sdh5 steady-state	Sdh1-Sdh5 interaction
H90S	Yes	Yes	Down	Stable	Attenuated
*sdh5*Δ	Yes	Yes	Down		
ClipK	No	No	Absent	ND	ND
C630A,R638A	No	No	Absent	Unstable	Attenuated
R582A	No	No	Absent	Unstable	Attenuated

One major question emerging from the present studies concerns the role of the C-terminal Arg residues in Sdh1 flavinylation. These mutations do not appear to destabilize the Sdh1 polypeptide; rather, they only impair Sdh1 maturation. Three candidate roles for the C-terminal Arg residues may be envisioned. One candidate link involves the binding of Sdh5 and its importance in Sdh1 flavinylation. Sdh5 levels are dependent on the presence of Sdh1. The reduced steady-state levels of Sdh5 in the Sdh1 mutants may reflect attenuated binding. However, cells harboring the mutant Sdh1 alleles are markedly impaired in SDH assembly, whereas *sdh5*Δ cells are only partially attenuated in SDH stability as seen by the variable levels of the assembled SDH complex in our series of isolates. Thus, the phenotypes observed with either the R582A or double C630A,R638A mutants appear distinct from that of *sdh5*Δ cells.

A second scenario is that the flavinylation may occur in a nascent conformation of Sdh1 that is somewhat distinct from the final mature conformation. In this scenario, the C-terminal Arg residues may be in juxtaposition for FAD flavinylation. The G70V second site suppressor mutation in the SDH-deficient R638A Sdh1 mutant is consistent with this postulate of a distinct nascent conformation in which these two residues are now in closer proximity. However, two observations argue against this model. The observation that citric acid cycle intermediates can stimulate the flavinylation process (10) suggests that a flavinylation-competent conformation may have a preformed native-like substrate binding site. The dependence of Sdh2 on efficient Sdh1 flavinylation suggests that the flavinylation-competent conformation of Sdh1 must be quite similar to the final mature fold enabling Sdh2 association. In the flavoprotein vanilly-alcohol oxidase containing a histidyl-linked FAD, structural similarity between the holo- and the apo-forms indicates that FAD and substrate bind to a folded, highly preorganized cofactor/active site cavity, followed by autocatalytic covalent flavinylation (27).

A third candidate role for the C-terminal Arg residues may relate to FAD binding. Although the C-terminal Arg residues are distantly removed from the FAD or substrate site in the mature Sdh1 structure, the Arg residues may be important in recruitment and/or guidance of FAD and or succinate to the substrate site. As mentioned, flavinylation of Sdh1 is dependent on succinate (10).

Another conserved Arg residue (human Arg^{408}) stabilizes succinate or inhibitor binding through two hydrogen bonds. Mutations in the human gene yielding a R408C substitution was reported in a patient with a late onset neurodegenerative disease (28). Engineering the corresponding mutation in the *E. coli* enzyme resulted in impaired covalent flavinylation and the absence of membrane-associated enzyme (28).

The impaired assembly of SDH with the C-terminal Sdh1 mutants suggests that FAD binding is important to stabilize the Sdh1 conformation enabling association with Sdh2 and the membrane anchor subunits. To address the role of FAD binding in SDH assembly, we utilized a yeast *flx1*Δ deletion strain. This mutant was reported to have attenuated levels of matrix FAD levels (23), and we confirmed this observation. Cells lacking Flx1 are known to be deficient in two FAD-containing enzymes SDH and lipoamide dehydrogenase (22). We show the mutant cells are also impaired in SDH assembly and stability of Sdh2. The impaired SDH assembly in the FAD-deficient *flx1*Δ cells suggests that FAD binding is important for Sdh1 maturation enabling assembly of the tetrameric enzyme. Cells containing the H90S Sdh1 mutant that precludes covalent flavinylation assemble into the SDH complex consistent with a non-covalent association of FAD as was reported previously (8).

The covalent addition of FAD to Sdh1 likely occurs in a specific folded conformation of Sdh1 that brings a set of amino acids in juxtaposition for the autocatalytic addition. Sdh5 as well as succinate as a substrate are proposed to stabilize the flavinylation-competent conformation of Sdh1 for the reaction. The conserved C-terminal Arg residues (Arg^{582} and Arg^{638}) could contribute to FAD recruitment and or its binding prior to formation of the covalent attachment. The G70V second site suppressor mutation in the SDH-deficient R638A Sdh1 mutant may merely partially deform the Sdh1 conformation allowing FAD binding in the absence of Arg^{638}. The C-terminal Arg residues may also have a secondary role in the binding of Sdh5.

The propensity of Sdh1 to adsorb onto heme-agarose beads may relate to either a hydrophobic pocket that fortuitously accommodates heme with no physiological consequence of this binding. Alternatively, the presence of the positively charged Arg residues in the C-terminal segment could interact electrostatically with the dianionic propionate groups of heme, facilitating the association of Sdh1 with heme-agarose. This interaction may be analogous to the possible dianionic succinate or phosphates of FAD. Thus, in this scenario, heme is acting merely as a dianionic mimic of FAD or succinate. This notion is supported by the fact that protoporphyrin IX (heme lacking the iron center, but still possessing the dianionic propionates) can compete for heme binding to Sdh1 (results not shown). This observation argues that the iron center is not important for binding to Sdh1. Thus, the increased affinity of Sdh1 to heme in the presence of a reductant may be more related to the reduced state of Sdh1 than the heme iron.

A third less likely scenario is that heme has an effector role in the flavinylation reaction. We have no evidence that SDH biogenesis requires heme for Sdh1 maturation. Because heme is essential for cell survival and important in yeast for Hap1-mediated gene expression of mitochondrial proteins, the investigation of a role of heme in Sdh1 maturation is challenging and will be the topic of future studies.

REFERENCES

1. Sun, F., Huo, X., Zhai, Y., Wang, A., Xu, J., Su, D., Bartlam, M., and Rao, Z. (2005) Crystal structure of mitochondrial respiratory membrane protein complex II. *Cell* **121,** 1043–1057
2. Hägerhäll, C. (1997) Succinate: quinone oxidoreductases. Variations on a conserved theme. *Biochim. Biophys. Acta* **1320,** 107–141
3. Oyedotun, K. S., and Lemire, B. D. (2001) The quinone-binding sites of the *Saccharomyces cerevisiae* succinate-ubiquinone oxidoreductase. *J. Biol. Chem.* **276,** 16936–16943
4. Silkin, Y., Oyedotun, K. S., and Lemire, B. D. (2007) The role of Sdh4 Tyr-89 in ubiquinone reduction by the *Saccharomyces cerevisiae* succinate dehydrogenase. *Biochim. Biophys. Acta* **1767,** 143–150
5. Maklashina, E., Rajagukguk, S., McIntire, W. S., and Cecchini, G. (2010) Mutation of the heme axial ligand of *Escherichia coli* succinate-quinone reductase: implications for heme ligation in mitochondrial complex II from yeast. *Biochim. Biophys. Acta* **1797,** 747–754
6. Tomasiak, T. M., Maklashina, E., Cecchini, G., and Iverson, T. M. (2008) A threonine on the active site loop controls transition state formation in *Escherichia coli* respiratory complex II. *J. Biol. Chem.* **283,** 15460–15468
7. Lemire, B. D., and Oyedotun, K. S. (2002) The *Saccharomyces cerevisiae* mitochondrial succinate:ubiquinone oxidoreductase. *Biochim. Biophys. Acta* **1553,** 102–116
8. Robinson, K. M., Rothery, R. A., Weiner, J. H., and Lemire, B. D. (1994) The covalent attachment of FAD to the flavoprotein of *Saccharomyces cerevisiae* succinate dehydrogenase is not necessary for import and assembly into mitochondria. *Eur. J. Biochem.* **222,** 983–990
9. Hägerhäll, C., Sled, V., Hederstedt, L., and Ohnishi, T. (1995) The trinuclear iron-sulfur cluster S3 in *Bacillus subtilis* succinate:menaquinone reductase; effects of a mutation in the putative cluster ligation motif on enzyme activity and EPR properties. *Biochim. Biophys. Acta* **1229,** 356–362
10. Robinson, K. M., and Lemire, B. D. (1996) Covalent attachment of FAD to the yeast succinate dehydrogenase flavoprotein requires import into mitochondria, presequence removal, and folding. *J. Biol. Chem.* **271,** 4055–4060
11. Hao, H. X., Khalimonchuk, O., Schraders, M., Dephoure, N., Bayley, J. P., Kunst, H., Devilee, P., Cremers, C. W., Schiffman, J. D., Bentz, B. G., Gygi, S. P., Winge, D. R., Kremer, H., and Rutter, J. (2009) SDH5, a gene required for flavination of succinate dehydrogenase, is mutated in paraganglioma. *Science* **325,** 1139–1142
12. Rutter, J., Winge, D. R., and Schiffman, J. D. (2010) Succinate dehydrogenase - Assembly, regulation, and role in human disease. *Mitochondrion* **10,** 393–401
13. McNeil, M. B., Clulow, J. S., Wilf, N. M., Salmond, G. P., and Fineran, P. C. (2012) SdhE is a conserved protein required for the flavinylation of succinate dehydrogenase in bacteria. *J. Biol. Chem.* **287,** 18418–18428.
14. Heuts, D. P., Scrutton, N. S., McIntire, W. S., and Fraaije, M. W. (2009) What's in a covalent bond? On the role and formation of covalently bound flavin cofactors. *FEBS J.* **276,** 3405–3427
15. Longtine, M. S., McKenzie, A., 3rd, Demarini, D. J., Shah, N. G., Wach, A., Brachat, A., Philippsen, P., and Pringle, J. R. (1998) Additional modules for versatile and economical PCR-based gene deletion and modification in *Saccharomyces cerevisiae*. *Yeast* **14,** 953–961
16. Glick, B. S., and Pon, L. A. (1995) Isolation of highly purified mitochondria from *Saccharomyces cerevisiae*. *Methods Enzymol.* **260,** 213–223
17. Diekert, K., De Kroon, A. I., Kispal, G., and Lill, R. (2001) Isolation and subfractionation of mitochondria from the yeast *Saccharomyces cerevisiae*. *Methods Cell Biol.* **65,** 37–51
18. Bradford, M. M. (1976) A rapid and sensitive method for the quantitation of microgram quantities of protein utilizing the principle of protein-dye binding. *Anal. Biochem.* **72,** 248–254
19. Smith, P. K., Krohn, R. I., Hermanson, G. T., Mallia, A. K., Gartner, F. H., Provenzano, M. D., Fujimoto, E. K., Goeke, N. M., Olson, B. J., and Klenk, D. C. (1985) Measurement of protein using bicinchoninic acid. *Anal. Biochem.* **150,** 76–85
20. Schägger, H., and von Jagow, G. (1991) Blue native electrophoresis for isolation of membrane protein complexes in enzymatically active form. *Anal. Biochem.* **199,** 223–231
21. Robinson, K. M., and Lemire, B. D. (1995) Flavinylation of succinate: ubiquinone oxidoreductase from *Saccharomyces cerevisiae*. *Methods Enzymol.* **260,** 34–51
22. Bafunno, V., Giancaspero, T. A., Brizio, C., Bufano, D., Passarella, S., Boles, E., and Barile, M. (2004) Riboflavin uptake and FAD synthesis in *Saccharomyces cerevisiae* mitochondria: involvement of the Flx1p carrier in FAD export. *J. Biol. Chem.* **279,** 95–102
23. Tzagoloff, A., Jang, J., Glerum, D. M., and Wu, M. (1996) FLX1 codes for a carrier protein involved in maintaining a proper balance of flavin nucleotides in yeast mitochondria. *J. Biol. Chem.* **271,** 7392–7397
24. Burnichon, N., Brière, J. J., Libé, R., Vescovo, L., Rivière, J., Tissier, F., Jouanno, E., Jeunemaitre, X., Bénit, P., Tzagoloff, A., Rustin, P., Bertherat, J., Favier, J., and Gimenez-Roqueplo, A. P. (2010) SDHA is a tumor suppressor gene causing paraganglioma. *Hum. Mol. Genet.* **19,** 3011–3020
25. Wu, M., Repetto, B., Glerum, D. M., and Tzagoloff, A. (1995) Cloning and characterization of FAD1, the structural gene for flavin adenine dinucleotide synthetase of *Saccharomyces cerevisiae*. *Mol. Cell. Biol.* **15,** 264–271
26. Giancaspero, T. A., Wait, R., Boles, E., and Barile, M. (2008) Succinate dehydrogenase flavoprotein subunit expression in *Saccharomyces cerevisiae*–involvement of the mitochondrial FAD transporter, Flx1. *FEBS J.* **275,** 1103–1117
27. Fraaije, M. W., van Den Heuvel, R. H., van Berkel, W. J., and Mattevi, A. (2000) Structural analysis of flavinylation in vanillyl-alcohol oxidase. *J. Biol. Chem.* **275,** 38654–38658
28. Birch-Machin, M. A., Taylor, R. W., Cochran, B., Ackrell, B. A., and Turnbull, D. M. (2000) Late-onset optic atrophy, ataxia, and myopathy associated with a mutation of a complex II gene. *Ann. Neurol.* **48,** 330–335

CHAPTER 3

THE LYR FACTORS SDHAF1 AND SDHAF3 MEDIATE MATURATION OF THE IRON-SULFUR SUBUNIT OF SUCCINATE DEHYDROGENASE

Un Na,[*] Wendou Yu,[*] James Cox, Daniel K. Bricker, Knut Brockmann, Jared Rutter, Carl S. Thummel, Dennis R. Winge

[*]Co-first authors

Reprinted with permission from Cell Metabolism

Vol.20, pp.253-266, August 5, 2014

Cell Metabolism
Article

The LYR Factors SDHAF1 and SDHAF3 Mediate Maturation of the Iron-Sulfur Subunit of Succinate Dehydrogenase

Un Na,[1,2,5] Wendou Yu,[3,5,6] James Cox,[2] Daniel K. Bricker,[3] Knut Brockmann,[4] Jared Rutter,[2] Carl S. Thummel,[3] and Dennis R. Winge[1,2,*]
[1]Department of Medicine, University of Utah Health Sciences Center 5C426 School of Medicine, 30 North 1900 East, Salt Lake City, UT 84132-2408, USA
[2]Department of Biochemistry, University of Utah, 15 North Medical Drive East, Salt Lake City, UT 84112-5650, USA
[3]Department of Human Genetics, University of Utah, 15 North 2030 East, Salt Lake City, UT 84112-5330, USA
[4]Departments of Pediatrics and Pediatric Neurology, Faculty of Medicine, University of Göttingen, Robert Koch Strasse 40, 37075 Göttingen, Germany
[5]Co-first authors
[6]Present address: Interdisciplinary Stem Cell Institute, Department of Pediatrics, Leonard M. Miller School of Medicine, University of Miami, Miami, FL 33101, USA
*Correspondence: dennis.winge@hsc.utah.edu
http://dx.doi.org/10.1016/j.cmet.2014.05.014

SUMMARY

Disorders arising from impaired assembly of succinate dehydrogenase (SDH) result in a myriad of pathologies, consistent with its unique role in linking the citric acid cycle and electron transport chain. In spite of this critical function, however, only a few factors are known to be required for SDH assembly and function. We show here that two factors, Sdh6 (SDHAF1) and Sdh7 (SDHAF3), mediate maturation of the FeS cluster SDH subunit (Sdh2/SDHB). Yeast and *Drosophila* lacking SDHAF3 are impaired in SDH activity with reduced levels of Sdh2. *Drosophila* lacking the Sdh7 ortholog SDHAF3 are hypersensitive to oxidative stress and exhibit muscular and neuronal dysfunction. Yeast studies revealed that Sdh6 and Sdh7 act together to promote Sdh2 maturation by binding to a Sdh1/Sdh2 intermediate, protecting it from the deleterious effects of oxidants. These studies in yeast and *Drosophila* raise the possibility that SDHAF3 mutations may be associated with idiopathic SDH-associated diseases.

INTRODUCTION

Succinate dehydrogenase (SDH) is an integral component of both the mitochondrial respiratory chain and the tricarboxylic acid (TCA) cycle. It catalyzes the two-electron oxidation of succinate to fumarate with the reduction of ubiquinone to ubiquinol (succinate:ubiquinone oxidoreductase). SDH is embedded within the inner membrane (IM) of mitochondria and consists of four nuclear-encoded subunits, designated Sdh1 through Sdh4 in yeast and SDHA through SDHD in mammalian cells. SDH deficiency in humans results in infant encephalomyopathy, myopathy, or tumorigenesis in the adult (Finsterer, 2008; Rustin and Rötig, 2002). Loss-of-function mutations in human genes for SDHA, SDHB, SDHC, and SDHD are strongly linked with susceptibility to familial paraganglioma, pheochromocytoma, gastrointestinal stromal tumors, and renal cell carcinoma (Bardella et al., 2011; Baysal et al., 2000; Feichtinger et al., 2010; Janeway et al., 2011). Tumorigenesis arising from SDH deficiency is purportedly related to the deleterious effects of supraphysiological levels of succinate, which is a known inhibitor of a myriad of α-ketoglutarate (αKG)-dependent enzymes, including prolyl hydroxylases, histone, and DNA demethylases (Selak et al., 2005; Xiao et al., 2012).

This tetrameric enzyme contains five redox cofactors, including a covalently bound FAD and three iron-sulfur (FeS) clusters in a hydrophilic segment consisting of two subunits (Sdh1 and Sdh2) and a heme-containing membrane anchor domain consisting of Sdh3 and Sdh4 subunits (Robinson and Lemire, 1996). The FeS clusters facilitate electron transfer to the ubiquinone-binding site formed between Sdh2 and the membrane subunits (Sun et al., 2005).

Assembly factors are often used to facilitate cofactor insertion in mitochondrial respiratory complexes and mitigate unwanted reactions during biogenesis. Recently, two SDH assembly factors associated with human pathogenesis were identified. Succinate dehydrogenase assembly factor 1 (SDHAF1) was found in a study of infantile mitochondrial diseases in which two families had multiple children afflicted with leukoencephalopathy (Ghezzi et al., 2009). Biochemical analyses revealed a SDH deficiency in muscle samples and fibroblasts from these patients along with missense mutations in SDHAF1. Deletion of the yeast ortholog of *SDHAF1* (*SDH6*) resulted in a respiratory deficiency and a specific reduction in SDH activity (Ghezzi et al., 2009). SDH deficiency has subsequently been reported in other patients that carry *SDHAF1* mutations (Ohlenbusch et al., 2012). Succinate dehydrogenase assembly factor 2 (SDHAF2 or yeast Sdh5) was shown to be required for the covalent attachment of FAD to the catalytic SDHA (Sdh1) subunit (Hao et al., 2009). Yeast lacking Sdh5 were respiratory deficient due to an absence of SDH activity. Germline loss-of-function mutations in *SDHAF2*

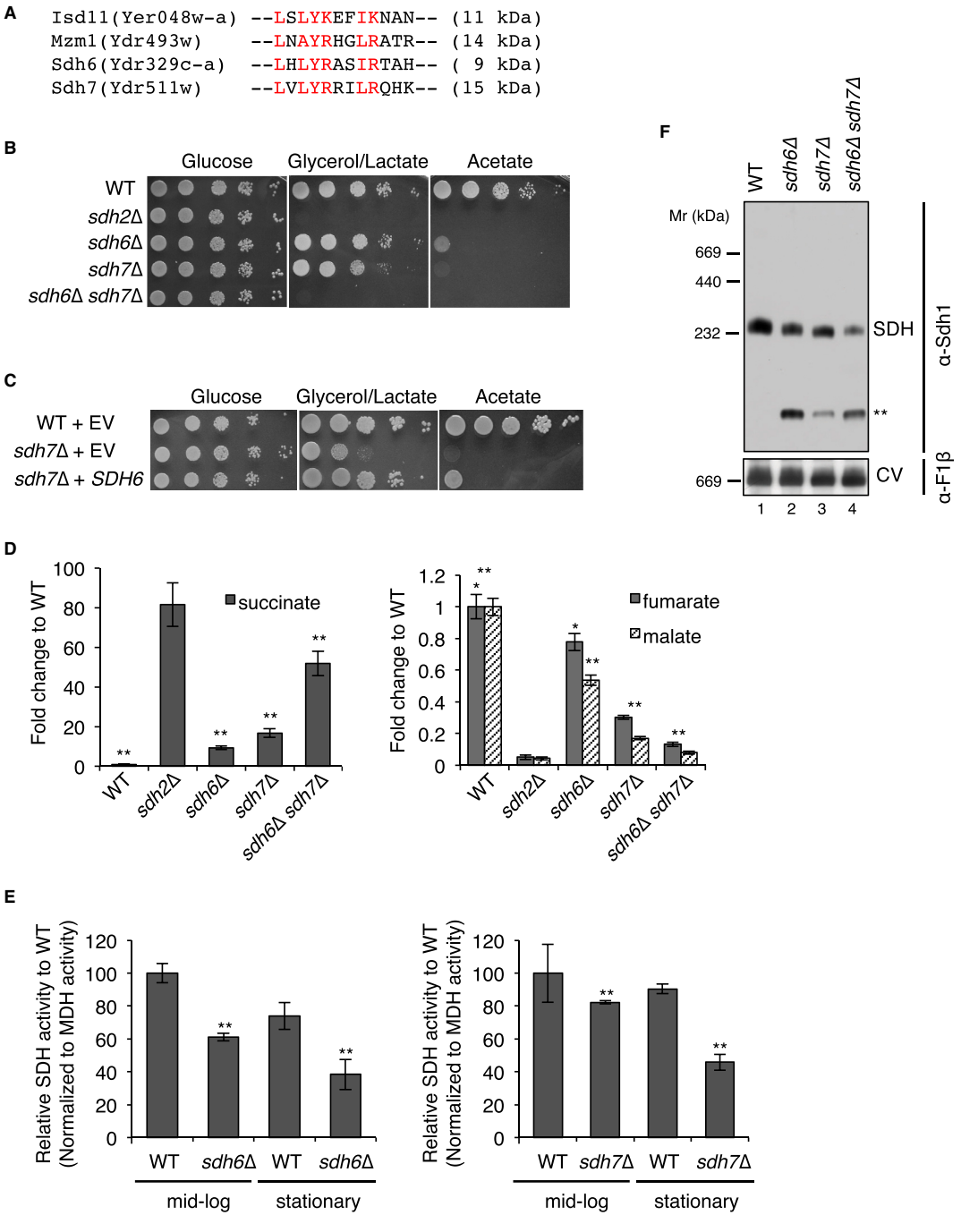

(legend on next page)

were identified in SDH-deficient neuroendocrine paraganglioma tumors (Hao et al., 2009). A number of SDH-deficient pathologies, including Leigh syndrome, gastrointestinal stromal tumors, and neuroblastomas, have also been reported that lack mutations in known SDH assembly factors or SDH structural subunits (Feichtinger et al., 2010; Janeway et al., 2011). Thus, additional SDH assembly factors may remain to be discovered, potentially providing insights into the causes of idiopathic SDH-associated diseases.

Sdh6 is a member of the LYR protein family that consists of ten proteins in the human proteome and four in the yeast proteome (Figure 1A). Within yeast, the founding member is the mitochondrial Isd11 protein that functions in the matrix FeS biogenesis pathway as an effector of the Nfs1 cysteine desulfurase (Adam et al., 2006; Wiedemann et al., 2006). We demonstrated that a second LYR protein Mzm1 is a chaperone for the Rieske FeS subunit of complex III (Atkinson et al., 2011; Cui et al., 2012). The remaining yeast LYR proteins are Sdh6 and Acn9 (human ortholog ACN9). Although Sdh6 is required for proper SDH activity, its molecular mechanism remains unknown. Moreover, Acn9 (designated Sdh7 in yeast and SDHAF3 in humans and flies) has no known function. Here we show that these two factors are required for SDH biogenesis in eukaryotes. Both Sdh6 and Sdh7 protect Sdh2 maturation from the deleterious effects of endogenous reactive oxygen species. We also report that loss of *SDHAF3* in *Drosophila* cells leads to a marked SDH deficiency analogous to that in yeast, with defects in muscular and neuronal function in mutant flies. This study identifies functions of two SDH assembly factors, providing a more complete understanding of its critical role in cellular energy production and a potential molecular framework for defining currently idiopathic SDH-associated diseases.

RESULTS

Cells Lacking Sdh6 and Sdh7 Exhibit SDH Deficiency

As a first step toward characterizing Sdh6 and Sdh7 function, we examined the growth phenotypes of *sdh6*Δ or *sdh7*Δ mutants on nonfermentable carbon sources using *S. cerevisiae*. Compared to wild-type cells, cells lacking Sdh6 or Sdh7 exhibited a partial growth defect on glycerol/lactate medium and a severe growth defect on acetate medium (Figure 1B), which is consistent with previous studies (Ghezzi et al., 2009; McCammon, 1996). We confirmed that the respiratory growth defects of *sdh6*Δ and *sdh7*Δ mutants were attributed to deletions of *SDH6* and *SDH7*, as respiratory growth of *sdh6*Δ and *sdh7*Δ cells was restored with epitope-tagged Sdh6 and Sdh7, respectively (Figure S1A, available online). Since both Sdh6 and Sdh7 belong to the LYR motif protein family (Figure 1A), we looked for genetic interactions between their encoded proteins. The *sdh6*Δ *sdh7*Δ double-deletion strain exhibited a marked synthetic growth defect on glycerol/lactate medium (Figure 1B). In addition, the overexpression of *SDH6* partially suppressed the respiratory growth defect of *sdh7*Δ cells (Figure 1C); however, overexpression of *SDH7* failed to restore respiratory function of *sdh6*Δ cells.

Metabolomic profiling was used to identify the biological process impaired in *sdh6*Δ and *sdh7*Δ mutants, assaying the levels of approximately 100 polar metabolites. We cultured cells in synthetic minimal medium with 2% raffinose and 0.2% glucose to stationary phase. Metabolites extracted from cells were analyzed using gas chromatography-mass spectrometry (GC-MS) (Figure 1D). Cells lacking either Sdh6 or Sdh7 exhibited elevated succinate levels and attenuated fumarate and malate levels, consistent with impaired conversion of succinate to fumarate by SDH in the citric acid cycle. These observations in *sdh6*Δ cells are consistent with the previous study in fibroblasts harboring a mutated *SDHAF1* gene (Ghezzi et al., 2009). Moreover, the *sdh6*Δ *sdh7*Δ double mutant showed an enhanced accumulation in succinate, consistent with the synergistic respiratory growth defects in these cells.

To confirm that the increased succinate/fumarate ratio in *sdh7*Δ mutants was due to impaired SDH function, we quantified SDH activity in mitochondria purified from wild-type (WT) and mutant cells lacking Sdh6 or Sdh7. Mitochondria isolated from *sdh6*Δ and *sdh7*Δ cells harvested at mid-log phase exhibited modest diminutions of SDH activity, but the deficit was magnified in stationary-phase cells (Figure 1E). The *sdh6*Δ *sdh7*Δ double mutant showed markedly decreased SDH activity in mid-log cultures (34% of WT; Figure S1B) relative to the single mutants, in accordance with the synergistic respiratory growth defect and TCA cycle intermediates in *sdh6*Δ *sdh7*Δ double mutants. Enzymatic activities of pyruvate dehydrogenase, α-ketoglutarate dehydrogenase, aconitase, malate dehydrogenase, and bc_1 complex III were unaffected in cells lacking Sdh6 or Sdh7 (Figures S1B and S1C).

A moderate diminution of the assembled tetrameric SDH complex was seen in mitochondria isolated from late-log cultures of *sdh6*Δ or *sdh7*Δ mutants as visualized by blue native (BN)-PAGE (Figure 1F). The abundance of the SDH complex was further

Figure 1. Succinate Dehydrogenase Deficiency in Cells Lacking Two LYR Motif Family Proteins, Sdh6 and Sdh7

(A) LX(L/A)YRXX(L/I)(R/K) motif conserved in four LYR motif family proteins in yeast. Isd11, a chaperone required for cysteine desulfurase activity in FeS biogenesis pathway (Adam et al., 2006); Mzm1, a protein facilitating the Rieske FeS protein insertion into bc_1 (Cui et al., 2012); Sdh6 (SDHAF1); and Sdh7.

(B) Serial dilutions (10-fold) of cells starting from optical density 600 (OD_{600}) = 0.5 were spotted on synthetic complete (SC) media containing different carbon sources, as indicated, and incubated at 30°C.

(C) Serial dilutions (10-fold) of cells were spotted on SC media lacking uracil and incubated at 30°C. EV, empty vector.

(D) Metabolites extracted from cells cultured in synthetic minimal media containing 2% raffinose/0.2% glucose were analyzed using GC-MS. Cells were harvested at OD_{600} = 2. Relative levels of metabolites to WT are represented as mean ± SEM (n ≥ 4 biological replicates; *p < 0.05; **p < 0.005).

(E) Relative SDH activity in isolated mitochondria compared to WT. Mitochondria were isolated from cells grown in SC media plus 2% raffinose/0.2% glucose for 24 hr (mid-log) and 48 hr (stationary). Data are shown as mean ± SD (n = 3; **p < 0.05).

(F) Blue native (BN)-PAGE analysis to visualize protein complexes. Mitochondria isolated from the strains harvested at late-log phase were solubilized with 1% digitonin. After clarification, soluble fractions were separated on BN-PAGE and then transferred to membranes for immunoblotting. Sdh1, a FAD-containing subunit of SDH; F1β, a subunit of ATP synthase (complex V, CV) in oxidative phosphorylation. The band highlighted by ** is the Sdh1 assembly intermediate. This band is visualized by antisera to Sdh1, but not Sdh2. See also Figures S1 and S2.

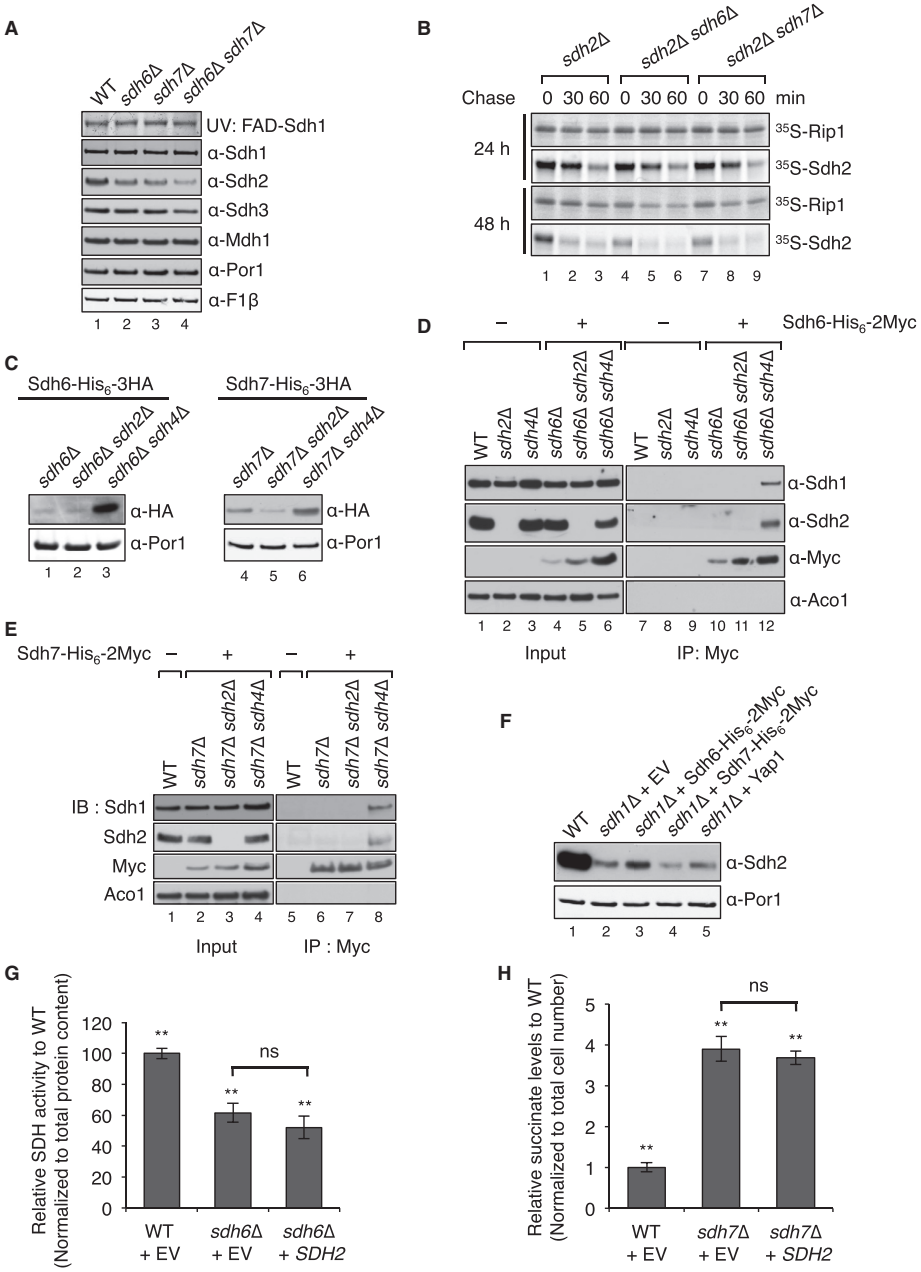

Figure 2. Sdh6 or Sdh7 Functions Are Linked to the Fe/S Sdh2 Subunit

(A) FAD-containing Sdh1 was visualized by UV excitation. Other proteins visualized by immunoblotting include Mdh1 (malate dehydrogenase) and Por1 (porin) (loading control).

(B) ^{35}S-methionine-labeled proteins were incubated with isolated mid-log versus stationary phase mitochondria for 30 min (pulse), followed by blocking protein import with valinomycin for 30 and 60 min (chase), respectively. Radiolabeled proteins were resolved on SDS-PAGE and detected by autoradiography.

(legend continued on next page)

attenuated in *sdh6*Δ *sdh7*Δ double-mutant cells. Thus, Sdh6 and Sdh7 are required to maintain normal SDH levels and activity in yeast. In addition to reduced levels of tetrameric SDH in the mutant cells, a Sdh1 subcomplex is evident, and the same subcomplex is seen in cells lacking Sdh2 or Sdh4 (** in Figures 1F and S2). Therefore, Sdh6 and Sdh7 appear to function in SDH assembly rather than in the regulation of SDH activity.

Maturation of Sdh2 Is Impaired in the Absence of Sdh6 or Sdh7

To characterize the roles of Sdh6 and Sdh7, the steady-state levels of SDH subunits were quantified in mitochondria isolated from mutant cells. The levels of Sdh2 were attenuated in both *sdh6*Δ and *sdh7*Δ mutants and further diminished in the *sdh6*Δ *sdh7*Δ double mutant (Figure 2A). In contrast, Sdh1 levels were unchanged in the mutant cells, and covalent flavinylation of Sdh1 was not significantly altered (Figure 2A). Cells lacking Sdh5 are compromised in Sdh1 flavinylation, leading to a reduced stability of Sdh1 (Hao et al., 2009; Kim et al., 2012).

A mitochondrial in vitro protein import assay was used to address a role for Sdh6 and Sdh7 in Sdh2 maturation. The import assay consisted of the in vitro import of ^{35}S-methionine-labeled Sdh2 into purified mitochondria isolated from *sdh2*Δ cells. Sdh2-deficient mitochondria were used to ensure that a pool of unassociated Sdh1 would be available for a stabilizing interaction with imported Sdh2. Furthermore, the use of *sdh2*Δ cells negates any changes in the mitochondrial membrane potential (which drives protein import) by the loss of Sdh6 or Sdh7. The stability of ^{35}S-Sdh2 as monitored during the chase phase of the reaction was compromised in cells lacking Sdh6 or Sdh7, especially in mitochondria isolated from stationary-phase cultures (Figure 2B). This result is consistent with the exacerbated defect in SDH activity seen in mutant cells at late stages of growth. Unlike Sdh2, radioisotope-labeled Rip1, a target of the LYR protein Mzm1, remained unaffected by loss of either Sdh6 or Sdh7.

Sdh1 and Sdh2 accumulate in cells lacking the membrane anchor subunits Sdh3 and/or Sdh4 (Figure S3A) (Kim et al., 2012). We observed that cells depleted of the membrane anchor contain increased steady-state levels of both Sdh6 and Sdh7 (Figure 2C). These results suggest that Sdh6 and Sdh7 may form stalled preassembly intermediates with Sdh1 and/or Sdh2. We performed coimmunoprecipitation on epitope-tagged Sdh6 and Sdh7 in mitochondria from WT cells and cells stalled in SDH assembly. A fraction of Sdh1 and Sdh2 was copurified with either Sdh6 or Sdh7 from cells lacking the membrane anchor domain, but not in cells devoid of Sdh2 (Figures 2D, 2E, and S3B). These interactions are seen in the presence and absence of crosslinking prior to resin adsorption. These results suggest that Sdh6 and Sdh7 interact with Sdh2 within a Sdh1/Sdh2 subcomplex, which is known to accumulate in cells lacking the membrane anchor domain (Kim et al., 2012). Moreover, these interactions appear to occur in the mitochondrial matrix, consistent with the known matrix location of Sdh1, Sdh2, and Sdh6 (Ghezzi et al., 2009). Sdh7 is also a matrix protein, as revealed by proteinase K treatment of purified mitochondria, which degrades Sdh7 only in the presence of detergents and not upon hypotonic disruption of only the outer membrane. (Figure S3C).

The physical interactions of Sdh6 and Sdh7 with Sdh2 prompted the hypothesis that Sdh6 and Sdh7 may be chaperones for Sdh2. To test this, we first examined the ability of overexpressed Sdh6 or Sdh7 to stabilize the highly labile Sdh2 present in *sdh1*Δ cells (Kim et al., 2012). Elevated levels of Sdh6, but not Sdh7, led to increased steady-state Sdh2 levels under these conditions (Figure 2F). This result raised a possibility that Sdh6 may function as a chaperone for Sdh2 prior to its interaction with Sdh1. We tested whether *SDH2* overexpression in *sdh6*Δ mutants or *sdh7*Δ mutants would restore SDH activity and suppress the respiratory growth defects. However, *SDH2* overexpression neither restored SDH activity nor reversed succinate accumulation or rescued respiratory growth of *sdh6*Δ mutants and *sdh7*Δ mutants (Figures 2G, 2H, S4A, and S4B).

Once a holo-Sdh2/Sdh1 complex forms, the final step in SDH biogenesis is the addition of the Sdh3/Sdh4 membrane anchor. To address whether Sdh6 and Sdh7 are involved in the recruitment of the membrane anchor, we tested whether co-overexpression of *SDH3* and *SDH4* would suppress the respiratory defect in the *sdh6*Δ and *sdh7*Δ mutant cells. No restoration of growth on acetate medium was observed with elevated cellular levels of Sdh3 and Sdh4 (Figures S4C and S4D). Thus, Sdh6 and Sdh7 do not likely facilitate the recruitment of the Sdh3/Sdh4 membrane anchor.

We conducted a series of studies to assess whether Sdh6 or Sdh7 has an active role in FeS cluster insertion. These studies failed to reveal a direct role of either factor in FeS cluster insertion. First, affinity purification of Sdh2 in yeast leads to copurification of Nfu1, Isu1, and Isa2, three key matrix proteins involved in FeS biogenesis (data not shown). However, affinity purification of Sdh6-His$_6$-2Myc or Sdh7-His$_6$-2Myc failed to adsorb Isu1 or Isa2, whereas Sdh2 was associated. Second, whereas overexpression of *ISA1* or *ISA2* restores respiratory growth in *grx5*Δ

(C) Sdh6-His$_6$-3HA or Sdh7-His$_6$-3HA under their own endogenous promoters was expressed from plasmids in cells lacking either Sdh2 or Sdh4, along with endogenous Sdh6 or Sdh7 depleted, respectively. Steady-state levels are shown by immunoblotting.
(D) Coimmunoprecipitation of Sdh6-His$_6$-2Myc after crosslinking. Mitochondria were solubilized with 1% digitonin in the presence of 1 mM dithiobis(succinimidylpropionate). The crosslinking reaction was stopped with Tris buffer (pH 7.4), and the supernatants were absorbed to anti-Myc antibody-conjugated magnetic beads. Bound substances to Myc beads were resolved on SDS-PAGE and detected by immunoblotting. Input, 4% of total lysates; Aco1, FeS aconitase.
(E) Standard coimmunoprecipitation of Sdh7-His$_6$-2Myc was performed with isolated mitochondria without crosslinking. Input, 2% of total lysates.
(F) Steady-state levels of Sdh2 in *sdh1*Δ mutants with overexpression of proteins indicated. Yap1, transcription factor upregulating oxidative stress response genes.
(G) SDH activity in *sdh6*Δ mutants with *SDH2* overexpression was detected as described in Figure 1E. Data are represented as mean ± SD (n = 3; **$p < 0.05$; ns, not significant).
(H) Succinate levels in *sdh7*Δ mutants with *SDH2* overexpression were measured as described in Figure 1D. Mean ± SEM is shown (n = 6; **$p < 0.05$; ns, not significant). See also Figure S3.

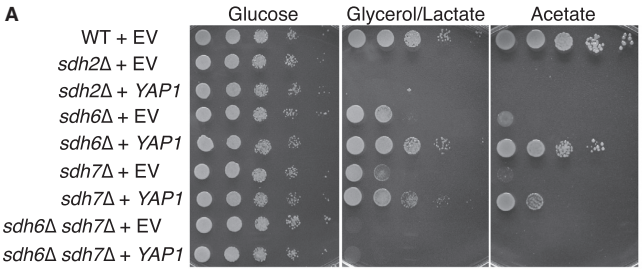

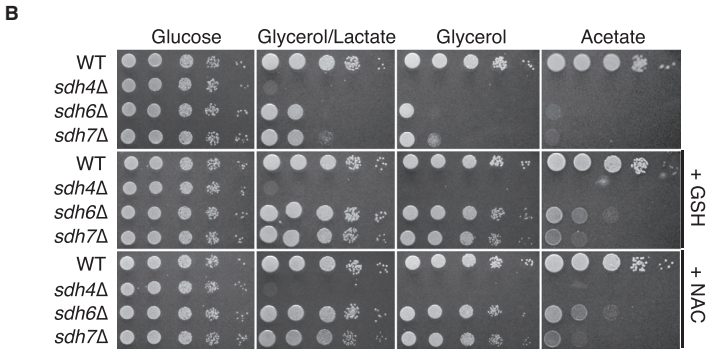

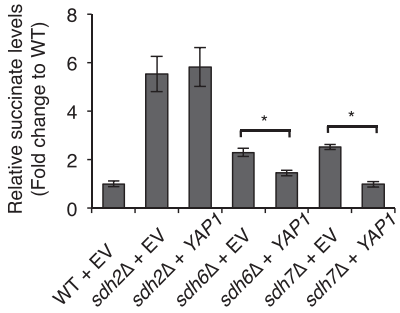

Figure 3. Exogenous Antioxidants Rescue the Growth Defect of *sdh6*Δ and *sdh7*Δ Mutants

(A) Cells harboring either empty vector (EV) or high-copy *YAP1* plasmid were spotted on SC media lacking leucine by 10-fold serial dilutions and incubated at 30°C.

(B) Serial dilutions (10-fold) of cells were spotted on SC medium with the indicated carbon sources with or without 5 mM N-acetylcysteine or 2 mM glutathione and incubated at 30°C.

(C) Succinate levels in cells overexpressing *YAP1* were measured as described in Figure 1D. Cells were harvested at OD_{600} = 1. Mean ± SEM is shown (n = 6; *p < 0.005).

mutant cells (Kim et al., 2010; Rodríguez-Manzaneque et al., 2002), overexpression of *ISA1*, *ISA2*, *NFU1*, or *ISU1* failed to suppress the respiratory defect of *sdh6*Δ or *sdh7*Δ cells (data not shown). Third, ^{55}Fe incorporation into Sdh2-His_6-2Myc was quantified in cells either containing or lacking Sdh6 or Sdh7. Immunocapture of Sdh2 failed to show any clear diminution in ^{55}Fe in the mutant cells (Figure S4E). However, interpretation of the ^{55}Fe study is complicated, since Sdh2 has three distinct FeS centers, and Sdh6 or Sdh7 may have a restricted role with one cluster. In addition, ascorbate is used during ^{55}Fe labeling and, as a reductant, may mimic the exogenous reductants in suppressing the defects in the mutant cells.

Antioxidants Ameliorate Defects in *sdh6*Δ Mutants and *sdh7*Δ Mutants

Further clues to the function of Sdh6 emerged from a genetic suppressor study in which extragenic suppressors of the acetate growth defect of *sdh6*Δ mutants were recovered. We generated a high-copy plasmid library with partially digested genomic DNA from *sdh6*Δ mutants. This library was transformed to *sdh6*Δ mutants, and the transformants that exhibited enhanced growth on acetate medium were collected. Interestingly, multiple independent suppressors were recovered that encoded Yap1, which is a transcriptional activator that induces the expression of a battery of antioxidant genes, including thioredoxin, thioredoxin reductase, and glutathione reductase, in response to oxidative stress (Fernandes et al., 1997). The overexpression of *YAP1* in subcloned vectors robustly suppressed the acetate growth defect of cells lacking Sdh6 (Figure 3A). Consistent with the antioxidant role of Yap1 expression, supplemental glutathione or N-acetylcysteine also restored limited respiratory growth in *sdh6*Δ mutants (Figure 3B).

Since we observed a genetic interaction between *SDH6* and *SDH7* (Figure 1), we tested whether overexpression of *YAP1* could also restore respiratory growth in *sdh7*Δ mutants. Indeed, *YAP1* overexpression suppressed the respiratory growth defect of *sdh7*Δ mutants, although the suppression was less pronounced compared to *sdh6*Δ mutants (Figure 3A). Moreover, the addition of exogenous reductants restored limited respiratory growth of *sdh7*Δ mutants (Figure 3B). To confirm that *YAP1* overexpression restored SDH activity in *sdh6*Δ and *sdh7*Δ single-mutant cells, we assessed SDH activity by measuring succinate levels using metabolomics. Indeed, *YAP1* overexpression decreased succinate levels in both *sdh6*Δ and *sdh7*Δ mutants significantly, while *YAP1* overexpression did not affect succinate levels in *sdh2*Δ mutants as a negative control (Figure 3C).

Therefore, we conclude that *YAP1* overexpression contributes to the restoration of SDH activity in *sdh6*Δ and *sdh7*Δ mutants. Elevated levels of Yap1, however, have no effect on the respiratory growth defects in *sdh6*Δ *sdh7*Δ double mutants (Figure 3A).

Sdh2 Is Stabilized by Sdh6 and Sdh7 under Oxidative Stress Conditions

We hypothesized that Sdh6 and Sdh7 may be important for SDH maturation under oxidative stress conditions. Initially, we tested whether cells lacking Sdh6 or Sdh7 were hypersensitive to the superoxide anion generator paraquat. The respiratory growth defect of *sdh6*Δ and *sdh7*Δ single mutants was dramatically exacerbated in the presence of paraquat (Figure 4A). Likewise, steady-state levels of Sdh2 were markedly attenuated in paraquat-treated *sdh6*Δ and *sdh7*Δ mutants compared to WT cells (Figure 4B). In contrast, steady-state levels of other mitochondrial FeS containing proteins were not significantly altered by paraquat in the mutant cells (Figure 4B).

The paraquat sensitivity of *sdh6*Δ and *sdh7*Δ mutants may arise from either enhanced ROS damage or the accumulation of a pro-oxidant in the mutants. We observed that ROS levels were not changed in untreated *sdh6*Δ and *sdh7*Δ mutants using two different assays. First, we quantified aconitase (Aco1) activity. The 4Fe-4S cluster in aconitase is susceptible to ROS damage (Gardner, 2002); thus, aconitase activity is an indicator of ROS stress in vivo. No diminution of aconitase activity was seen in *sdh6*Δ and *sdh7*Δ mutants compared to WT (Figure 4C). Second, we tested the mutant cells for hydrogen peroxide sensitivity on rich glucose medium. As cells accumulate ROS, they become sensitized to exogenous ROS and subsequently lose viability (Khalimonchuk et al., 2007). After 2 hour treatment of cells with 6 mM H_2O_2, the viability of *sdh2*Δ, *sdh3*Δ, and *sdh4*Δ mutant strains was significantly compromised (Figure 4D). However, *sdh6*Δ and *sdh7*Δ mutant cells exhibited no growth defects. The lack of impairment in aconitase activity and hydrogen peroxidase sensitivity suggest that ROS levels are not elevated in *sdh6*Δ and *sdh7*Δ mutants as compared to WT cells. It is notable that *sdh1*Δ and *sdh5*Δ single mutants and the *sdh4*Δ *sdh5*Δ double mutant did not show hydrogen peroxide sensitivity compared to *sdh2*Δ, *sdh3*Δ, and *sdh4*Δ strains, which suggests that an assembly intermediate containing FAD-Sdh1 may be the source for electron leakage for the generation of ROS in *sdh2*Δ, *sdh3*Δ, and *sdh4*Δ single mutants.

The observed hypersensitivity of *sdh6*Δ and *sdh7*Δ mutant cells to paraquat may imply that Sdh6 and Sdh7 are shielding the FeS clusters in Sdh2 prior to full assembly. Superoxide inactivation of the 4Fe-4S center in aconitase leads to a dissociation of one iron ion forming an inactive 3Fe-4S center that can be reactivated by supplemental iron salts (Gardner and Fridovich, 1992). We tested whether supplemental iron salts would restore respiratory function to *sdh6*Δ and *sdh7*Δ mutant cells. Supplemental $FeCl_2$, but not $ZnCl_2$, restored limited glycerol growth to both mutant cells (Figure 4E). These data are consistent with a candidate role of Sdh6 and Sdh7 in FeS cluster protection in SDH maturation.

Drosophila Sdhaf3 Mutants Are Sensitive to Oxidative Stress

The *Drosophila* genome encodes a close ortholog of Sdh7 (Figure S5A) but has only a weak candidate homolog of Sdh6. Accordingly, we examined the functions of Sdh7 in *Drosophila* to determine if its roles in SDH assembly and activity have been conserved through evolution and to define its possible physiological functions. Gene targeting was used to generate a null mutation in the *Drosophila sdh7* ortholog (*CG14898*), which we refer to here as *dSdhaf3* (Figures S5B and S5C). These mutants were outcrossed for six generations to w^{1118}, which was used as a control for most studies. *dSdhaf3* mutants progress normally through development and have a normal lifespan when maintained on standard growth media. These animals are, however, sensitive to ethanol (Figure 5A) and oxidative stress, resulting from either paraquat treatment (Figure 5B) or hyperoxia (Figure 5C). The response to hyperoxia is most pronounced, with a 50% reduction in lifespan relative to controls, although $SdhB^{12081}$ hypomorphic mutants display a more severe effect (Walker et al., 2006). Interestingly, most *dSdhaf3* mutants exposed to 100% oxygen for 4 days held their wings erect, a hallmark of mitochondrial dysfunction and muscle degeneration (DeSimone et al., 1996; Greene et al., 2003). A similar abnormal wing posture was observed in $SdhB^{12081}$ mutants maintained under normal conditions (10%–15%) or exposed to hyperoxia (80%–100%).

dSdhaf3 Mutants Display Reduced SdhB Protein Levels and SDH Activity

If the function of *dSdhaf3* has been conserved through evolution, then *dSdhaf3* mutants should display a specific defect in SDH function. Consistent with this possibility, metabolomic profiling of *dSdhaf3* mutants revealed elevated succinate and reduced levels of fumarate and malate (Figure 5D). Biochemical analysis of mitochondrial extracts from *dSdhaf3* mutants demonstrated that *dSdhaf3* mutants have normal levels of SdhA, but significantly reduced levels of SdhB (Figure 5E), resulting in an approximate 50% reduction in SDH enzymatic activity (Figures 5F and 5G), similar to the phenotypes of *sdh7*Δ yeast. SdhA is also flavinylated normally in *dSdhaf3* mutants, as expected (Figure S5E). Combining the hypomorphic $SdhB^{12081}$ allele with the *dSdhaf3* mutation resulted in a dramatic decrease in viability, demonstrating a strong genetic interaction, consistent with the reduced levels of SdhB in *dSdhaf3* mutants and confirming the functional interaction between dSdhaf3 and SDH (Figure S6A).

Interestingly, although *dSdhaf3* mutants are fully viable and fertile, they display a clear age-dependent reduction in movement (Figure 5H). While mutants at 1 week of adult life show no difference in motility relative to controls, mutants display an approximately 50% reduction in movement by 2 weeks of age and a more severe motility defect at later stages (Figure 5H). Mutants are also significantly more sensitive to paralysis by 2 weeks of age, relative to controls (Figure S5F). Thus, like its counterpart in yeast, dSdhaf3 is required to maintain normal SDH levels and activity and proper wing muscle function and motility in *Drosophila*.

Antioxidant and Genetic Rescue of *dSdhaf3* Mutants

Consistent with the ability of antioxidants to suppress the growth defects in *sdh7*Δ yeast mutants, either a dietary (N-acetylcysteine) or genetic (Sod2 expression) reduction in oxidative stress rescued the hyperoxia sensitivity of *dSdhaf3* mutants (Figures 6A and 6B). Unlike the yeast studies, however,

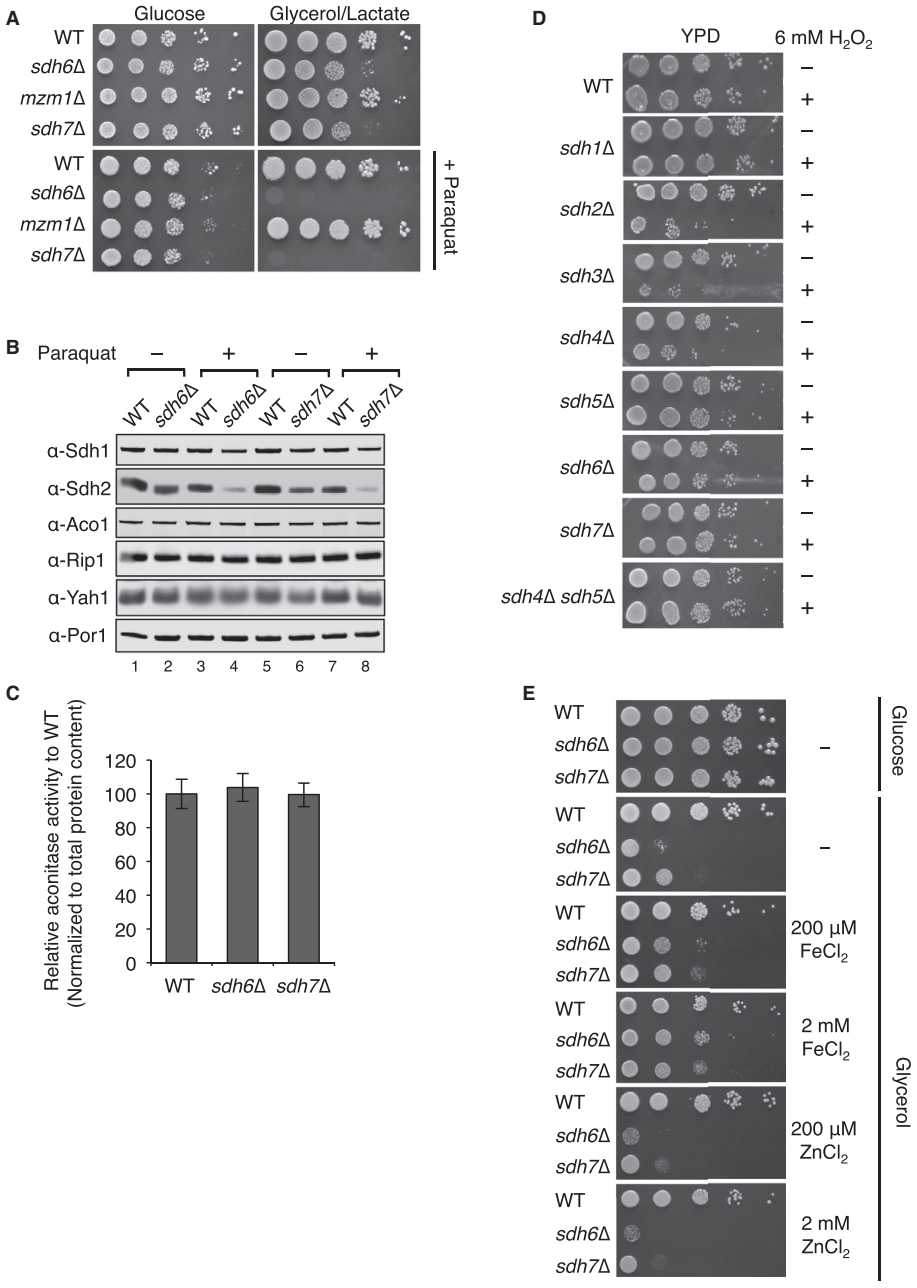

Figure 4. *sdh6*Δ and *sdh7*Δ Mutants Are Sensitive to Oxidative Stress

(A) Serial dilutions (10-fold) of cells were spotted on SC media with or without 2 mM paraquat with indicated carbon sources and incubated at 30°C.

(B) Steady-state levels of proteins in mitochondria isolated from strains cultured in the presence of 2 mM paraquat. Yah1, ferredoxin of the mitochondrial matrix.

(C) Aconitase activity specific to *cis*-aconitate conversion in isolated mitochondria. Data are shown as mean ± SD (n = 3).

(legend continued on next page)

overexpression of the putative Sdh6 homolog (encoded by *CG34229*), using *Act5C-GAL4* to drive a *UAS-CG34229* transgene in *dSdhaf3* mutants, had no effect on their sensitivity to hyperoxia (Figure S6B). This result, however, is difficult to interpret because there is only limited sequence homology between CG34229 and Sdh6. We conclude that this functional interaction between Sdh6 and Sdh7 may not be conserved through evolution or, alternatively, that CG34229 is not a functional homolog of Sdh6.

The wing posture and motility defects in *dSdhaf3* mutants suggested that these animals suffer from muscular and neuronal dysfunction. Consistent with this model, widespread expression of WT *dSdhaf3* (*Act > dSdhaf3)* in *dSdhaf3* mutants fully rescues their sensitivity to hyperoxia (Figure 6C), while muscle-specific (*C57 > dSdhaf3*) or neuronal-specific (*elav > dSdhaf3*) expression provides partial rescue (Figure 6D). Similar effects are seen on the climbing defects in *dSdhaf3* mutants (Figures 6E and 6F). Genetic rescue in the fat body (*Cg-GAL4*) or intestine (*Mex-GAL4*), however, provided no significant rescue (data not shown). Widespread overexpression of *dSdhaf3* in wild-type flies has no significant effect on their resistance to hyperoxia (data not shown). Taken together, we conclude that dSdhaf3 function is conserved through evolution and that proper SDH levels and activity are required for resistance to oxidative stress as well as muscular and neuronal function, consistent with their dependence on mitochondrial oxidative phosphorylation.

SDHB Is Specifically Impaired in Human Cells Deficient in Wild-Type SDHAF1

The human Sdh6 ortholog, SDHAF1, was shown previously to be important for SDH activity and abundance in fibroblasts (Ghezzi et al., 2009); however, its mechanism of action remained undefined. We addressed whether SDHAF1 protects SDHB (the human Sdh2 ortholog) from ROS damage similar to yeast Sdh6. First, we determined steady-state levels of SDH structural subunits in SDHAF1-depleted human embryonic kidney 293 (HEK293) cells by siRNA knockdown. SDHB and SDHC levels were significantly reduced upon SDHAF1 depletion (Figure 7A). SDHA levels, however, remained unaffected. Next, we tested the effects of paraquat on SDHAF1-depleted HEK293 cells. In accordance with the yeast and fly data, SDHB levels were further attenuated in SDHAF1-deficient cells (Figure 7B). The sensitivity to paraquat also suggests that SDHAF1 resembles Sdh6 in protecting holo-SDHB from ROS damage.

We also examined the steady-state SDHB levels in patient fibroblasts with a known *SDHAF1* mutation (Ohlenbusch et al., 2012). Both SDHB and SDHC levels were diminished in mitochondria isolated from the patient fibroblasts, whereas SDHA levels remained unaffected compared to controls (Figure 7C). SDHB protein levels were <50% of wild-type controls, and SDH enzyme activity was 52% and 40% in patients 1 and 2 relative to control values. Thus, the limited SDHB levels in the patient cells likely contribute to reduced SDH function.

DISCUSSION

The present work demonstrates that maturation of the FeS subunit of Sdh2 (SDHB) requires the participation of two assembly factors, Sdh6 (SDHAF1) and Sdh7 (SDHAF3). These factors are shown to guide Sdh2 maturation within the mitochondrial matrix in the midst of endogenous oxidants. Yeast, flies, and mammalian cells lacking one of these factors are impaired in SDH activity and assembly, with Sdh2 exhibiting a heightened susceptibility to oxidants. Normal oxidative metabolism in the mitochondria leads to the formation of superoxide anions from the one-electron reduction of O_2. Superoxide anions can readily dissociate FeS clusters, rendering the assembly of FeS cluster centers in mitochondrial enzymes susceptible to oxidative damage. The present studies in yeast, flies, and mammalian cells suggest that Sdh6 and Sdh7 shield one or more of the three FeS clusters in Sdh2 from oxidants during assembly.

Yeast studies reveal that Sdh6 and Sdh7 act in concert in the maturation of Sdh2 with a limited redundancy in function. Yeast lacking either factor show a marked SDH deficiency in late-log cultures that rely on oxidative metabolism. Under these conditions, the mutant cells contain a reduced level of the assembled tetrameric enzyme. These cells exhibit a hypersensitivity to the superoxide generator paraquat. The respiratory defect of these mutants is readily suppressed by overexpression of the Yap1 transcriptional activator of oxidative stress genes or exogenous reductants. These studies highlight the role of Sdh6 and Sdh7 in shielding Sdh2 maturation from deleterious effects of oxidants.

Flies lacking the Sdh7 ortholog SDHAF3, likewise, are hypersensitive to paraquat and hyperoxia. The mutant flies show diminished levels of active SDH and, as a result, accumulate succinate. The *dSdhaf3* mutants are viable and fertile yet display impaired movement that intensifies with age. The erect wing phenotype exhibited under hyperoxic conditions and the motility defects evident in aged mutant flies are consistent with muscular and neuronal dysfunction. Moreover, neuronal or muscle-specific expression of wild-type *dSdhaf3* is sufficient to partially rescue the hyperoxia sensitivity of the mutants, demonstrating the importance of SDH function in these tissues that rely heavily on oxidative phosphorylation (OXPHOS). The hyperoxia sensitivity of *dSdhaf3* mutants is also partially suppressed by dietary N-acetylcysteine or overexpression of the matrix manganosuperoxide dismutase Sod2. These effects of antioxidants mimic the rescue of yeast *sdh7*Δ mutant oxidative growth and demonstrate the apparent close conservation of Sdh7/SDHAF3 function through evolution.

Conservation in Sdh6/SDHAF1 function between yeast and humans also exists. Attenuation of SDHAF1 in HEK293 culture cells leads to a hypersensitivity in the stability of the FeS SDHB subunit to paraquat. SDHB instability is also seen in two SDHAF1 patient fibroblast lines. One implication of the observed antioxidant rescue of the defect of *sdh6*Δ yeast cells and *dSdhaf3* mutant flies is the potential use of antioxidant therapeutics for patients afflicted with SDHAF1 (and perhaps SDHAF3)

(D) Precultures grown up to late-log phase in YPD media were diluted 2-fold, followed by addition of 6 mM H_2O_2 and incubated for 2 hr at 30°C. Cells were washed with sterile water, and 10-fold serial dilutions were spotted on YPD plate, followed by incubation at 30°C.
(E) Enhanced respiratory growths of *sdh6Δ* mutants and *sdh7Δ* mutants with iron supplementation. Serial dilutions (10-fold) of cells were spotted on SC media with or without $FeCl_2$ or $ZnCl_2$ with the indicated concentrations and then incubated at 30°C.

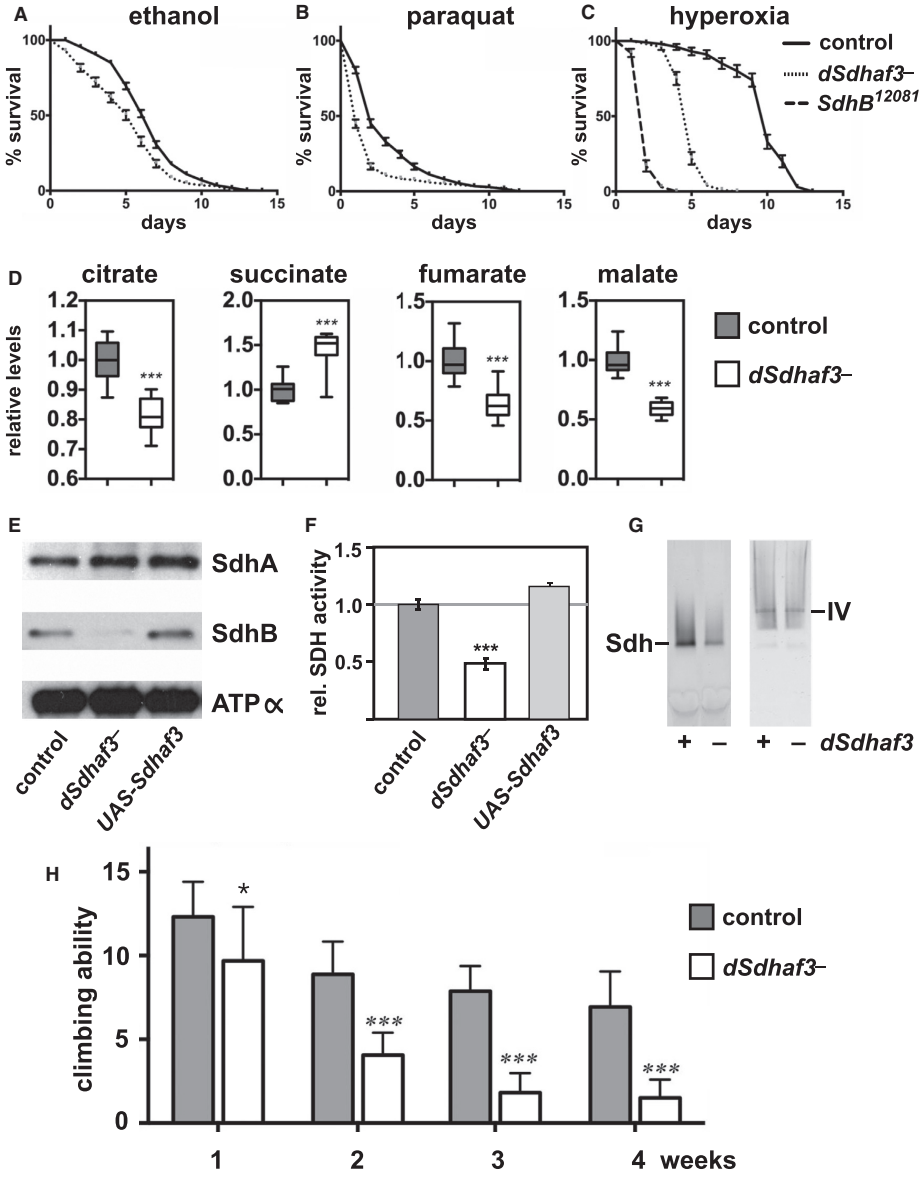

Figure 5. *dSdhaf3* Mutants Are Sensitive to Oxidative Stress and Display Reduced Levels of SdhB, Reduced SDH Activity, and Motility Defects

(A–C) w^{1118} control (solid line) and *dSdhaf3* mutant (dotted line) males (5 days old) were transferred to vials with (A) 5% ethanol, 1% agar in PBS, (B) 30 mM paraquat in semidefined medium, or (C) 100% O_2 with standard medium, and living animals were scored daily. Homozygous $SdhB^{12081}$ mutants (dashed line) were included in the hyperoxia experiment. Each graph was compiled from 3–5 experiments, using a total of 15–21 vials with 20 animals per vial. Error bars represent ±SEM. *dSdhaf3* mutants are significantly more sensitive than controls under each condition; $p < 0.001$.

(D) GC-MS was used to compare the relative levels of small metabolites in wild-type controls (gray boxes) and *dSdhaf3* mutants (white boxes). n = 12 samples from two independent experiments with 20 flies/sample (5 days old). ***$p < 0.001$.

(E) Proteins were extracted from mitochondria isolated from w^{1118} controls, *dSdhaf3* mutants, or *UAS-dSdhaf3*/+ transformants and analyzed by immunoblotting to detect SdhA, SdhB, and ATPα (subunit of complex V).

(legend continued on next page)

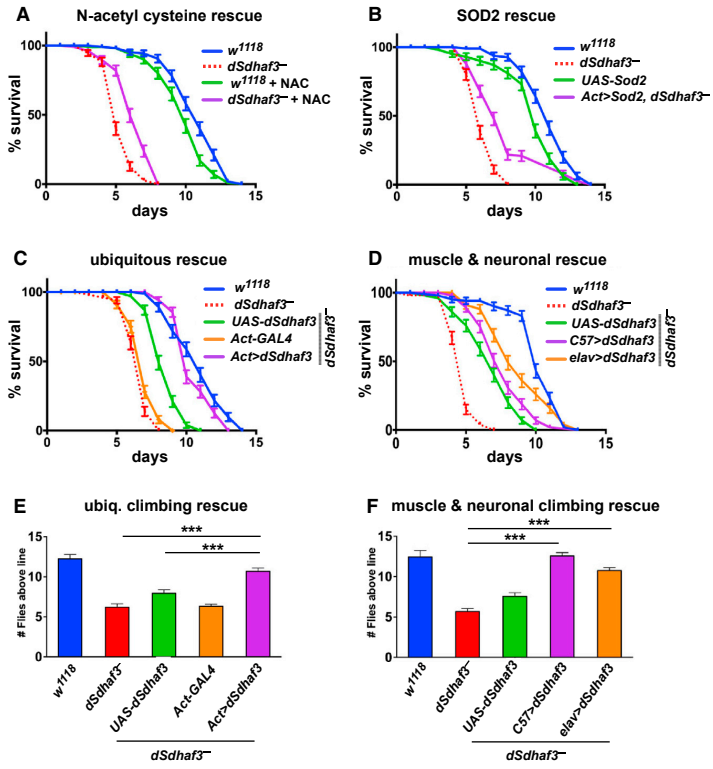

Figure 6. *dSdhaf3* Function Is Required in the Muscles and Nervous System

w^{1118} control (blue solid line) and *dSdhaf3* mutant (red dotted line) males (5 days old) were transferred to vials with 100% O_2 with standard medium, and living animals were scored daily.

(A) 0.1% N-acetylcysteine was added to the culture medium for a quarter of the vials.

(B) Expression of *Sod2* using the ubiquitous *Act5C-GAL4* driver (*Act>Sod2*; purple line) partially rescues the hyperoxia sensitivity of *dSdhaf3* mutants. Both NAC treatment and *Sod2* expression significantly rescue the hyperoxia sensitivity of *dSdhaf3* mutants; $p < 0.001$.

(C) Expression of wild-type *dSdhaf3* using the ubiquitous *Act5C-GAL4* driver (*Act>dSdhaf3*; purple line) rescues the hyperoxia sensitivity of *dSdhaf3* mutants ($p < 0.001$).

(D) The muscle-specific *C57-GAL4* driver provides minor, but significant ($p < 0.01$), rescue of the hyperoxia sensitivity of *dSdhaf3* mutants (purple line) relative to the control that carries the *UAS-dSdhaf3* transgene alone (green line), while the CNS-specific *elav-GAL4* driver provides more efficient rescue (orange line) ($p < 0.001$).

(E and F) Expression of wild-type *dSdhaf3* by using either (E) the ubiquitous *Act5C-GAL4* driver (purple), (F) the muscle-specific *C57-GAL4* driver (purple), or (F) the CNS-specific *elav-GAL4* driver (orange) rescues the climbing defect in *dSdhaf3* mutants.

The *Act>dSdhaf3* rescue in (C) and (E) was performed in females, and other rescue studies were performed in males (A, B, D, and F). The apparent partial rescue of *dSdhaf3* mutants by a single copy of the *UAS-dSdhaf3* transgene (C and D, green line) appears to be due to genetic background since *UAS-dSdhaf3* transformants have normal levels of SdhB and SDH activity (E and F). Each graph was compiled from two experiments with a total of 10 vials with 20 animals per vial. ***$p < 0.001$.

mutations. Patients with SDHAF1 mutations have presented with SDH-deficient leukoencephalopathy (Ghezzi et al., 2009; Ohlenbusch et al., 2012) and have a survival window that may be amenable to antioxidant therapy. Two case studies were reported that attempted to alleviate clinical symptoms in SDH-deficient patients harboring SDHAF1 mutations by supplementing riboflavin and CoQ10. The clinical outcomes, however, were not significantly improved (Jain-Ghai et al., 2013). More recently, a candidate therapeutic, EPI-743, is being tested for treatment of Leigh syndrome patients (Martinelli et al., 2012). EPI-743 is a vitamin E quinone that is orally bioavailable and crosses the blood-brain barrier (Shrader et al., 2011). Future studies will focus on the efficacy of antioxidants with SDHAF1 patient fibroblasts. In addition, it is important to note that every gene encoding an SDH subunit or known assembly factor is causally associated with human disease. We thus anticipate that SDHAF3 mutations will be associated with one or more previously idiopathic SDH-associated diseases and propose that SDHAF1 and SDHAF3 are candidate susceptibility factors for undefined SDH-deficient tumors.

The present work provides insights into the physiological function of Sdh6 and Sdh7 in Sdh2 maturation. Sdh6 and Sdh7 are shown to bind to the Sdh1/Sdh2 assembly intermediate that accumulates in mutants lacking the SDH membrane anchor. In addition, both Sdh6 and Sdh7 accumulate in the membrane anchor mutant cells. Sdh6 was found to impart stabilization to Sdh2 in cells lacking the FAD subunit Sdh1, suggesting that at least Sdh6 has a specific interface for Sdh2. These assembly factors do not appear to be apo-Sdh2 chaperones, since elevated levels of Sdh2 do not suppress the respiratory defects of *sdh6*Δ or

(F) A continuous colorimetric assay was used to measure SDH enzyme activity in extracts of purified mitochondria from w^{1118} controls, *dSdhaf3* mutants, and *UAS-dSdhaf3*/+ transformants. ***$p < 0.001$.

(G) Proteins from purified mitochondria were extracted from w^{1118} controls and *dSdhaf3* mutants, fractionated by nondenaturing PAGE, and analyzed for SDH and complex IV activity.

(H) Control w^{1118} flies and *dSdhaf3* mutants were tested for motility in three independent experiments using a total of 18 vials with 20 adults/vial at 1, 2, 3, or 4 weeks of age. Climbing ability is reported as the number of flies that climbed above a line drawn 4 cm above the bottom of the vial 5 s after being tapped to the bottom. *$p < 0.05$; ***$p < 0.001$.

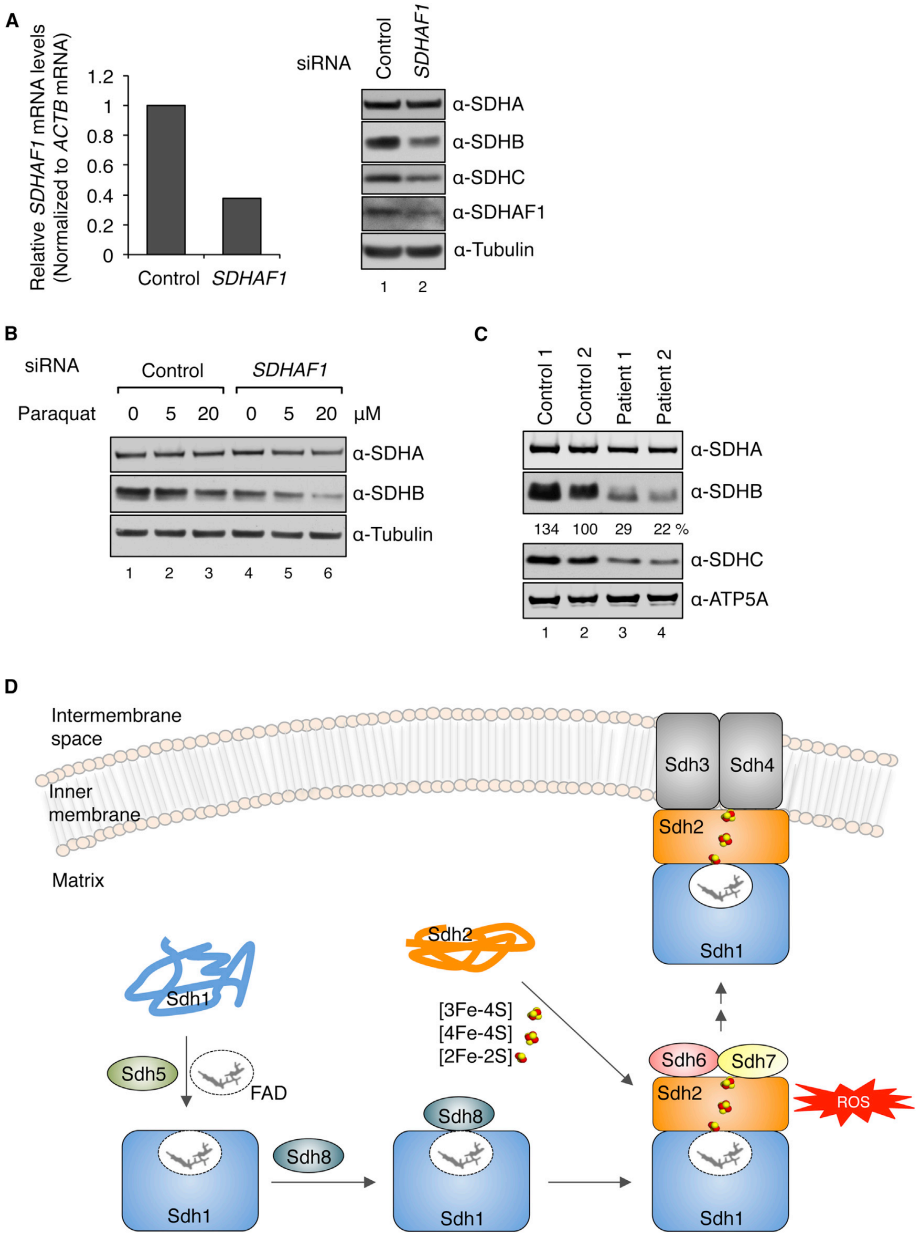

Figure 7. SDHB Is Destabilized in Human Cells with Reduced Levels of SDHAF1

(A) Relative *SDHAF1* mRNA levels in HEK293 cells 72 hr after *SDHAF1* knockdown using siRNA (left panel) and steady-state levels of proteins from total cell lysates (right panel).

(B) HEK293 cells were treated with either control siRNA or *SDHAF1* siRNA. Paraquat was added to cultures 24 hr after siRNA transfection. Total cell lysates were obtained 48 hr after paraquat treatment.

(legend continued on next page)

*sdh7*Δ mutants. Sdh6 and Sdh7 appear to be key chaperones in holo-Sdh2 maturation during oxidative growth. However, a recent report implicated SDHAF1 in an active role in FeS cluster insertion (Maio et al., 2014).

The observation that the two LYR proteins Sdh6 and Sdh7 function with the FeS cluster Sdh2 subunit has significant implications for the uncharacterized LYR proteins present in the human proteome. Our studies raise the possibility that future functional studies of LYRM1, LYRM2, LYRM5, and LYRM9 will reveal roles in maturation of mammalian-specific FeS cluster enzymes.

EXPERIMENTAL PROCEDURES

Yeast Strains and Plasmids

All *S. cerevisiae* strains and plasmids used are listed in Tables S1 and S2, respectively. Culture media and conditions are described in detail in the Supplemental Experimental Procedures.

Mitochondrial Enzymatic Activity Assay

Succinate dehydrogenase (SDH) and aconitase activity assays were performed as described previously (Atkinson et al., 2011). For SDH activity, quinone-mediated reduction of dichlorophenolindophenol (DCPIP) upon succinate oxidation was measured with isolated mitochondria spectrophotometrically at 600 nm. Aconitase activity was measured with 100 μM *cis*-aconitate in 50 mM Tris (pH 7.4) at 240 nm in soluble fractions of mitochondria disrupted by repetitive freeze-thaw. For malate dehydrogenase (MDH) activity, soluble mitochondrial fractions were obtained using sonication. Oxidation of 0.2 mM NADH was monitored in the presence of 2 mM oxaloacetate in 100 mM Tris (pH 7.4) at 340 nm (Hayes et al., 1991).

Mitochondrial Protein Import Assay

Mitochondrial protein import assay was performed as described previously (Wagener et al., 2011). Briefly, *SDH2* and *RIP1* open reading frames were subcloned in pGEM-4Z for in vitro transcription and translation, respectively. Radiolabeled precursor proteins were obtained using reticulocyte lysate (Promega) in the presence of ^{35}S-Met. Precursors were imported into 75 μg of isolated mitochondria in 50 mM HEPES-KOH (pH 7.2) buffer containing 0.6 M sorbitol, 0.5 mg/ml BSA, 2 mM potassium phosphate, 75 mM KCl, 10 mM magnesium acetate, 2 mM EDTA, 2.5 mM $MnCl_2$, 2 mM ATP, 2 mM NADH, 10 mM creatine phosphate, 0.1 mg/ml creatine kinase, 2.5 mM malate, and 2.5 mM succinate for 30 min at 25°C for pulse. Import was stopped by adding 5 μM valinomycin and then chased for the periods of time indicated. Nonimported precursors were degraded by proteinase K on ice. Samples were separated on SDS-PAGE and detected by autoradiography.

Coimmunoprecipitation

Mitochondria were solubilized in 10 mM sodium phosphate (pH 7.4), 500 mM NaCl, 1 mM EDTA, 1% digitonin, and 1× protease inhibitor cocktail (Roche) for 30 min on ice. Crosslinking was performed with solubilization by adding 1 mM of dithiobis(succinimidylpropionate) (Pierce) for 30 min at room temperature (RT). After centrifugation at 14,000 × *g*, supernatants were incubated with magnetic anti-Myc beads (Cell Signaling Technology) for 4 hr at 4°C. Beads were washed with 10 mM sodium phosphate (pH 7.4), 500 mM NaCl, 1 mM EDTA, 0.1% digitonin, and 1 mM PMSF. After washing three times, bound substances were recovered by boiling with 2× SDS-PAGE sample buffer, which was subjected to immunoblotting.

Drosophila Strains

Flies were maintained on standard Bloomington Stock Center medium with malt at 25°C. The following stocks were obtained from the Bloomington Stock Center: $SdhA^{HP21216}$/*CyO* (Bloomington #22087), $SdhB^{12081}$/*CyO* (Walker et al., 2006), *da-Gal4* (Wodarz et al., 1995), and *Act5C-Gal4*/*CyO* (Bloomington #25374). The *UAS-dSdhaf3* transformants were generated as described in the Supplemental Experimental Procedures.

Statistics

Yeast data were analyzed using Microsoft Excel 2011. Data are presented as mean ± SD or mean ± SEM, as indicated. Statistical significance was evaluated using Student's t test. $p < 0.05$ was considered significant. Statistical analysis and graphical presentation for *Drosophila* studies were performed using PRISM software. Student's t test was used for pairwise comparisons, and one-way ANOVA was used for multiple comparisons. Fly metabolomic data are graphically represented as box plots, with the box representing the lower and upper quartiles, the horizontal line representing the median, and the bars representing the minimum and maximum data points. All other data are shown as the mean ± SEM.

SUPPLEMENTAL INFORMATION

Supplemental Information includes Supplemental Experimental Procedures, six figures, and two tables and can be found with this article online at http://dx.doi.org/10.1016/j.cmet.2014.05.014.

AUTHOR CONTRIBUTIONS

U.N. designed the experiments, performed the cellular and biochemical analyses with yeast and mammalian cells, and wrote the paper. W.Y. designed the experiments and performed the genetic experiments with *Drosophila*, J.C. performed the metabolomics analyses, and D.K.B. initiated the *Drosophila* study. K.B. provided the SDHAF1 patient fibroblast cells, J.R. provided the tissue culture facility, and C.S.T. conceived the *Drosophila* studies, interpreted results, and contributed to the writing and financial support. D.R.W. conceived the yeast and mammalian study and design, contributed to writing the paper, interpreted results, provided financial support, and finalized the manuscript. U.N. and W.Y. contributed equally to this work.

ACKNOWLEDGMENTS

We thank the Bloomington Stock Center for providing fly stocks and FlyBase for information used for this study. We acknowledge support of funds in conjunction with grant P30 CA042014 awarded to Huntsman Cancer Institute. D.K.B. was supported by the NIH Genetics Predoctoral Training Grant T32 GM007464. This research was supported by NIH RO1 ES03817 (D.R.W.) and 1R01 GM094232 (C.S.T.).

Received: January 6, 2014
Revised: April 8, 2014
Accepted: May 16, 2014
Published: June 19, 2014

REFERENCES

Adam, A.C., Bornhövd, C., Prokisch, H., Neupert, W., and Hell, K. (2006). The Nfs1 interacting protein Isd11 has an essential role in Fe/S cluster biogenesis in mitochondria. EMBO J. *25*, 174–183.

Atkinson, A., Smith, P., Fox, J.L., Cui, T.Z., Khalimonchuk, O., and Winge, D.R. (2011). The LYR protein Mzm1 functions in the insertion of the Rieske Fe/S protein in yeast mitochondria. Mol. Cell. Biol. *31*, 3988–3996.

Bardella, C., Pollard, P.J., and Tomlinson, I. (2011). SDH mutations in cancer. Biochim. Biophys. Acta *1807*, 1432–1443.

Baysal, B.E., Ferrell, R.E., Willett-Brozick, J.E., Lawrence, E.C., Myssiorek, D., Bosch, A., van der Mey, A., Taschner, P.E., Rubinstein, W.S., Myers, E.N., et al.

(C) Steady-state levels of proteins in mitochondria isolated from control fibroblasts and patient fibroblasts harboring mutations on *SDHAF1* (Ohlenbusch et al., 2012). The indicated percentages are relative levels of SDHB normalized to ATP5A levels by densitometry.
(D) Model of the role of Sdh6(SDHAF1) and Sdh7(SDHAF3) in maturation of Sdh2(SDHB). Sdh6 and Sdh7 associate with Sdh2 within a Sdh1/Sdh2 intermediate. Sdh1 maturation requires covalent flavinylation by Sdh5, followed by formation of the Sdh1/Sdh2 subcomplex that is chaperoned by Sdh8 (see accompanying paper Van Vranken et al., 2014).

(2000). Mutations in SDHD, a mitochondrial complex II gene, in hereditary paraganglioma. Science *287*, 848–851.

Cui, T.Z., Smith, P.M., Fox, J.L., Khalimonchuk, O., and Winge, D.R. (2012). Late-stage maturation of the Rieske Fe/S protein: Mzm1 stabilizes Rip1 but does not facilitate its translocation by the AAA ATPase Bcs1. Mol. Cell. Biol. *32*, 4400–4409.

DeSimone, S., Coelho, C., Roy, S., VijayRaghavan, K., and White, K. (1996). ERECT WING, the Drosophila member of a family of DNA binding proteins is required in imaginal myoblasts for flight muscle development. Development *122*, 31–39.

Feichtinger, R.G., Zimmermann, F., Mayr, J.A., Neureiter, D., Hauser-Kronberger, C., Schilling, F.H., Jones, N., Sperl, W., and Kofler, B. (2010). Low aerobic mitochondrial energy metabolism in poorly- or undifferentiated neuroblastoma. BMC Cancer *10*, 149.

Fernandes, L., Rodrigues-Pousada, C., and Struhl, K. (1997). Yap, a novel family of eight bZIP proteins in *Saccharomyces cerevisiae* with distinct biological functions. Mol. Cell. Biol. *17*, 6982–6993.

Finsterer, J. (2008). Leigh and Leigh-like syndrome in children and adults. Pediatr. Neurol. *39*, 223–235.

Gardner, P.R. (2002). Aconitase: sensitive target and measure of superoxide. Methods Enzymol. *349*, 9–23.

Gardner, P.R., and Fridovich, I. (1992). Inactivation-reactivation of aconitase in *Escherichia coli*. A sensitive measure of superoxide radical. J. Biol. Chem. *267*, 8757–8763.

Ghezzi, D., Goffrini, P., Uziel, G., Horvath, R., Klopstock, T., Lochmüller, H., D'Adamo, P., Gasparini, P., Strom, T.M., Prokisch, H., et al. (2009). SDHAF1, encoding a LYR complex-II specific assembly factor, is mutated in SDH-defective infantile leukoencephalopathy. Nat. Genet. *41*, 654–656.

Greene, J.C., Whitworth, A.J., Kuo, I., Andrews, L.A., Feany, M.B., and Pallanck, L.J. (2003). Mitochondrial pathology and apoptotic muscle degeneration in *Drosophila* parkin mutants. Proc. Natl. Acad. Sci. USA *100*, 4078–4083.

Hao, H.X., Khalimonchuk, O., Schraders, M., Dephoure, N., Bayley, J.P., Kunst, H., Devilee, P., Cremers, C.W., Schiffman, J.D., Bentz, B.G., et al. (2009). SDH5, a gene required for flavination of succinate dehydrogenase, is mutated in paraganglioma. Science *325*, 1139–1142.

Hayes, M.K., Luethy, M.H., and Elthon, T.E. (1991). Mitochondrial malate dehydrogenase from corn : purification of multiple forms. Plant Physiol. *97*, 1381–1387.

Jain-Ghai, S., Cameron, J.M., Al Maawali, A., Blaser, S., MacKay, N., Robinson, B., and Raiman, J. (2013). Complex II deficiency—a case report and review of the literature. Am. J. Med. Genet. A. *161A*, 285–294.

Janeway, K.A., Kim, S.Y., Lodish, M., Nosé, V., Rustin, P., Gaal, J., Dahia, P.L., Liegl, B., Ball, E.R., Raygada, M., et al.; NIH Pediatric and Wild-Type GIST Clinic (2011). Defects in succinate dehydrogenase in gastrointestinal stromal tumors lacking KIT and PDGFRA mutations. Proc. Natl. Acad. Sci. USA *108*, 314–318.

Khalimonchuk, O., Bird, A., and Winge, D.R. (2007). Evidence for a pro-oxidant intermediate in the assembly of cytochrome oxidase. J. Biol. Chem. *282*, 17442–17449.

Kim, K.D., Chung, W.H., Kim, H.J., Lee, K.C., and Roe, J.H. (2010). Monothiol glutaredoxin Grx5 interacts with Fe-S scaffold proteins Isa1 and Isa2 and supports Fe-S assembly and DNA integrity in mitochondria of fission yeast. Biochem. Biophys. Res. Commun. *392*, 467–472.

Kim, H.J., Jeong, M.Y., Na, U., and Winge, D.R. (2012). Flavinylation and assembly of succinate dehydrogenase are dependent on the C-terminal tail of the flavoprotein subunit. J. Biol. Chem. *287*, 40670–40679.

Maio, N., Singh, A., Uhrigshardt, H., Saxena, N., Tong, W.H., and Rouault, T.A. (2014). Cochaperone binding to LYR motifs confers specificity of iron sulfur cluster delivery. Cell Metab. *19*, 445–457.

Martinelli, D., Catteruccia, M., Piemonte, F., Pastore, A., Tozzi, G., Dionisi-Vici, C., Pontrelli, G., Corsetti, T., Livadiotti, S., Kheifets, V., et al. (2012). EPI-743 reverses the progression of the pediatric mitochondrial disease—genetically defined Leigh Syndrome. Mol. Genet. Metab. *107*, 383–388.

McCammon, M.T. (1996). Mutants of Saccharomyces cerevisiae with defects in acetate metabolism: isolation and characterization of Acn- mutants. Genetics *144*, 57–69.

Ohlenbusch, A., Edvardson, S., Skorpen, J., Bjornstad, A., Saada, A., Elpeleg, O., Gärtner, J., and Brockmann, K. (2012). Leukoencephalopathy with accumulated succinate is indicative of SDHAF1 related complex II deficiency. Orphanet J. Rare Dis. *7*, 69.

Robinson, K.M., and Lemire, B.D. (1996). Covalent attachment of FAD to the yeast succinate dehydrogenase flavoprotein requires import into mitochondria, presequence removal, and folding. J. Biol. Chem. *271*, 4055–4060.

Rodríguez-Manzaneque, M.T., Tamarit, J., Bellí, G., Ros, J., and Herrero, E. (2002). Grx5 is a mitochondrial glutaredoxin required for the activity of iron/sulfur enzymes. Mol. Biol. Cell *13*, 1109–1121.

Rustin, P., and Rötig, A. (2002). Inborn errors of complex II—unusual human mitochondrial diseases. Biochim. Biophys. Acta *1553*, 117–122.

Selak, M.A., Armour, S.M., MacKenzie, E.D., Boulahbel, H., Watson, D.G., Mansfield, K.D., Pan, Y., Simon, M.C., Thompson, C.B., and Gottlieb, E. (2005). Succinate links TCA cycle dysfunction to oncogenesis by inhibiting HIF-alpha prolyl hydroxylase. Cancer Cell *7*, 77–85.

Shrader, W.D., Amagata, A., Barnes, A., Enns, G.M., Hinman, A., Jankowski, O., Kheifets, V., Komatsuzaki, R., Lee, E., Mollard, P., et al. (2011). α-Tocotrienol quinone modulates oxidative stress response and the biochemistry of aging. Bioorg. Med. Chem. Lett. *21*, 3693–3698.

Sun, F., Huo, X., Zhai, Y., Wang, A., Xu, J., Su, D., Bartlam, M., and Rao, Z. (2005). Crystal structure of mitochondrial respiratory membrane protein complex II. Cell *121*, 1043–1057.

Van Vranken, J.G., Bricker, D.K., Dephoure, N., Gygi, S.P., Cox, J.E., Thummel, C.S., and Rutter, J. (2014). SDHAF4 promotes mitochondrial succinate dehydrogenase activity and prevents neurodegeneration. Cell Metab. *20*. Published online June 19, 2014. http://dx.doi.org/10.1016/j.cmet.2014.05.012.

Wagener, N., Ackermann, M., Funes, S., and Neupert, W. (2011). A pathway of protein translocation in mitochondria mediated by the AAA-ATPase Bcs1. Mol. Cell *44*, 191–202.

Walker, D.W., Hájek, P., Muffat, J., Knoepfle, D., Cornelison, S., Attardi, G., and Benzer, S. (2006). Hypersensitivity to oxygen and shortened lifespan in a *Drosophila* mitochondrial complex II mutant. Proc. Natl. Acad. Sci. USA *103*, 16382–16387.

Wiedemann, N., Urzica, E., Guiard, B., Müller, H., Lohaus, C., Meyer, H.E., Ryan, M.T., Meisinger, C., Mühlenhoff, U., Lill, R., and Pfanner, N. (2006). Essential role of Isd11 in mitochondrial iron-sulfur cluster synthesis on Isu scaffold proteins. EMBO J. *25*, 184–195.

Wodarz, A., Hinz, U., Engelbert, M., and Knust, E. (1995). Expression of crumbs confers apical character on plasma membrane domains of ectodermal epithelia of *Drosophila*. Cell *82*, 67–76.

Xiao, M., Yang, H., Xu, W., Ma, S., Lin, H., Zhu, H., Liu, L., Liu, Y., Yang, C., Xu, Y., et al. (2012). Inhibition of α-KG-dependent histone and DNA demethylases by fumarate and succinate that are accumulated in mutations of FH and SDH tumor suppressors. Genes Dev. *26*, 1326–1338.

CHAPTER 4

ANALYSIS OF SDHAF3 IN FAMILIAL AND SPORADIC PHEOCHROMOCYTOMA AND PARAGANGLIOMA

Trisha Dwight,[1,2,9] Un Na,[3,4,9] Edward Kim,[1,2] Ying Zhu,[5] Anne Louise Richardson,[1] Bruce G Robinson,[1,2] Katherine M Tucker,[6] Anthony J Gill,[2,7,8] Diana E Benn,[1,2] Roderick J Clifton-Bligh,[1,2,10] Dennis R Winge[3,10]

[1]Cancer Genetics, Hormones and Cancer Group, Kolling Institute of Medical Research, Royal North Shore Hospital, Sydney 2065, Australia; [2]University of Sydney, Sydney 2006, Australia; Departments of Medicine[3] and Biochemistry[4], University of Utah Health Sciences Center, Salt Lake City, Utah 84132, United States of America; [5]Hunter New England Health, Royal North Shore Hospital, Sydney 2065, Australia; [6]Hereditary Cancer Service, Prince of Wales Hospital, Sydney 2031, Australia; [7]Department of Anatomical Pathology, Royal North Shore Hospital, Sydney 2065, Australia; [8]Northern Cancer Translational Research Unit, Royal North Shore Hospital, Sydney 2065, Australia. [9]TD and UN contributed equally; [10]RJCB and DRW contributed equally.

Abstract

SDH assembly factors have been identified as playing a role in maturation of individual SDH subunits and assembly of the functioning SDH complex. Using massively parallel sequencing, we identified a variant in SDH assembly factor 3 (*SDHAF3*), c.157T>C (p.Phe53Leu), associated with increased prevalence in familial and sporadic pheochromocytoma and/or paraganglioma (6.6%) compared to a normal population (2.1% [Exome Aggregation Consortium]; p=0.0063). *In silico* prediction tools suggest this variant is probably damaging to protein function, hence we assessed functional consequences of the resulting amino acid change (p.Phe53Leu) in yeast and human cells. Through our analysis in yeast, we showed that introduction of SDHAF3 p.Phe53Leu into *Sdh7* null yeast (ortholog of *SDHAF3* in humans) resulted in impaired function, as observed by its failure to restore SDH activity when expressed in *Sdh7* null yeast relative to WT SDHAF3. As SDHAF3 is involved in maturation of SDHB, we tested the functional impact of *SDHAF3* c.157T>C and various clinically relevant *SDHB* mutations on this interaction. Our in vitro studies in human cells show that SDHAF3 interacts with SDHB (residues 46 and 242), with impaired interaction observed in the presence of the *SDHAF3* c.157T>C variant. Our studies reveal novel insights into the biogenesis of SDH, uncovering a vital interaction between SDHAF3 and SDHB. We have shown that SDHAF3 interacts directly with SDHB (residue 242 being key to this interaction), and that a variant in *SDHAF3* (c.157T>C [p.Phe53Leu]) is more prevalent in individuals with pheochromocytoma and/or paraganglioma, and is hypomorphic via impaired interaction with SDHB.

Introduction

Succinate dehydrogenase (SDH) plays an integral role in both the tricarboxylic acid (TCA) cycle, where it catalyses the oxidation of succinate to fumarate; and electron transport chain (ETC), where succinate oxidation is coupled to ubiquinone reduction. SDH is comprised of four nuclear encoded subunits (SDHA, B, C and D), and germline mutations in any of these SDH subunits are associated with a variable risk of developing neoplasia (*1*). Nevertheless, discordant phenotypes are observed both within and between families carrying the same *SDH* mutation, suggesting that other environmental, genetic or epigenetic factors influence the clinical phenotype.

SDH genes (*SDHA*, *SDHB*, *SDHC*, *SDHD*) act as classical tumor suppressors, such that germline heterozygous inactivating mutations coupled with somatic loss of the remaining wild-type allele leads to complete loss of enzyme function and development of associated tumors. *SDHx* mutations have been linked to tumorigenesis as a result of a number of downstream consequences. SDH deficiency results in succinate accumulation, due to inability of SDH to catalyze the oxidation of succinate to fumarate. In turn, the elevated succinate can inhibit α-ketoglutarate-dependent dioxygenases, resulting in pseudo-hypoxia and hypermethylation of histones and DNA. Inhibition of the α-ketoglutarate-dependent dioxygenase, prolyl hydroxylase (PHD), leads to HIF stabilization, increased expression of HIF targets and ultimately induction of a hypoxic response under normoxic conditions (pseudo-hypoxia). In line with this proposed mechanism of action, both increased stability of HIF and increased expression of HIF targets have been identified in *SDHx*-mutated paragangliomas and pheochromocytomas (*2-4*). Additionally, accumulated succinate inhibits other α-ketoglutarate-dependent

dioxygenases, such as histone demethylases of the Jumonji demethylase family and TET hydroxylases, resulting in hypermethylation of histones and DNA. This mechanism has been observed recently in *SDHx*-mutated paragangliomas, pheochromocytomas and gastrointestinal stromal tumors (*5-7*).

Recently, SDH assembly factors (SDHAF1, SDHAF2, SDHAF3 and SDHAF4) have been identified as being crucial for maturation and effective functioning of SDH within mitochondria (*8-10*). To date, mutations affecting *SDHAF1* (involved in maturation of SDHB) and *SDHAF2* (required for covalent attachment of FAD to SDHA) have been associated with human diseases. *SDHAF1* mutations have been identified in individuals with leukoencephalopathy (*11, 12*), but not yet in subjects with paragangliomas or pheochromocytomas. A *SDHAF2* loss-of-function mutation (p.Gly78Arg) has been reported in two unrelated families with head and neck paragangliomas (*8, 13, 14*). In the tumors of affected individuals, this mutation was shown to impair flavinylation of SDHA. Additionally, in vitro experiments showed that the p.Gly78Arg mutant leads to complete loss of SDH activity, through impaired covalent flavinylation of SDHA and destabilization of the SDHAF2 protein. Subsequent studies in large cohorts of apparently sporadic paragangliomas and pheochromocytomas have failed to identify germline or somatic *SDHAF2* mutations, suggesting that mutations within *SDHAF2* may be rare (*13, 14*).

Recently, yeast studies showed that two LYR motif proteins Sdh6 (SDHAF1, human ortholog) and Sdh7 (SDHAF3, human ortholog) act in concert to promote the maturation of Sdh2 (SDHB, human ortholog) by shielding one or more of the three Fe-S clusters in Sdh2 from the deleterious effects of oxidants during assembly (*9*). LYR motifs

were also observed in SDHB itself in residues 44-46 and 240-242. These were implicated in the insertion of Fe-S clusters (*15*). We therefore hypothesized that mutations within the newly identified SDH assembly factor, SDHAF3, may be associated with the pathogenesis of pheochromocytoma and/or paraganglioma syndromes. Furthermore, given SDHAF3 is involved in the maturation of SDHB, we hypothesized that mutations within either of these genes may impair this process.

Materials and methods

Subjects and samples

DNA was extracted from peripheral blood leukocytes of 37 individuals (from 23 families) with germline *SDH* mutations (16 *SDHB,* 1 *SDHC* and 6 *SDHD* families) and 100 individuals with no known disease (i.e., unaffected control population). Additionally, DNA was extracted from 15 fresh-frozen pheochromocytoma/paraganglioma (PC/PGL) samples of apparently sporadic origin, as well as 3 paraffin embedded PC/PGL samples associated with familial disease. SDHB immunohistochemical assessment of the 3 paraffin embedded PC/PGL samples was also performed, as previously described (*16*). Informed consent was obtained for the collection and study of all samples, with approval for research being granted by the Northern Sydney Local Health District Human Research Ethics Committee (Kolling Neuroendocrine Tumour Bank Protocol #11011-361M, Australian SHD Consortium Protocol #1103-101M, and Kolling Institute Healthy Volunteers Bank Protocol HVBMC#14-06).

Massively parallel sequencing

A custom gene panel (TruSeq® Custom Amplicon Assay, Illumina) was developed, encompassing our candidate gene - *SDHAF3* (NM_020186); as well as eight known PC/PGL suseptibility genes (*MAX* [NM_002382], *SDHB* [NM_003000], *SDHC* [NM_003001], *SDHD* [NM_003002], *SDHAF2* [NM_017841], *RET* [NM_020975], *TMEM127* [NM_017849] and *VHL* [NM_000551]). The panel included the protein-coding exons and flanking intronic regions of each of the genes and was created using DesignStudio (Illumina). DNA libraries were prepared (using 250 ng of DNA from each sample) and sequenced on a MiSeq platform (using 2 x 150 bp paired end reads) according to the manufacturer's instructions (Illumina). FASTQ files (containing reads and their base call quality scores) were generated for each sample, and alignment of reads (banded Smith-Waterman algorithm) and variant calling (GATK (*17*)) was processed by MiSeq Reporter (version 2.0, Illumina). Annotation of functional consequences to variant calls was performed using ANNOVAR (version 2013Jul (*18*)), which incorporates various *in silico* tools, including (but not limited to) PolyPhen-2, SIFT, MutationTaster. Visualisation of reads was performed using IGV (v2.1).

Sanger sequencing

SDHAF3 variants identified by massively parallel sequencing were confirmed by Sanger sequencing. Mutation analysis of the entire coding sequence, including exon-intron boundaries, was performed for the two exons of *SDHAF3*. Primer sequences were as follows: exon 1-forward (5'-gtctgccttccggttcacta-3'), exon 1-reverse (5'-gaacaggttgctgctctgttta-3'), exon 2-forward (5'-tccttaaccaaatgcttctgc-3'), exon 2-reverse

(5'-tgatcttgatccatatactgcaa-3'). In some instances, two rounds of PCR were required to amplify the DNA from paraffin embedded tissues; in such cases, each mutation was confirmed by sequencing of two independent PCRs.

Strains and plasmids for studies in yeast

S. cerevisiae strains used in this study were from a previous study (*9*). Yeast cells were grown in synthetic complete or minimal media containing 2% raffinose and 0.2% glucose, unless indicated otherwise. To clone *SDHAF3* in yeast plasmids, the PCR-amplified *SDHAF3* ORF from a human cDNA library was ligated into pRS416 with *MET25* promoter and *CYC1* terminator. For *SDHAF3* and *SDH2* sequence variants, site-directed mutagenesis was carried out using Phusion high-fidelity DNA polymerase (Thermo Fisher Scientific). The full-length *SDH2* with its own promoter and terminator were cloned into pRS416. Plasmids expressing Sdh2-His_6Myc_2 and Rip-Myc were from a previous study (*19*).

Co-immunoprecipitation of yeast proteins

SDHAF3 immunoprecipitation with anti-SDHAF3 antibody was performed using protein A magnetic beads. Briefly, mitochondria were solubilized in 10 mM Tris-HCl (pH 7.4), 150 mM NaCl, 1 mM EDTA, 1% digitonin and 1X protease inhibitor cocktail (Roche) for 30 min on ice. Supernatants after centrifugation at 14,000 x g were incubated with appropriate antibodies for 16 hours at 4°C. Protein A magenetic beads (New England Biolabs, Inc.) were added and incubated for 4 hours at 4°C. Beads were washed three times with 10 mM Tris-HCl (pH 7.4), 150 mM NaCl, 1 mM EDTA, 0.1 % digitonin

and 1 mM PMSF. Beads were resuspended in 2X SDS-PAGE sample buffer, which was subjected to immunoblotting.

Enzyme activity assay

Succinate dehydrogenase (SDH) and succinate:quinone oxidoreductase (SQR) activity assays were performed as previously described, with slight modifications (*23*). Briefly, isolated mitochondria were incubated in 40 mM potassium phosphate (pH 7.4) buffer with 0.5% Tween 80, 20 mM succinate and 20 μM antimycin A for 5 min at room temperature. The reaction was initiated by adding 90 μM decylubiquinone for SQR or 120 μM phenazine methosulfate for SDH with 120 μM dichlorophenolindophenol (DCPIP). The rate of reduction of DCPIP was measured spectrophotometrically at 600 nm for 5 min.

Plasmid constructs and site-directed mutagenesis for studies in mammalian cells

Site-directed mutagenesis (QuikChange Lightning Site-Directed Mutagenesis Kit, Agilent) was used to produce the *SDHAF3* variant (p.Phe53Leu [c.157T>C, NM_020186]) and *SDHB* mutants (p.Ala43Pro [c.127G>C, NM_003000], p.Arg46Gly [c.136C>G], p.Arg46Gln [c.137G>A], p.Cys101Tyr [c.302G>A], p.Ile127Ser [c.380T>G], p.Pro197Arg [c.590C>G], p.Arg242His [c.725G>A]). The *SDHAF3* variant was generated in a commercially available plasmid, pCMV6-SDHAF3-Myc-DDK (RC204626, Origene); while the *SDHB* mutants were generated in a plasmid (pEGFP-N1; 6085-1, Clonetech) containing wild-type *SDHB*. Briefly, normal *SDHB* cDNA was

generated from human adrenal total RNA and inserted into pEGFP-N1, using EcoRI and BamHI restriction sites, as previously described (*24*). Sanger sequencing was used to confirm the presence of wild-type or variant sequences, and that they were in-frame with the respective tag.

Co-immunoprecipitation of mammalian proteins

Human embryonic kidney 293 (HEK293) cells, cultured in DMEM with 10% fetal bovine serum, were seeded at 1.0 x 10^6 cells/25 cm^2 flask and left to settle for 24 hours. Co-transfections were then performed using 7.5 µg of DNA (pCMV6-SDHAF3-Myc-DDK and pEGFP-N1-SDHB) using Lipofectamine™ 2000 (Life Technologies) and Opti-MEM® (Life Technologies) according to the manufacturers' instructions. Twenty-four hours post transfection, cells were washed (PBS), pelleted and lysed using co-immunoprecipitation (Co-IP) buffer (20 mM Tris pH7.5, 150 mM NaCl, 1 mM EGTA, 1 mM EDTA, 0.1% Triton X100), which was also used for whole cell lysates. Dynabeads® M-280 sheep anti-mouse IgG (Life Technologies) were incubated with either mouse IgG antibody (dilution 1:2000, Thermo-Fisher, Waltham, MA, USA) for negative control or mouse monoclonal anti-DDK (dilution 1:2000, OriGene [TA50011], MD, USA) for 2 hours prior to washing; then incubated overnight with cell extracts at 4°C under gentle rotation. Proteins not associated with DDK-tagged SDHAF3 were removed (3 x 10 minutes gentle agitation washes) using Co-IP lysis buffer with a higher salt concentration (500 mM NaCl). To remove immunoprecipitated material from beads, cell lysates were mixed with NuPAGE® LDS sample buffer (Invitrogen) and dithiothreitol and incubated at 95°C for 5 min. Extracts were removed from beads, sonicated and separated by SDS-

PAGE (4-12% NuPAGE Bis-Tris gels, Invitrogen) under reducing conditions. Proteins were transferred (nitrocellulose membrane) and the membrane blocked with 5% skim milk (in TBST) for 1 hour at room temperature. The membranes were probed with the following antibodies: GFP (dilution 1:2000, Roche [11814460001], Basel, Switzerland), DDK (dilution 1:2000, OriGene [TA50011], MD, USA), GAPDH (dilution 1:5000, Cell Signaling [D16H11], MA, USA) and incubated overnight at 4°C. Immunoblots were washed three times with TBST for 5-10 min and incubated with the relevant secondary antibody conjugated to horseradish peroxidase (HRP). Blots were then washed (three times in TBST for 5 minutes) and protein detected (ECL Plus Western Blotting Detection Reagent [GE Healthcare, Little Chalfont, UK]) on a LAS-3000 (Fujifilm, Brookvale, Australia).

Immunoblotting

Isolation of yeast mitochondria was performed using the method of Glick and Pon (*20*). BN-PAGE was performed as described previously with mitochondrial lysates in 1 % digitonin solution (*21*). Samples were separated on 4-16% NativePAGE Bis-Tris gels (Life Technologies) and transferred to PVDF membrane for immunodetection. Anti-Sdh1, Sdh2 and Sdh3 were from a previous study (*22*). Antibodies to Por1 were from Molecular Probes. Protein concentration was determined by the Bradford assay.

Statistical analyses

Chi-squared tests were used to compare allele counts in the disease-affected and disease-free cohorts, with $p<0.05$ considered significant (GraphPad Software, Inc). Yeast

data were analyzed using Microsoft Excel 2011, with data presented as mean ± SD or mean ± SEM as indicated. Statistical significance was evaluated using Student's test, with $p<0.05$ considered significant.

Results

Massively parallel sequencing identifies germline variants arising in SDHB and SDHAF3 in the same individual

During validation of our targeted PC/PGL gene panel (MiSeq platform), we noted that one individual (S11_1) with a previously identified germline *SDHB* splice-site mutation (within intron 3 [IVS3]) also harbored a germline *SDHAF3* c.157T>C (p.Phe53Leu) variant (rs62624461). Pheochromocytoma was first diagnosed in this individual at the age of 18 years, and subsequent recurrence and spinal metastasis was noted at 24 years of age. Although this *SDHAF3* variant has been identified in population studies (minor allele frequency [MAF] 0.014 [1000 Genomes_Phase 1_ALL] and 0.021 [Exome Aggregation Consortium, ExAC]), it is predicted to be damaging by several *in silico* tools (score of 0.777 [PolyPhen-2 v2.2.2r398], score of 0 [SIFT]). Since SDHAF3 was recently shown to be involved in mediating SDHB maturation(*9*), we determined the prevalence of the *SDHAF3* c.157T>C variant among other subjects either with SDH-related PC/PGL or apparently sporadic PC/PGL, in comparison with normal controls.

Analysis of SDHAF3 c.157T>C variant in a normal population

The frequency of *SDHAF3* c.157T>C in our Australian population was determined by direct sequencing of 100 healthy controls (48% males) with no known

familial association to SDH-related disease. Of 200 alleles assessed, 6 were found to exhibit the minor allele (c.157C [NM_020186], p.Phe53Leu, rs62624461), resulting in a minor allele frequency (MAF) of 0.03, which is consistent with the MAF reported in both 1000 Genomes (Phase 1_ALL) and Exome Aggregation Consortium populations (Table 4.1).

Analysis of SDHAF3 c.157T>C in individuals with SDH-related familial pheochromocytoma and/or paraganglioma

In addition to individual S11_1, an additional 22 unrelated individuals with *SDH* germline mutations and evidence of disease (i.e., presence of pheochromocytoma and/or paraganglioma) were assessed for the presence of *SDHAF3* c.157T>C (Table 4.2). Of these, one additional individual was found to carry *SDHAF3* c.157T>C (S55). This individual (S55) had multiple head and neck paragangliomas, the first (glomus jugulare tumor) being resected at the age of 48. A nodule at the left carotid bifurcation was noted at age 49 (MRI) and has subsequently been monitored, with no evidence of enlargement to date. Taken together, of 23 individuals with *SDH*-related familial pheochromocytoma and/or paraganglioma, two were heterozygous for *SDHAF3* c.157T>C, giving a MAF of 0.043 (Table 4.1) which was not significantly different from our Australian population of healthy controls (p=0.64) nor from the 1000 Genomes (Phase 1_ALL) (p=0.10) or Exome Aggregation Consortium (p=0.2855) populations (Table 4.1). Interestingly, both S11_1 and S55 had germline *SDHB* mutations in addition to the *SDHAF3* c.157T>C variant; and if only *SDHB*-mutated individuals from our cohort were considered, then co-carriage of *SDHAF3* c.157T>C (MAF 0.063) was significantly different from the 1000

Table 4.1. Summary of SDHAF3 c.157T>C (p.Phe53Leu) variant analysis in familial and suspected sporadic pheochromocytoma and/or paraganglioma

Cohort	SDHAF3 F53 germline allele count (T)	SDHAF3 F53L germline allele count (C)	MAF	p value[a] (Australian)	p value[a] (1000Genome)	p value[a] (ExAC)
Disease-affected						
Unrelated SDH-mutation carrier with disease (n=23; alleles=46)	44	2	0.043	0.64	0.1	0.2855
Unrelated SDHB-mutation carrier with disease (n=16; alleles=32)	30	2	0.063	0.35	0.025	0.1005
Apparently sporadic (n=15; alleles=30)	27	3	0.1	0.07	0.0002	0.0025
All disease-affected (familial and sporadic; n=38; alleles=76)	71	5	0.066	0.17	0.0004	0.0063
Disease-free						
Australian (n=100; alleles=200)	194	6	0.03			
1000Genome_Phase 1_ALL[b] (n=1092; alleles=2184)	2153	31	0.014			
ExAC[c] (alleles=120844)	118315	2529	0.02093			

[a]Chi-squared test; [b]McVean *et al* (2012) An integrated map of genetic variation from 1,092 human genomes *Nature* 491:56-65; [c]Exome Aggregation Consortium (ExAC), Cambridge, MA (URL: http://exac.broadinstitute.org), 16 February 2015.

Table 4.2. Summary of SDHAF3 p.Phe53Leu variant analysis in familial SDH-associated individuals

Family ID	Individual ID	Tumor Details	Primary Germline Mutation	Somatic *SDHB* Mutation/Allele Status	Germline *SDHAF3* c.157T>C Status	Somatic *SDHAF3* c.157T>C/Allele Status
S11	1	PC (metastatic)	SDHB (splice-site)	IVS3 + loss normal allele	c.157T>C	c.157T>C + retention normal allele
S50	1	PGL	SDHB (nonsense)	nd	WT	nd
S15	1	PC (metastatic)	SDHB (splice-site)	nd	WT	nd
S18	1	PGL	SDHB (frameshift)	nd	WT	nd
S24	1	PGL	SDHB (splice-site)	nd	WT	nd
S26	1	PGL	SDHB (missense)	nd	WT	nd
S27	1	PGL	SDHB (frameshift)	nd	WT	nd
S52	1	HN PGL	SDHB (nonsense)	nd	WT	nd
S55	1	HN PGL	SDHB (frameshift)	nd	c.157T>C	nd
S59	1	HN PGL	SDHB (nonsense)	nd	WT	nd
S25	1	HN PGL	SDHB (missense)	nd	WT	nd
S10	1	PGL (metastatic)	SDHB (missense + splice-site)	nd	WT	nd
S16	1	PGL (metastatic)	SDHB (splice-site)	nd	WT	nd
S20	1	PC	SDHB (splice-site)	nd	WT	nd
S37	1	PC (metastatic)	SDHB (splice-site)	nd	WT	nd
S44	1	PC (metastatic)	SDHB (frameshift)	nd	WT	nd
S69	1	PGL	SDHC (nonsense)	nd	WT	nd
S82	1	HN PGL	SDHD (missense)	nd	WT	nd
S83	1	PGL	SDHD (missense)	nd	WT	nd
S84	1	HN PGL	SDHD (frameshift)	nd	WT	nd
S88	1	HN PGL	SDHD (frameshift)	nd	WT	nd
S93	1	PC + HN PGL	SDHD (nonsense)	nd	WT	nd
S105	1	HN PGL	SDHA (missense)	nd	WT	nd

Abbreviations: IVS, intervening sequence; nd, not done; PC, pheochromocytoma; PGL, paraganglioma (extra adrenal thoracic/abdominal); HNPGL, head and neck paraganglioma; WT, wild-type

Genomes (Phase 1_ALL) population (p=0.025) but still not different from the Exome Aggregation Consortium (p=0.1005) (Table 4.1).

Analysis of SDHAF3 c.157T>C in individuals with apparently sporadic pheochromocytoma and/or paraganglioma

To further assess the potential role of *SDHAF3* in pheochromoctyomas and/or paragangliomas, 15 tumors of apparently sporadic origin were assessed for the presence of the *SDHAF3* c.157T>C (Table 4.3). Three samples were found to be heterozygous for this variant, giving a MAF of 0.1 (Table 4.1), which was significantly different from the 1000 Genomes (Phase 1_ALL) (p=0.0002) and Exome Aggregation Consortium (p= 0.0025) populations (Table 4.1).

Extension of SDHAF3 c.157T>C analysis in Family S11

In addition to individual S11_1, an additional 14 *SDHB* mutation carrying members of this family (S11) were assessed (Table 4.4). The *SDHAF3* c.157T>C variant was identified in an additional seven *SDHB* mutation carrying family members. Five individuals in this family have (to date) presented with pheochromocytoma and/or paraganglioma (S11_1, S11_2, S11_3, S11_4 and S11_5). Of those with germline *SDHB* mutation and *SDHAF3* variant (n=7), three (43%) have developed pheochromocytomas or paragangliomas (S11_1, S11_2 and S11_3); while two (25%) of those with germline *SDHB* mutation and wild-type *SDHAF3* (n=8) have developed paragangliomas (p=0.47, Chi-squared test). Of note, the tumors of individuals S11_1, S11_2 and S11_4 all exhibited loss of the normal *SDHB* allele and retention of the mutated allele (*SDHB* IVS3

Table 4.3. Summary of SDHAF3 c.157T>C (p.Phe53Leu) variant analysis in pheochromocytoma and/or paraganglioma of suspected sporadic origin

Tumor ID	Tumor Type	Primary Germline Mutation	Somatic *SDHAF3* c.157T>C Status	Germline *SDHAF3* c.157T>C Status
1	PC (benign, 23 years)	none known[a]	WT	nd
2	PC (benign, 45years)	none known[a]	c.157T>C (heterozygous)	c.157T>C (heterozygous)
3	PC (benign, 47 years)	none known[a]	WT	nd
4	PC (benign, 67 years)	none known[a]	WT	nd
5	PC (benign, 58 years)	none known[a]	c.157T>C (heterozygous)	c.157T>C (heterozygous)
6	PC (benign, 75 years)	none known[a]	WT	nd
7	PC (benign, 68 years)	none known[a]	WT	nd
8	PC (benign, 64 years)	none known[a]	WT	nd
9	PC (benign, 47 years)	none known[a]	c.157T>C (heterozygous)	c.157T>C (heterozygous)
10	PC (benign, 67 years)	none known[a]	WT	nd
11	PGL (benign, 36 years)	none known[a]	WT	nd
12	PC (malignant, 56 years)	none known[a]	WT	nd
13	PC (malignant, 52 years)	none known[a]	WT	nd
14	PC (malignant, 49 years)	none known[a]	WT	nd
15	PC (malignant, 37 years)	none known[a]	WT	nd

Abbreviations: nd, not done; PC, pheochromocytoma; PGL, paraganglioma (extra adrenal thoracic/abdominal); WT, wild-type

[a]Germline tests included SDHB (all exons),SDHD (all exons), RET (exon 11 only), and VHL (all exons), and were performed using PCR and denaturing high performance liquid chromatography (dHPLC) as previously described (Meyer-Rochow et al., 2010).

Table 4.4. Summary of SDHAF3 c.157T>C (p.Phe53Leu) variant analysis in Family S11

Family ID	Individual ID	Tumor Details	Primary Germline Mutation	Somatic *SDHB* Mutation/Allele Status	Germline *SDHAF3* c.157T>C Status	Somatic *SDHAF3* c.157T>C/Allele Status
S11	1	PC (18 years) (metastatic, 24 years)	SDHB (IVS3)	IVS3 + loss normal allele	c.157T>C (heterozygous)	c.157T>C + retention normal allele
	2	PC (metastatic, 59 years)	SDHB (IVS3)	IVS3 + loss normal allele	c.157T>C (heterozygous)	na
	3	PGL (30 years)	SDHB (IVS3)	nd	c.157T>C (heterozygous)	nd
	4	PGL (11 years)	SDHB (IVS3)	IVS3 + loss normal allele	WT	WT
	5	PGL (34 years)	SDHB (IVS3)	nd	WT	nd
	6	No evidence of PC/PGL (66 years)	SDHB (IVS3)	nd	c.157T>C (heterozygous)	nd
	7	No evidence of PC/PGL (22 years)	SDHB (IVS3)	nd	c.157T>C (heterozygous)	nd
	8	No evidence of PC/PGL (62 years)	SDHB (IVS3)	nd	c.157T>C (heterozygous)	nd
	9	No evidence of PC/PGL (57 years)	SDHB (IVS3)	nd	c.157T>C (heterozygous)	nd
	10	No evidence of PC/PGL (35 years)	SDHB (IVS3)	nd	WT	nd
	11	No evidence of PC/PGL (34 years)	SDHB (IVS3)	nd	WT	nd
	12	No evidence of PC/PGL (29 years)	SDHB (IVS3)	nd	WT	nd
	13	No evidence of PC/PGL (26 years)	SDHB (IVS3)	nd	WT	nd
	14	No evidence of PC/PGL (23 years)	SDHB (IVS3)	nd	WT	nd
	15	No evidence of PC/PGL (66 years)	SDHB (IVS3)	nd	WT	nd

Abbreviations: IVS, intervening sequence; na, not able to amplify; nd, not done; PC, pheochromocytoma; PGL, paraganglioma; WT, wild-type

splice-site mutation). Additionally, immunohistochemical assessment demonstrated loss of SDHB staining in all three tumors from individuals S11_1, S11_2 and S11_4.

Functional characterization of SDHAF3 p.Phe53Leu in yeast

To test whether the substitution of p.Phe53 residue with Leu is pathogenic, we exploited *S. cerevisiae* as a model organism to conduct biochemical and molecular biological characterization of the p.Phe53Leu variant. The expression of wild-type (WT) SDHAF3 in yeast cells lacking *Sdh7*, a yeast ortholog of *SDHAF3*, enhanced respiratory growth of mutant cells; however, the SDHAF3 p.Phe53Leu variant failed to fully rescue the respiratory growth defect (Fig. 4.1A). Cells lacking *Sdh7* exhibit a modest diminution in SDH activity (*9*). Interestingly, the SDHAF3 p.Phe53Leu variant did not restore SDH activity in *sdh7*Δ cells, in contrast to the effect of WT SDHAF3 (Fig. 4.1B), suggesting that the p.Phe53Leu substitution in SDHAF3 is a hypomorphic mutation that contributes to SDH deficiency.

Since SDHAF3 p.Phe53Leu appeared to be impaired functionally, we first examined whether expression of SDHAF3 p.Phe53Leu is compromised. We found that steady-state levels of SDHAF3 p.Phe53Leu were equal to those of WT SDHAF3 in *sdh7*Δ cells, consistent with stable expression of SDHAF3 p.Phe53Leu (Fig. 4.1C, Lane 1 and 3). Meanwhile, substitution of residues in the LYR motif (p.Tyr13Ala and p.Arg14Ala) dramatically decreased SDHAF3 levels (Fig. 4.1C, Lane 5). Since SDHAF3 p.Phe53Leu appeared to be well expressed compared to WT SDHAF3 in *sdh7*Δ cells, we next interrogated whether SDHAF3 p.Phe53Leu was competent to interact with Sdh2 (a yeast ortholog of *SDHB*) during SDH assembly. Previously, we showed that the steady-

Fig. 4.1. Phe53 substitution with Leu in SDHAF3 leads to the loss of function of SDHAF3 in yeast. **(A)** Respiratory growth of yeast cells expressing a human Sdh7 ortholog, SDHAF3, and its sequences variants. Precultured cells in synthetic complete (SC) media were serially diluted and then spotted on SC media containing different carbon sources, as indicated. Cells were incubated at 30 °C. **(B)** Relative succinate:quinone oxidoreductase (SOQ) activity in isolated mitochondria. Mitochondria were isolated from cells grown until late-log phase in SC media plus 2% raffinose/0.2% glucose. Data are shown as mean ± SD ($n = 3$; $^{**}p < 0.05$). **(C)** Steady-state levels of SDHAF3 proteins in *sdh4*Δ cells. Human SDHAF3 and its mutants under yeast *MET25* promoter were expressed from plasmids in cells. Por1 (porin) is a loading control. **(D)** Steady-state levels of SDHAF3 proteins in response to ectopic expression of Sdh2-His_6Myc_2. Rip1 is the Fe-S cluster subunit of *bc1* complex. **(E)** Co-immunoprecipitation of SDHAF3 was performed with mitochondrial isolated from cells expressing Sdh2-His_6Myc_2 using anti-SDHAF3 antibody and protein A magnetic beads. Anti-HA antibody is a negative control. *, nonspecific reactivity; Input, 1% of total lysates.

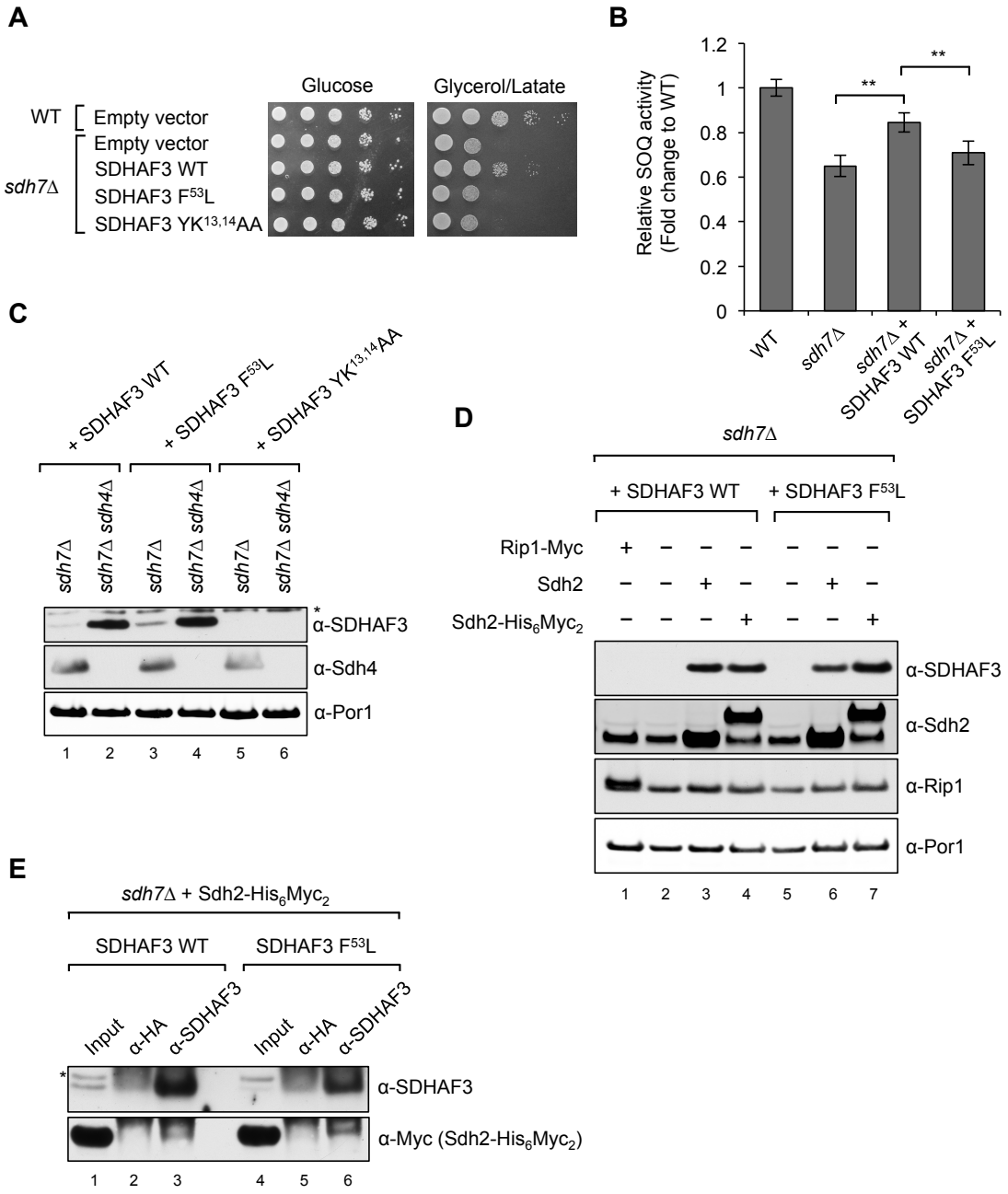
A
Glucose
Glycerol/Latate
WT
Empty vector
sdh7Δ
Empty vector
SDHAF3 WT
SDHAF3 F53L
SDHAF3 YK13,14AA
B
Relative SOQ activity (Fold change to WT)
1.2
1
0.8
0.6
0.4
0.2
0
**
**
WT
sdh7Δ
sdh7Δ + SDHAF3 WT
sdh7Δ + SDHAF3 F53L
C
+ SDHAF3 WT
+ SDHAF3 F53L
+ SDHAF3 YK13,14AA
sdh7Δ
sdh7Δ sdh4Δ
α-SDHAF3
α-Sdh4
α-Por1
1 2 3 4 5 6
D
sdh7Δ
+ SDHAF3 WT
+ SDHAF3 F53L
Rip1-Myc
Sdh2
Sdh2-His6Myc2
α-SDHAF3
α-Sdh2
α-Rip1
α-Por1
1 2 3 4 5 6 7
E
sdh7Δ + Sdh2-His6Myc2
SDHAF3 WT
SDHAF3 F53L
Input
α-HA
α-SDHAF3
α-SDHAF3
α-Myc (Sdh2-His6Myc2)
1 2 3 4 5 6

state levels of Sdh7 increased in cells lacking the membrane anchor domain of SDH as a consequence of the enhanced interaction between Sdh7 and an Sdh1/Sdh2 pre-stalled intermediate (Sdh1, yeast ortholog of SDHA) (*9*). Therefore, we measured SDHAF3 levels in *sdh4*Δ cells where an Sdh1/Sdh2 intermediate accumulates. SDHAF3 p.Phe53Leu as well as WT SDHAF3 accumulated in *sdh4*Δ cells (Fig. 4.1C, Lane 2 and 4), suggesting that SDHAF3 p.Phe53Leu may be capable of interacting with Sdh2. Recently, we observed that Sdh7 levels increased in response to an ectopic expression of Sdh2 in the presence of endogenous Sdh2 (data not shown). Therefore, we tested whether WT SDHAF3 and SDHAF3 p.Phe53Leu levels would also increase when Sdh2 is overexpressed in yeast cells. Indeed, an ectopic expression of Sdh2 or Sdh2-His_6Myc_2 in *sdh7*Δ cells harboring human SDHAF3 alleles resulted in increased levels SDHAF3, regardless of the p.Phe53Leu variation; however, the expression of Myc-tagged Rip1, a target of another LYR motif protein, Mzm1, failed to do so (Fig. 4.1D). We exploited this phenotype to further confirm the physical interaction between SDHAF3 p.Phe53Leu and Sdh2. We performed immunoprecipitation of SDHAF3 p.Phe53Leu with mitochondrial lysates from *sdh7*Δ cells wherein Sdh2-His_6Myc_2 is exogenously expressed. Indeed, Sdh2-His_6Myc_2 was co-precipitated with SDHAF3 p.Phe53Leu by anti-SDHAF3 antibodies, indicating that SDHAF3 p.Phe53Leu can interact with Sdh2 (Fig. 4.1E).

Functional characterization of SDHAF3 p.Phe53Leu
in mammalian cells

Physical interaction between SDHB and SDHAF3 was validated in mammalian cells by co-immunoprecipitation of overexpressed SDHB (GFP-tagged) and SDHAF3

(DDK-tagged) in HEK293 cells. Similar to our observations in yeast, WT SDHB and WT SDHAF3 were shown to interact (Fig. 4.2A). This interaction was impaired with the introduction of the SDHAF3 p.Phe53Leu variant (Fig. 4.2B).

Further assessment of the interaction between SDHB and SDHAF3 was carried out using clinically relevant SDHB mutants. Introduction of SDHB mutants with wild-type SDHAF3 impaired normal SDHB-SDHAF3 interaction to varying degrees (Fig. 4.2A). Interestingly, complete abrogation of the SDHB-SDHAF3 interaction was seen with the SDHB p.Arg242His mutant; reduced interaction was observed for all other mutants, with the exception of the SDHB p.Ile127Ser mutant that appeared to be unaffected. Coupled with the stable SDHB expression observed in whole cell lysates (Fig. 4.2A), the complete loss of interaction observed on introduction of the SDHB p.Arg242His mutant is highly suggestive of this being a putative interaction site for SDHAF3.

The interaction observed between WT SDHB and SDHAF3 p.Phe53Leu was also impaired, to varying degrees, with the introduction of SDHB mutants (Fig. 4.2B). Complete loss of interaction was not only observed with the SDHB p.Arg242His mutant but also with mutants affecting residue 46 (p.Arg46Gly and p.Arg46Gln). Interestingly, enhanced binding was observed with SDHB p.Ile127Ser and p.Cys101Tyr mutants; whereas no effect on interaction was evident with SDHB p.Ala43Pro and p.Pro197Arg mutants. Stable expression of SDHB in whole cell lysates (Fig. 4.2B) indicates these observed changes in SDHB levels, following immunoprecipitation with SDHAF3, are reflective of changes to the SDHB-SDHAF3 interaction. Complete abrogation of SDHB-SDHAF3 interaction, following introduction of SDHB p.Arg46Gly and p.Arg46Gln

Fig. 4.2. SDHAF3 interacts with SDHB in vitro. SDHAF3-SDHB complexes pulled down by DDK-tagged SDHAF3, following 24 hours co-transfection with GFP-tagged SDHB in HEK293 cells, were immunoblotted for GFP and DDK. Stability of SDHB expression was assessed (whole cell lysates), following 24 hours co-transfection with DDK-tagged SDHAF3 and GFP-tagged SDHB in HEK293 cells, when immunoblotted for GFP and GAPDH. **(A)** Interaction of wild-type SDHAF3 with wild-type SDHB is evident (Lane 1); complete abrogation of this interaction can be seen when the SDHB p.Arg242His mutant is introduced (Lane 9); reduced interaction was observed for all other mutants (Lanes 3-5, 7-8) with the exception of SDHB p.Ile127Ser whose interaction was unaffected. Stable SDHB expression was observed in whole cell lysates. **(B)** Introduction of SDHAF3 p.Phe53Leu with wild-type SDHB leads to reduced SDHAF3-SDHB interaction (Lane 1); complete loss of interaction was observed with SDHB p.Arg242His (Lane 9), p.Arg46Gly (Lane 4) and p.Arg46Gln (Lane 5); interaction with SDHB p.Ala43Pro and p.Pro197Arg was unaffected; while binding was enhanced with SDHB p.Ile127Ser and p.Cys101Tyr mutants. Stable SDHB expression was observed in whole cell lysates. **(C)** Relative succinate dehydrogenase (SDH) and succinate:quinone oxidoreductase (SQR) activity with Sdh2 $R^{235}H$ in isolated mitochondria. Mitochondria were isolated from cells grown until late-log phase in SC media plus 2% raffinose/0.2% glucose. Data are shown as mean ± SD ($n = 3$; $^{**}p < 0.05$). **(D)** Blue native-PAGE analysis to visualize mature SDH complexes. Mitochondrial lysates extracted with 1% digitonin were separated on BN-PAGE and then transferred to membranes for immunoblotting. III_2IV_2 is a supercomplex consisting of complex III and complex IV as a loading control. **(E)** Porcine succinate dehydrogenase (PDB: 1ZOY). SDHA (gray ribbon); SDHB (blue ribbon); SDHC (green ribbon); SDHD (Brown ribbon); Fe-S centers, [2Fe–2S], [4Fe–4S], [3Fe–4S] from the bottom (red and yellow sphere); Ubiquinone in the Q binding site (magenta stick); Arg242, corresponding to Arg235 in yeast (red stick).

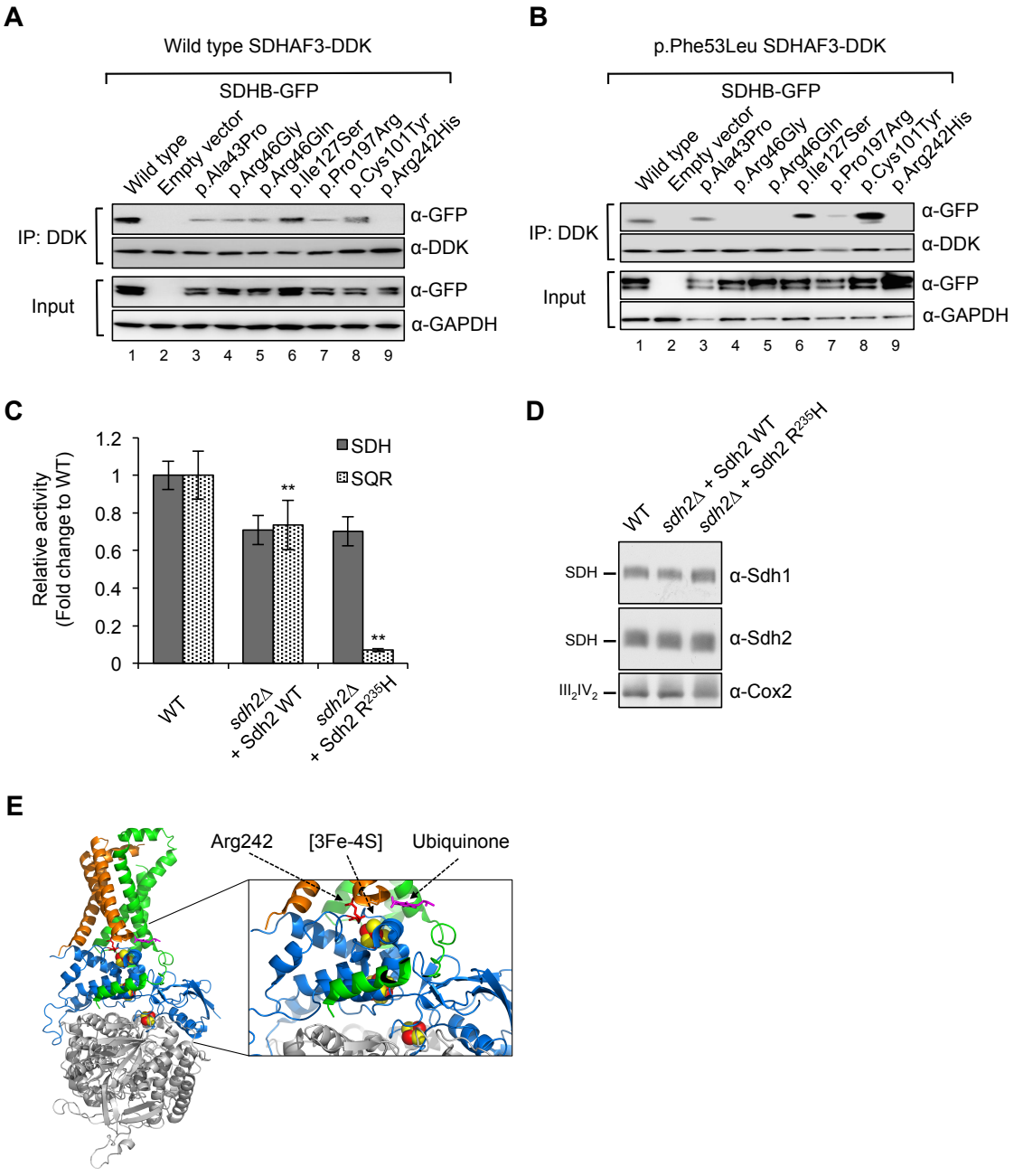
A
Wild type SDHAF3-DDK
SDHB-GFP
Wild type
Empty vector
p.Ala43Pro
p.Arg46Gly
p.Arg46Gln
p.Ile127Ser
p.Pro197Arg
p.Cys101Tyr
p.Arg242His
IP: DDK
α-GFP
α-DDK
Input
α-GFP
α-GAPDH
1 2 3 4 5 6 7 8 9
B
p.Phe53Leu SDHAF3-DDK
SDHB-GFP
Wild type
Empty vector
p.Ala43Pro
p.Arg46Gly
p.Arg46Gln
p.Ile127Ser
p.Pro197Arg
p.Cys101Tyr
p.Arg242His
IP: DDK
α-GFP
α-DDK
Input
α-GFP
α-GAPDH
1 2 3 4 5 6 7 8 9
C
Relative activity
(Fold change to WT)
1.2
1
0.8
0.6
0.4
0.2
0
SDH
SQR
**
**
WT
sdh2Δ + Sdh2 WT
sdh2Δ + Sdh2 R235H
D
WT
sdh2Δ + Sdh2 WT
sdh2Δ + Sdh2 R235H
SDH
α-Sdh1
SDH
α-Sdh2
III2IV2
α-Cox2
E
Arg242
[3Fe-4S]
Ubiquinone

mutants with SDHAF3 p.Phe53Leu (Fig. 4.2B), indicates that residue 46 of SDHB may also be involved in binding SDHAF3.

Additional studies in yeast revealed that Sdh2 p.Arg235His, which corresponds to the SDHB p.Arg242His mutation, resulted in impairment of SDH function. Compared to Sdh2 WT, *sdh2*Δ cells expressing Sdh2 p.Arg235His exhibited reduced succinate:quinone oxidoreductase (SQR) activity (Fig. 4.2C). Interestingly, the substitution of p.Arg235 with His did not affect succinate dehydrogenase (SDH) activity (Fig. 4.2C) and SDH assembly (Fig. 4.2D). The 3Fe-4S cluster in SDHB is in close juxtaposition to p.Arg242 (Fig. 4.2E). The 3Fe-4S cluster in SDHB is essential for electron transfer to ubiquinone in the Q binding site in between SDHB and SDHC. Previously, we have shown that SDHAF3 confers protection on SDHB against reactive oxygen species (ROS) during SDHB maturation with Fe-S clusters (*9*). Given that p.Arg242 in SDHB (p.Arg235 in Sdh2) is critical for the interaction between SDHB and SDHAF3 (Fig. 4.2A, lane 9), it is possible that the 3Fe-4S cluster may become more susceptible to ROS-related damage in SDHB p.Arg242His mutants. However, we cannot completely rule out the possibility that the Q binding site is altered in cells harboring SDHB p.Arg242His.

Discussion

In this study, we have identified a variant in the SDH assembly factor 3 (*SDHAF3*, c.157T>C [p.Phe53Leu]) associated with increased prevalence of pheochromocytoma and/or paraganglioma. Studies in yeast confirm this to be a loss-of-function variant, leading to reduced SDH activity. Furthermore, our in vitro studies in

human cells show that SDHAF3 interacts with SDHB (residues 46 and 242), and that interaction between SDHAF3 p.Phe53Leu and SDHB is impaired.

SDH plays an integral role in both the tricarboxylic acid cycle and electron transport chain. Germline mutations within any of its four subunits (SDHA, B, C and D) have been associated with development of a number of tumors, including pheochromocytoma and/or paraganglioma, gastrointestinal stromal tumors, renal cancer and pituitary adenomas (*1*). Recently, SDH assembly factors (SDHAF1-4) have been identified as playing a role in maturation of individual SDH subunits and assembly of the functioning SDH complex as a whole (*25*). To date, loss-of-function mutations in *SDHAF1* (biallelic) and *SDHAF2* have been associated with infantile leukoencephalopathy (*11, 12*) and head and neck paragangliomas (*8, 13, 14*), respectively. More recently, the yeast orthologs for SDHAF1 (Sdh6) and SDHAF3 (Sdh7) were shown to shield the Fe-S clusters of the yeast ortholog for SDHB (Sdh2), thereby promoting maturation of SDHB (*9*). Further, two LYR motifs within SDHB (residues 44-46 and 240-242) have been speculated to play a role in the incorporation of its Fe-S clusters (*15*). Taken together, we hypothesized that mutations within the newly identified SDH assembly factor, *SDHAF3*, may be associated with the pathogenesis of pheochromocytoma and/or paraganglioma syndromes.In this study, we identified a *SDHAF3* c.157T>C (p.Phe53Leu) variant in familial and sporadic cases of pheochromocytoma/paraganglioma (PC/PGL), observing a minor allele frequency (MAF) of 0.066. Although this variant (rs62624461) is reported with a MAF of 0.021 in the Exome Aggregation Consortium (ExAC) database (http://exac.broadinstitute.org/), reflecting exome variant data from over 60,000 individuals, the prevalence is

significantly higher in PC/PGL (6.6% versus 2.1%, p=0.0063). This prompted us to perform additional studies to clarify the role that the SDHAF3 p.Phe53Leu variant may play in the pathogenesis of PC/PGL. Through yeast studies, we were able to show that introduction of the SDHAF3 p.Phe53Leu variant into *Sdh7* null yeast (ortholog of *SDHAF3* in humans) resulted in impaired function, observed by its failure to fully restore SDH activity when expressed in *Sdh7* null yeast relative to wild-type (WT) SDHAF3. Taken together, these findings indicate that although SDHAF3 p.Phe53Leu is at best a very low penetrance allele for PC/PGL *per se*, it may play a modifying role as observed by its hypomorphic activity. Hypomorphic alleles of SDHAF3 may contribute to the pathology in SDH-deficient tumors with residual SDH subunits, or alternatively through a secondary unidentified function of SDHAF3. In this study, two PC/PGL tumors from patients harboring germline *SDHB* (IVS3 splice-site) mutation and *SDHAF3* (c.157T>C) variant showed loss of SDHB staining by immunohistochemistry. This raises the question of how *SDHAF3* c.157T>C can play a role in PC/PGL tumorigenesis, in SDH-deficient tumors. Clearly, by the time that inactivation of both *SDHB* alleles has occurred in the tumor, *SDHAF3* c.157T>C presumably has no additional role, as SDHAF3 appears to interact specifically with SDHB. Nevertheless, we conjecture that the germline presence of this hypomorphic *SDHAF3* c.157T>C allele may over time lead to instability of SDH. Further, as *SDHB* is a known tumor suppressor and hence requires inactivation of both alleles for tumorigenesis, the timeframe between *SDHB* germline (first hit) and somatic loss of the normal *SDHB* allele (second hit) provides a means by which the *SDHAF3* c.157T>C allele could act. Further research is needed to resolve this issue.

To further understand the role of SDHAF3, and the impact of p.Phe53Leu in

greater detail, we assessed its ability to interact with SDHB. Our in vitro studies in human cells, confirmed previous findings in yeast (*9*), with wild-type SDHAF3 shown to interact with SDHB. Interestingly, this interaction was attenuated on introduction of the p.Phe53Leu variant. We wanted to assess SDHAF3-SDHB interaction further by introducing clinically relevant SDHB mutations. Interaction between wild-type SDHAF3 and SDHB p.Arg242His mutant was not observed, implicating this region of SDHB as a direct binding site for SDHAF3. This finding is supported by observations in yeast, whereby Sdh6 and Sdh7 (orthologs of human SDHAF1 and SDHAF3, respectively) have been shown to interact with Sdh2 (ortholog of human SDHB) (*9*), although the specific binding site(s) enabling these interactions were not identified. Interestingly, Maio *et al* (2014) recently showed that the LYR motif of SDHB, affecting residues p.240-242, was not an SDHAF1 binding site, as substitution of these three residues with alanines failed to disrupt SDHBs ability to bind to SDHAF1 (*15*). Our study shows that SDHAF3, in fact, is a direct binding partner for the LYR motif of SDHB (p.240-242). Reduced interaction was observed in all other SDHB mutants, with the exception of p.Ile127Ser in which interaction between SDHAF3 and SDHB appeared to be unaffected, indicating that this residue has no bearing on SDHB interaction with SDHAF3.

On introduction of the SDHAF3 p.Phe53Leu variant, SDHAF3-SDHB interaction was completely lost for SDHB p.Arg46Gln and p.Arg46Glyn mutants, implicating residue 46 as another region of SDHB that may interact with SDHAF3. Although these two regions are spatially separated in two distinct sub-domains, SDHAF3 may bind residues in each domain. Alternatively, the impaired binding may arise from secondary consequences of the p.Arg46 mutation. Interestingly, our previous structural modeling of

these *SDHB* mutations had not identified the functional impact on SDHB, as both glycine and glutamine are capable of fitting within the space left by arginine, and the electron path is not nearby (*24*). The findings of our current study suggest that mutations affecting residue 46 of SDHB are pathogenic via preventing maturation of SDHB. A similar effect was noted by Maio *et al*. (2014), whereby the SDHB p.Arg46Gln mutation did not impair SDHB interaction with HSC20, although reduced binding to the HSC20 complex and SDHA were noted, suggestive of an effect on formation of a mature SDH complex (*15*).

Interestingly, introduction of the SDHAF3 p.Phe53Leu variant resulted in a stronger SDHAF3-SDHB interaction in the presence of the SDHB p.Cys101Tyr mutant. Since Cys101 is a ligand to the 2Fe-2S center in the N-terminal domain of SDHB, the enhanced interaction is suggestive that SDHAF3 interacts with apo-SDHB. Consistent with this prediction is the observation that over-expression of *SDH2* in yeast lacking Sdh1 results in a profound stabilization of Sdh7 (SDHAF3) (U.N., unpublished data). SDHAF3 may, therefore, contribute to the Fe-S cluster insertion process in SDHB.

Our studies have revealed novel insights into the biogenesis of SDH, uncovering a vital interaction between SDHAF3 and SDHB. We have shown that SDHAF3 interacts directly with SDHB (residue 242 being key to this interaction), and that a variant in *SDHAF3* (c.157T>C [p.Phe53Leu]) is more prevalent in individuals with pheochromocytomas and/or paragangliomas, and is hypomorphic via impaired interaction with SDHB.

Declaration of interest

The authors declare that there is no conflict of interest that could be perceived as prejudicing the impartiality of the research reported.

Funding

This work was supported by grants from the Hillcrest Foundation (Perpetual Trustees to D.E.B., B.G.R.), Pheo Para Alliance (T.D., R.C.B., D.E.B., K.M.T., B.G.R.), National Institutes of Health (RO1 GM110755-01 to D.R.W) and Huntsman Cancer Institute (P30 CA042014 to D.R.W).

Acknowledgements

The authors are extremely grateful to all of the patients, families and clinicians associated with the Australian SDH Consortium; the Kolling Neuroendocrine Tumour Bank; the Kolling Institute Healthy Volunteers Bank; and Adam Dwight for assistance with bioinformatics.

References

1. P. L. Dahia, Pheochromocytoma and paraganglioma pathogenesis: learning from genetic heterogeneity. *Nat. Rev. Cancer* **14**, 108-119 (2014).

2. N. Burnichon *et al.*, Integrative genomic analysis reveals somatic mutations in pheochromocytoma and paraganglioma. *Hum. Mol. Genet.* **20**, 3974-3985 (2011).

3. P. L. Dahia *et al.*, A HIF1alpha regulatory loop links hypoxia and mitochondrial signals in pheochromocytomas. *PLoS Genet.* **1**, 72-80 (2005).

4. E. Lopez-Jimenez *et al.*, Research resource: Transcriptional profiling reveals different pseudohypoxic signatures in SDHB and VHL-related pheochromocytomas. *Mol. Endocrinol.* **24**, 2382-2391 (2010).

5. J. K. Killian *et al.*, Succinate dehydrogenase mutation underlies global epigenomic divergence in gastrointestinal stromal tumor. *Cancer Discov.* **3**, 648-657 (2013).

6. E. Letouze *et al.*, SDH mutations establish a hypermethylator phenotype in paraganglioma. *Cancer Cell* **23**, 739-752 (2013).

7. M. Xiao *et al.*, Inhibition of alpha-KG-dependent histone and DNA demethylases by fumarate and succinate that are accumulated in mutations of FH and SDH tumor suppressors. *Genes Dev.* **26**, 1326-1338 (2012).

8. H. X. Hao *et al.*, SDH5, a gene required for flavination of succinate dehydrogenase, is mutated in paraganglioma. *Science* **325**, 1139-1142 (2009).

9. U. Na *et al.*, The LYR factors SDHAF1 and SDHAF3 mediate maturation of the iron-sulfur subunit of succinate dehydrogenase. *Cell Metab.* **20**, 253-266 (2014).

10. J. G. Van Vranken *et al.*, SDHAF4 promotes mitochondrial succinate dehydrogenase activity and prevents neurodegeneration. *Cell Metab.* **20**, 241-252 (2014).

11. D. Ghezzi *et al.*, SDHAF1, encoding a LYR complex-II specific assembly factor, is mutated in SDH-defective infantile leukoencephalopathy. *Nat. Genet.* **41**, 654-656 (2009).

12. A. Ohlenbusch *et al.*, Leukoencephalopathy with accumulated succinate is indicative of SDHAF1 related complex II deficiency. *Orphanet. J. Rare Dis.* **7**, 69 (2012).

13. J. P. Bayley *et al.*, SDHAF2 mutations in familial and sporadic paraganglioma and phaeochromocytoma. *Lancet Oncol.* **11**, 366-372 (2010).

14. H. P. Kunst *et al.*, SDHAF2 (PGL2-SDH5) and hereditary head and neck paraganglioma. *Clin. Cancer Res.* **17**, 247-254 (2011).

15. N. Maio *et al.*, Cochaperone binding to LYR motifs confers specificity of iron sulfur cluster delivery. *Cell Metab.* **19**, 445-457 (2014).

16. A. J. Gill *et al.*, Immunohistochemistry for SDHB triages genetic testing of SDHB, SDHC, and SDHD in paraganglioma-pheochromocytoma syndromes. *Hum. Pathol.* **41**, 805-814 (2010).

17. A. McKenna *et al.*, The Genome Analysis Toolkit: a MapReduce framework for analyzing next-generation DNA sequencing data. *Genome Res.* **20**, 1297-1303 (2010).

18. K. Wang, M. Li, H. Hakonarson, ANNOVAR: functional annotation of genetic variants from high-throughput sequencing data. *Nucleic Acids Res.* **38**, e164

(2010).

19. T. Z. Cui, A. Conte, J. L. Fox, V. Zara, D. R. Winge, Modulation of the respiratory supercomplexes in yeast: enhanced formation of cytochrome oxidase increases the stability and abundance of respiratory supercomplexes. *J. Biol. Chem.* **289**, 6133-6141 (2014).

20. B. S. Glick, L. A. Pon, Isolation of highly purified mitochondria from Saccharomyces cerevisiae. *Methods Enzymol.* **260**, 213-223 (1995).

21. I. Wittig, H. P. Braun, H. Schagger, Blue native PAGE. *Nat. Protoc.* **1**, 418-428 (2006).

22. H. J. Kim, M. Y. Jeong, U. Na, D. R. Winge, Flavinylation and assembly of succinate dehydrogenase are dependent on the C-terminal tail of the flavoprotein subunit. *J. Biol. Chem.* **287**, 40670-40679 (2012).

23. K. S. Oyedotun, P. F. Yau, B. D. Lemire, Identification of the heme axial ligands in the cytochrome b562 of the Saccharomyces cerevisiae succinate dehydrogenase. *J. Biol. Chem.* **279**, 9432-9439 (2004).

24. E. Kim *et al.*, Structural and functional consequences of succinate dehydrogenase subunit B mutations. *Endocr. Relat. Cancer* **22**, 387-397 (2015).

25. J. G. Van Vranken, U. Na, D. R. Winge, J. Rutter, Protein-mediated assembly of succinate dehydrogenase and its cofactors. *Crit. Rev. Biochem. Mol. Biol*. **50**, 168-180 (2015).

CHAPTER 5

ROLE OF NFU1 AND BOLA3 IN IRON-SULFUR CLUSTER TRANSFER TO MITOCHONDRIAL CLIENTS

Andrew Melber,[1] Un Na,[1] Ajay Vashisht,[2] James Wohlschlegel,[2] Dennis R. Winge[1]

[1] Departments of Medicine, Biochemistry, University of Utah Health Sciences Center, Salt Lake City, Utah 84132

[2] Department of Biological Chemistry, David Geffen School of Medicine at UCLA, Los Angeles, CA 90095-1737

Introduction

A severe syndrome characterized by the dysfunction of multiple mitochondrial enzymes has been described for a series of patients with mutations in three mitochondrial proteins IBA57, NFU1 and BOLA3 (*1-7*). These patients presented with lactic acidosis, nonketotic hyperglycinemia and infantile encephalopathy, typically leading to death in their first year of life. The biochemical phenotype was associated with an impairment of the 2-oxoacid dehydrogenases arising from defective lipoate synthesis and defects in respiratory complexes I and II in select tissues, including muscle and liver. The syndrome presents due to defective iron-sulfur (Fe-S) cluster synthesis within the mitochondria. The defect in protein lipolyation is due to impaired activity of lipoic acid synthetase, which requires a [4Fe-4S] cluster cofactor (*8*). The hyperglycinemic phenotype arises from failed lipolyation of the glycine cleavage enzyme. IBA57 is a known component of the ISA complex that functions in the formation of [4Fe-4S] clusters in mitochondria (*9, 10*). Yeast cells lacking Nfu1 are partially compromised in mitochondrial [4Fe-4S] cluster formation, but the defect is not as pronounced as in cells lacking the components of the ISA complex (Isa1, Isa2 and Iba57) (*3, 11*). As in patient cells with mutations in NFU1, yeast *nfu1*Δ cells have diminished protein lipoylation levels (*3*). Humans and yeast have two mitochondrial BolA proteins BolA1 (Bol1 in yeast) and BolA3 (Bol3 in yeast) (*12*), but little is known concerning their physiological function. The similarities in phenotypes of patients with mutations in NFU1 and BOLA3 suggest that BOLA3 may likewise function in mitochondrial Fe-S biogenesis.

Fe-S cluster synthesis within the mitochondria occurs on a scaffold complex and preformed clusters are subsequently transferred to recipient proteins (*13*). The initial

cluster formed is a [2Fe-2S] cluster assembled on the ISU complex consisting of four proteins, Nfs1, Isd11, Yfh1 and Isu1 (or Isu2; yeast nomenclature) (*13-15*). The sulfide ions are provided by the Nfs1 cysteine desulfurase, along with its effector proteins Isd11 and Yfh1 (*15-21*). Assembled [2Fe-2S] clusters on Isu1 are transferred to the monothiol glutaredoxin Grx5 through the action of the Ssq1 ATPase and DnaJ protein Jac1 (*22-24*). Two [2Fe-2S] clusters are condensed into a [4Fe-4S] cluster on the downstream ISA complex (Isa1, Isa2 and Iba57) (*9, 10, 25, 26*).

Nfu1 has been implicated to act as a late Fe-S maturation factor in bacteria and yeast (*3, 27*), but also suggested to be an alternate scaffold protein (*2, 28*). The lack of NfuA in *E. coli* and *Azobacter vinelandii* is associated with decreased viability under stress conditions (*27, 29, 30*). BolA proteins typically function with glutaredoxins (*31*); therefore, one prediction is that BolA3 and/or BolA1 has a role in conjunction with Grx5 downstream of [2Fe-2S] formation.

Nfu proteins from most species are multidomain proteins. One common feature of Nfu proteins is a conserved domain containing a functionally important CxxC sequence motif. The *E. coli* NfuA and human Nfu1 proteins consist of two domains with the C-terminal domain containing the key CxxC motif (*28, 29*). The N-terminal domains differ between the *E. coli* and human proteins and lack a conserved CxxC motif. The conserved CxxC-containing domain is known to bind a [4Fe-4S] cluster, likely at a homodimer interface (*28-30*). Recombinant expression and purification of *Azobacter* NfuA or human Nfu1 did not result in Fe-S cluster bound to the purified protein, but in vitro Fe-S reconstitution studies followed by Mössbauer spectral studies demonstrated the presence of a [4Fe-4S] cluster (*28-30*). The ability of Nfu1 to bind a [4Fe-4S] cluster supported the

suggestions that Nfu1 was either an alternative scaffold protein involved in Fe-S cluster formation or involved in a late cluster transfer step. The ability of bacterial NfuA to transfer its cluster to apo-aconitase is consistent with a role in late step cluster transfer (*29, 30*).

BolA proteins are also known to coordinate Fe-S clusters in conjunction with monothiol glutaredoxins. *Arabidopsis thaliana* contain three BolA proteins, one of which, BolA1, binds a [2Fe-2S] cluster in a complex with glutaredoxin (Grx) (*32*). In this BolA:Grx complex two thiolates, one each from Grx and an associated glutathione, and two histidyl residues from BolA1 coordinated the cluster. Likewise, the cytosolic BolA2 proteins of yeast and humans coordinate [2Fe-2S] clusters at the heterodimer interface with monothiol glutaredoxins (*31, 33*). Little is known about the physiological function of mitochondrial BolA proteins. BolA proteins are found only in aerobic species (*12*). Depletion of the mitochondrial BolA1 in HeLa cells caused an oxidative shift in the mitochondrial thiol/disulfide redox ratio (*12*).

We set out to define the functional steps of Nfu1 and the two mitochondrial BolA proteins in yeast. We report that Nfu1 and BolA3 function in late step transfer of Fe-S clusters from the ISA complex to mitochondrial client proteins. In contrast to BolA3, the related mitochondrial BolA1 shows an interaction with Grx5 but not Fe-S client proteins.

Results

Nfu1 is associated with mitochondrial [4Fe-4S] cluster formation

S. cerevisiae cells lacking the mitochondrial Nfu1 protein (*nfu1*Δ cells) are markedly impaired in growth on synthetic complete medium with acetate as a carbon

source (Fig. 5.1A). However, the cells exhibit only a modest growth impairment on glycerol/lactate medium, suggesting a partial defect in respiratory growth that is exacerbated with acetate as the carbon source. It was previously reported that *nfu1*Δ cells exhibit specific but partial defects in formation of [4Fe-4S] clusters analogous to phenotypes seen in patients with mitochondrial dysfunctions syndrome (*3*). We confirmed the defects in [4Fe-4S] enzymes reported for *nfu1*Δ cells showing that aconitase and succinate dehydrogenase (SDH) activities are markedly impaired, but residual active enzymes persist (Fig. 5.1B). Whereas aconitase activity is markedly attenuated in *nfu1*Δ yeast cells, its level is not significantly depleted in human *nfu1* patients (*2, 3*). No defect was observed in the yeast mutant in respiratory complex III, cytochrome bc_1, which requires a [2Fe-2S] cluster in its Rieske subunit (Fig. 5.1B). Consistent with the known defects of *nfu1*Δ yeast cells and human *nfu1* patients, lipoic acid (LA) conjugates on pyruvate dehydrogenase and oxoglutarate dehydrogenase were attenuated in *nfu1*Δ cells (Fig. 5.1C). As mentioned, lipoic acid formation is dependent on the [4Fe-4S] lipoic acid synthase Lip5 (*8*). Steady-state protein analysis by SDS-PAGE showed diminished Sdh2 levels, the Fe-S subunit of SDH. Sdh2 contains three distinct Fe-S clusters ([2Fe-2S], [4Fe-4S] and [3Fe-4S] clusters), which transfer electrons from the catalytic Sdh1 subunit to ubiquinone. In the absence of Fe-S cluster insertion, the Sdh2 stability is compromised (Fig. 5.1C). In contrast, aconitase protein stability is not as sensitive to the presence of its [4Fe-4S] cluster.

Two enzymes involved in yeast lysine biosynthesis Aco2 and Lys4 contain [4Fe-4S] clusters (*34*). Whereas yeast lacking the ISA complex are auxotrophic for lysine and accumulate homocitrate as a metabolic intermediate, *nfu1*Δ cells propagate normally in

Fig. 5.1. Cells lacking Nfu1 exhibit defects in [4Fe-4S] cluster enzymes in mitochondria. **(A)** Respiratory growth defects revealed by yeast drop-test. Cells harboring empty vectors (EV) or high-copy plasmids expressing designated genes were precultured in liquid synthetic complete (SC) glucose media lacking uracil. Serially diluted cells (10-fold) were spotted on SC media plates supplemented with different carbon sources, and then incubated at 30°C. **(B)** Relative activity of aconitase, SDH, cytochrome bc_1, cytochrome *c* oxidase (CcO), and malate dehydrogenase were measured in isolated mitochondria from cells cultured in SC media with 2% raffinose. Data are shown as mean ± SE (n=3). **(C)** Steady-state protein levels measured by SDS-PAGE followed by immunoblotting in isolated mitochondria. Anti-LA antibody is an antibody specific to lipoic acid (LA) that is conjugated to proteins. **(D)** Restoration of Sdh2 protein shown by SDS-PAGE followed by immunoblotting in isolated mitochondria from *nfu1*Δ cells over-expressing suppressors from panel A. Grx5 is a monothiol glutaredoxin. Isa1, Isa2 and Iba57 are subunits of the ISA scaffold complex required for [4Fe-4S] cluster synthesis. PDH is pyruvate dehydrogenase and KDH is α-ketoglutarate dehydrogenase. Sdh2 is the Fe-S cluster subunit of SDH. Aco1 is mitochondrial aconitase. Por1 is a mitochondrial loading control. Yap1 is a transcription factor that induces expression of anti-oxidant genes.

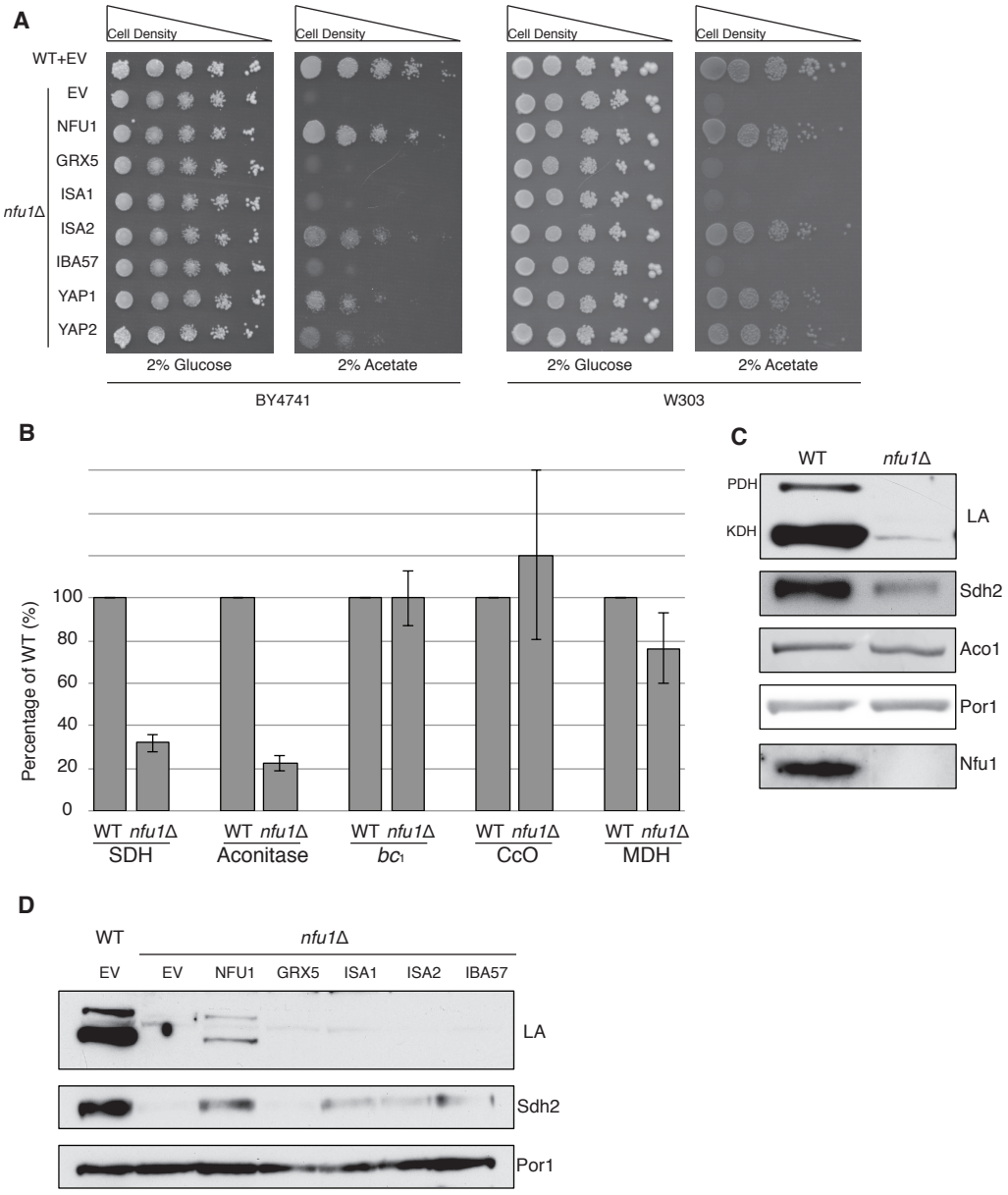
A
Cell Density
Cell Density
Cell Density
Cell Density
WT+EV
EV
NFU1
GRX5
ISA1
ISA2
IBA57
YAP1
YAP2
nfu1Δ
2% Glucose
2% Acetate
2% Glucose
2% Acetate
BY4741
W303
B
Percentage of WT (%)
100
80
60
40
20
0
WT nfu1Δ
SDH
WT nfu1Δ
Aconitase
WT nfu1Δ
bc1
WT nfu1Δ
CcO
WT nfu1Δ
MDH
C
WT
nfu1Δ
PDH
KDH
LA
Sdh2
Aco1
Por1
Nfu1
D
WT
nfu1Δ
EV
EV
NFU1
GRX5
ISA1
ISA2
IBA57
LA
Sdh2
Por1

medium lacking lysine and do not accumulate homocitrate as shown by GC-MS metabolomic studies (data not shown). Thus, sufficient [4Fe-4S] cluster synthesis and distribution occurs in *nfu1*Δ cells for lysine synthesis.

The growth defect of *nfu1*Δ yeast cells on acetate medium was severe, creating an opportunity to conduct screens for genetic suppressors of the respiratory defect. In a screen using transformants with a yeast high-copy cDNA library, we isolated respiratory competent vector-borne clones of *nfu1*Δ BY4741 cells containing *NFU1*, *ISA2*, and *YAP2*. Each gene was recloned into yeast vectors and *nfu1*Δ transformants of both BY4741 and W303 genetic backgrounds were analyzed for growth on acetate medium and respiratory function. Although Isa2 is a component of the mitochondrial ISA heterotrimeric complex comprised of Isa1, Isa2 and Iba57, overexpression of Isa2 was the only ISA component capable of restoring respiratory growth of *nfu1*Δ cells on acetate medium (Fig. 5.1A) and glycerol/lactate (data not shown). *ISA2* transformants of *nfu1*Δ cells showed restoration of SDH levels, suggesting that the respiratory capacity of the mutant cells was partially restored by elevated Isa2 levels (Fig. 5.1D). Thus, the respiratory function of Nfu1 can be partially replaced by super-physiological levels of the Isa2 component of the ISA complex.

Nfu1 is necessary for protecting Fe-S clusters from oxidative damage

Partial respiratory function of *nfu1*Δ cells was also restored by overexpression of Yap2 or its paralogue Yap1 (Fig. 5.1A). Yap1 and Yap2 are transcriptional activator that induces the expression of a battery of antioxidant genes, including thioredoxin, thioredoxin reductase and glutathione reductase, in response to oxidative stress (*35*). To

confirm that the suppression of *nfu1*Δ cells by the YAP transcription factors was specifically due to a recovery of the [4Fe-4S] centers, we analyzed mitochondria from the transformants to test for restoration of respiratory function. A modest restoration of LA conjugates of PDH and KDH was seen (Fig. 5.2A). The identification of *YAP1* and *YAP2* as high copy suppressors of *nfu1*Δ cells suggested the potential importance of Nfu1 during oxidative stress.

To further understand the importance of Nfu1 function during oxidative stress, we grew *nfu1*Δ cells on glycerol/lactate medium with or without paraquat, a superoxide generator. Interestingly, *nfu1*Δ cells with Isa2 overexpression, unlike the presence of Nfu1, did not exhibit any enhanced resistance to paraquat. The presence of paraquat in the growth medium exacerbated the respiratory growth defect of *nfu1*Δ cells (Fig. 5.2B). In addition, respiratory growth of *nfu1*Δ cells is partially restored with the addition of the antioxidants, GSH and N-acetyl cysteine (NAC) to the growth medium (Fig. 5.2C). These results support an important role for Nfu1 during oxidative metabolism.

If Nfu1 is important during oxidative cell conditions, we tested whether Nfu1 is expendable during anoxic growth. WT and *nfu1*Δ cells were cultured to mid-log growth in normoxic or anoxic conditions. Mitochondria isolated from the cells were analyzed by steady-state protein analysis and enzymatic function of various [4Fe-4S] cluster enzymes. Whereas normoxic *nfu1*Δ cells exhibited the expected marked attenuation in SDH and aconitase activities and reduced lipoic acid adducts, the anoxic cells did not exhibit a significant difference between WT and *nfu1*Δ cells (Fig. 5.2, D and E). It should be noted that anoxic WT cells showed a marked reduction in mitochondrial enzymatic activities and steady-state protein levels compared to normoxic WT cells, yet anoxic *nfu1*Δ cells

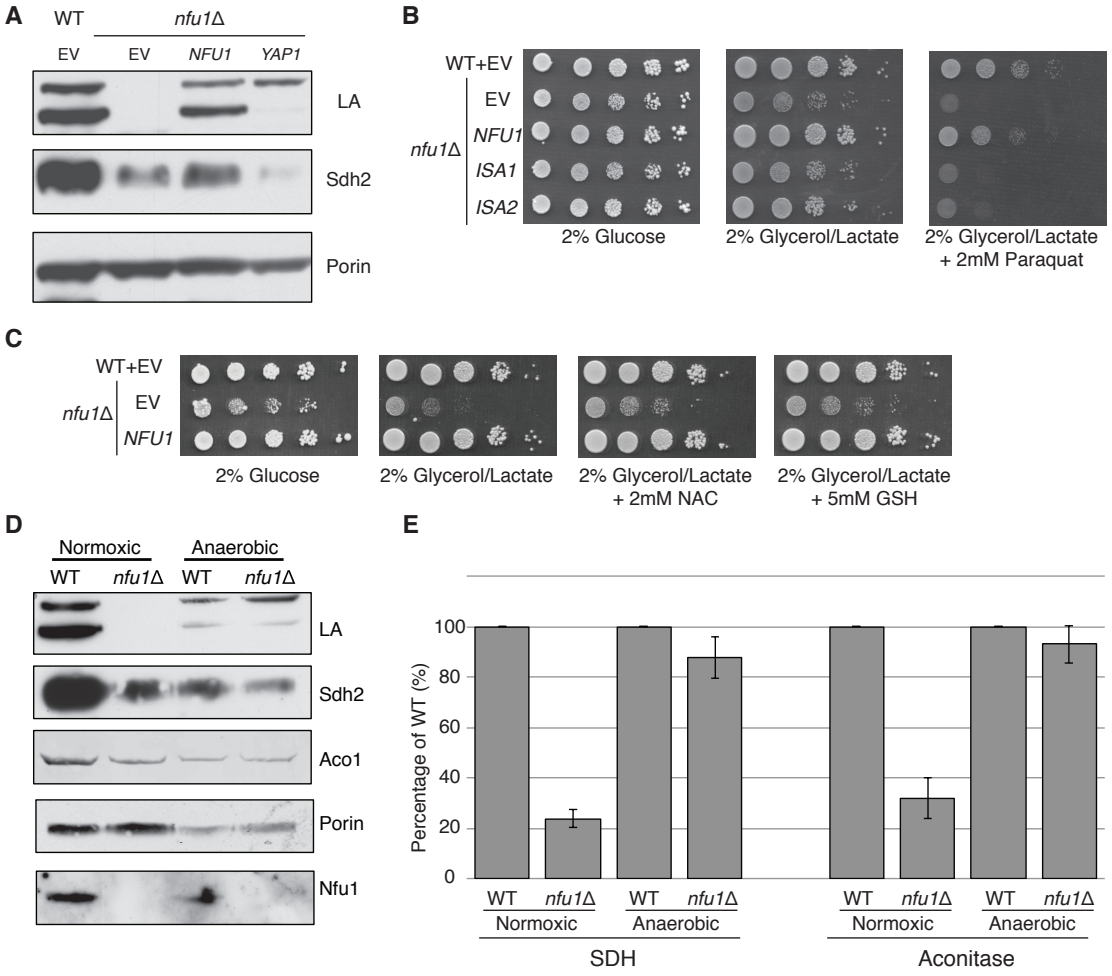

Fig. 5.2. Defects in cells lacking Nfu1 are pronounced under oxidative stress conditions. **(A)** Steady-state levels of proteins in isolated mitochondria from nfu1Δ cells harboring high-copy NFU1 plasmids or YAP1 plasmids. **(B)** Yeast drop-test with paraquat supplementation. **(C)** Yeast drop-test with n-acetyl cysteine (NAC) and glutathione (GSH). **(D)** Steady-state levels of proteins in isolated mitochondria from cells cultured under normoxic conditions or anaerobic conditions. **(E)** Relative activity of SDH and aconitase in mitochondria from panel D. Data are shown as mean ± SE (n=3).

did not show a marked further attenuation in SDH and lipoic acid conjugates. Thus, cells are more dependent on Nfu1 in oxidative metabolism.

Nfu1 binds the ISA complex and [4Fe-4S] client proteins

An association of Nfu1 with the mitochondrial ISA complex (involved in [4Fe-4S] clusters) was suggested by the observed suppression of the respiratory defect of *nfu1*Δ cells by Isa2 overexpression along with defects in 4Fe-4S mitochondrial enzymes. We tested if Nfu1 physically interacts with the ISA complex by co-immunoprecipitation studies using a functional C-terminal Strep tagged chimera of Nfu1. Affinity purification of Nfu1-Strep with Strep-Tactin beads showed co-purification of Isa1 and Isa2 (Fig. 5.3A). In addition to the interaction with Isa1 and Isa2, Nfu1 associated with three [4Fe-4S] client proteins: Aco1, Aco2 and Lys4 (Fig. 5.3, B and C).

The NifU domain of Nfu1 harbors a CxxC motif required for function

Nfu1 consists of two domains in addition to the N-terminal mitochondrial target sequence based on sequence homologies (Fig. 5.4A). The N-terminal domain (NfuN, residues 22-126) is only conserved within eukaryote species, while the C-terminal NifU-like domain (residues 143-256) is widely conserved in all species and contains the important Fe-S cluster binding CxxC motif (Fig. 5.4B). Both candidate domains were separately expressed with the endogenous mitochondrial targeting sequence of Nfu1 (1-21) to ensure proper delivery to the mitochondrial matrix.

Cells containing only the Nfu1 C-terminal NifU domain were capable of respiratory growth on either glycerol/lactate or acetate medium (Fig. 5.4C), whereas cells

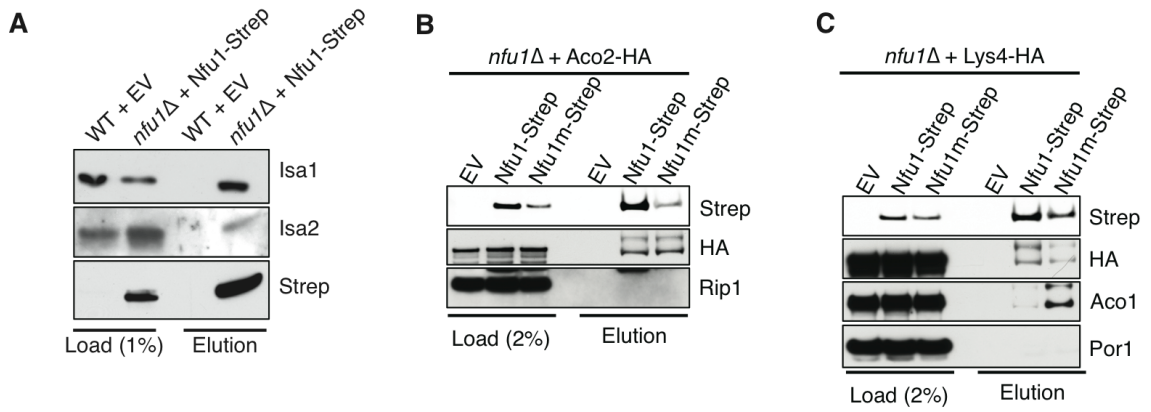

Fig. 5.3. Nfu1 interacts with the ISA complex and [4Fe-4S] cluster proteins. **(A)** Strep-tag affinity purification of Nfu1-Strep revealed the Nfu1 interaction with Isa1 and Isa2. Mitochondria were solubilized with 0.1 % n-dodecyl maltoside (DDM). Clarified lysates were incubated with Strep-Tactin superflow beads for 16 hours. After washing, proteins were eluted with 2.5 mM desthiobiotin, and then analyzed by immunoblotting. **(B)** Strep-tag affinity purification of Nfu1-Strep in the presence of ectopically expressed Aco2-HA. **(C)** Strep-tag affinity purification of Nfu1-Strep in the presence of ectopically expressed Lys4-HA.

Fig. 5.4. The CxxC motif is critical for Nfu1 function. **(A)** A schematic representation of Nfu1 domains. MTS, the mitochondrial targeting sequence; NfuN, the N-terminal domain of Nfu1; NifU, the C-terminal domain harboring the highly conserved CxxC motif. **(B)** The human NifU tertiary structure (PDB: 2M5O) and primary sequences showing the CxxC motif (red) and adjacent amino acids indicated in partial sequences (green). **(C)** The respiratory growth defect of *nfu1*Δ cells was rescued with NifU. Nfu1, NfuN, and NifU were all fused with a C-terminal Strep-tag and expressed exogenously using low-copy plasmids. **(D)** Restoration of Nfu1 target proteins by NifU expression in *nfu1*Δ cells. **(E)** Respiratory growths of *nfu1*Δ cells that express Nfu1 sequence variants were tested. All variants were fused with a Strep-tag and expressed on low-copy plasmids. **(F)** Strep-tag purification of Nfu1 sequence variants as described in Fig. 5.3A.

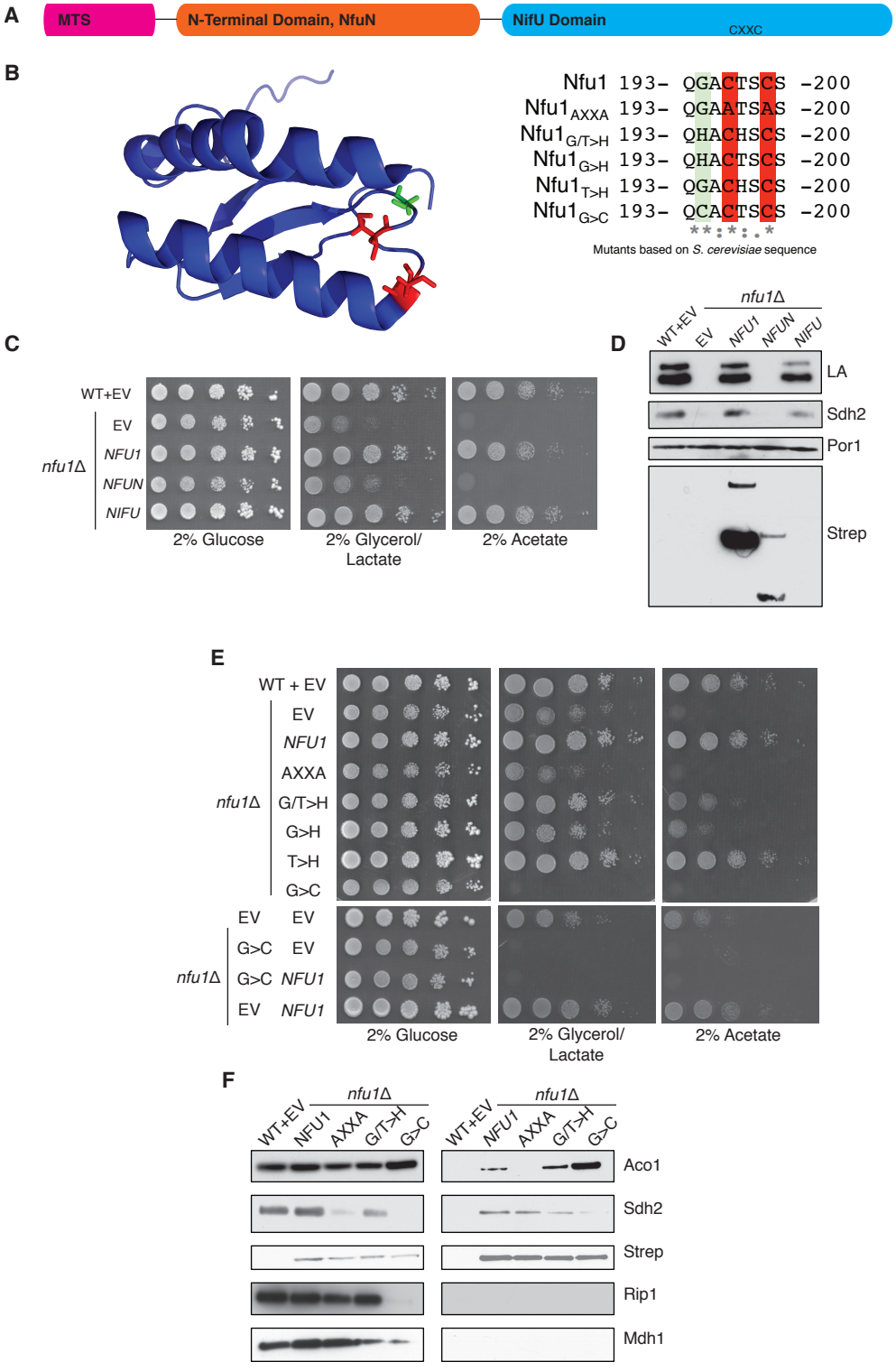
A
MTS
N-Terminal Domain, NfuN
NifU Domain
CXXC
B
Nfu1 193- QGACTSCS -200
Nfu1AXXA 193- QGAATSAS -200
Nfu1G/T>H 193- QHACHSCS -200
Nfu1G>H 193- QHACTSCS -200
Nfu1T>H 193- QGACHSCS -200
Nfu1G>C 193- QCACTSCS -200
Mutants based on S. cerevisiae sequence
C
WT+EV
nfu1Δ
EV
NFU1
NFUN
NIFU
2% Glucose
2% Glycerol/ Lactate
2% Acetate
D
nfu1Δ
WT+EV
EV
NFU1
NFUN
NIFU
LA
Sdh2
Por1
Strep
E
WT + EV
nfu1Δ
EV
NFU1
AXXA
G/T>H
G>H
T>H
G>C
EV EV
nfu1Δ G>C EV
G>C NFU1
EV NFU1
2% Glucose
2% Glycerol/ Lactate
2% Acetate
F
nfu1Δ
WT+EV
NFU1
AXXA
G/T>H
G>C
Aco1
Sdh2
Strep
Rip1
Mdh1

harboring only the Nfu1 N-terminal domain failed to propagate. Additionally, cells with the C-terminal, but not the N-terminal Nfu1 domain, showed normal Sdh2 and lipoic acid levels. Although the N-terminal Nfu1 domain failed to restore Nfu1 function, the fragment was well expressed in cells, unlike the functional C-terminal domain that was markedly attenuated in expression level (Fig. 5.4D).

To further address the functional importance of the C-terminal NifU domain, we generated a series of amino acid substitutions within and near the conserved CxxC motif (Fig. 5.4, B and E). One Nfu1 variant generated had the two cysteinyl residues in the CxxC motif (highlighted in red in Fig. 5.4B) replaced with alanines. Cells harboring Nfu1 with the two CxxC cysteinyl residues replaced by alanines exhibited a respiratory growth defect analogous to *nfu1*Δ cells, suggesting a loss-of-function phenotype. The critical role of the CxxC motif cysteines was previously shown in the *E. coli* NfuA (*29*).

A conserved glycine just upstream of the CxxC motif is commonly mutated to a cysteine in European patients with Multiple Mitochondrial Dysfunctions Syndrome (MMDS). We generated mutants with G>C or G>H substitutions and replaced the conserved threonine between the two cysteinyl residues by a histidyl residue. Each mutant of Nfu1 was expressed in *nfu1*Δ cells and tested for function. The most striking mutant was the $G^{194}C$ mutant that mimics the MMDS patient allele, which displayed a severe synthetic sick phenotype (Fig. 5.4E). This dominant negative phenotype was reversed when cells were plated on medium containing 5-fluoroorotic acid (5-FOA) to shed the *URA3*-containing plasmid harboring the $G^{194}C$ Nfu1 mutant (data not shown). In addition, co-expression of a wild-type Nfu1 with the $G^{194}C$ Nfu1 mutant failed to restore respiratory growth, demonstrating the dominant negative nature of this mutant (Fig.

5.4E).

We tested whether the dominant negative effect arises from changes in interactions between Nfu1 and client proteins. We performed affinity purification of Nfu1-Strep on Step-Tactin beads for the WT and mutant alleles. The loss-of-function AxxA Nfu1 mutant failed to show a detectable interaction with Aco1. In contrast, the $G^{194}C$ Nfu1 mutant exhibited an enhanced interaction with Aco1 (Fig. 5.4F). An interaction with Sdh2 is unclear, since Sdh2 levels are markedly depleted in $G^{194}C$ Nfu1 cells. These data show the importance of Nfu1's C-terminal NifU domain and the CxxC motif in [4Fe-4S] cluster transfer to client proteins.

The two BolA proteins of the mitochondria function in Fe-S cluster biogenesis

Patients presenting with MMDS have also been reported to have mutations in the mitochondrial BOLA3 protein (*1, 2, 6*). The clinical phenotypes of patients with mutations in NFU1 or BOLA3 were similar with neurological regression, infantile encephalopathy and hyperglycinemia (*2, 3*). In addition, related biochemical defects in protein lipolyation and succinate dehydrogenase were observed.

Due to the clinical and biochemical similarities in NFU1 or BOLA3 patients, we elected to evaluate the function of the yeast BOLA3 homolog, Bol3 and the related Bol1 protein (Fig. 5.5A). In human cells, BOLA1 and BOLA3 were shown to be mitochondrial proteins. We confirmed that Bol1 and Bol3 were likewise localized within the mitochondria of yeast cells (data not shown). Yeast lacking either Bol1 or Bol3 lack a clear respiratory phenotype, but a double *bol1*Δ*bol3*Δ null strain displayed a growth

Fig. 5.5. Bol1 and Bol3 play roles in Fe-S cluster biogenesis in mitochondria. **(A)** Partial sequences of yeast and human mitochondrial BolA proteins. Boxed are conserved motifs with proposed ISC ligands that were mutated in this work. **(B)** Respiratory growth defects of *bol1*Δ cells, *bol3*Δ cells and *bol1*Δ*bol3*Δ double mutants and complementation by plasmid-borne *BOL1* or *BOL3*. **(C)** Steady-state levels of LA-conjugated proteins and Sdh2 in cells lacking Bol1 and/or Bol3. **(D)** Relative activity of SDH, cytochrome bc_1 complex and aconitase were measured. Data are shown as mean ± SE (n=3). **(E)** Steady-state levels of LA-conjugated proteins and Sdh2 in response to overexpression of Grx5 or the ISA components in cells lacking Bol1 and Bol3. **(F)** Respiratory function of Bol1 and Bol3 sequence variants in conserved residues were examined by yeast drop-test. All Bol1 variants were fused with a C-terminal Strep-tag and expressed on low-copy plasmids. All Bol3 variants were fused with a N-terminal Strep-tag between the MTS and the remainder of the protein and expressed on low-copy plasmids.

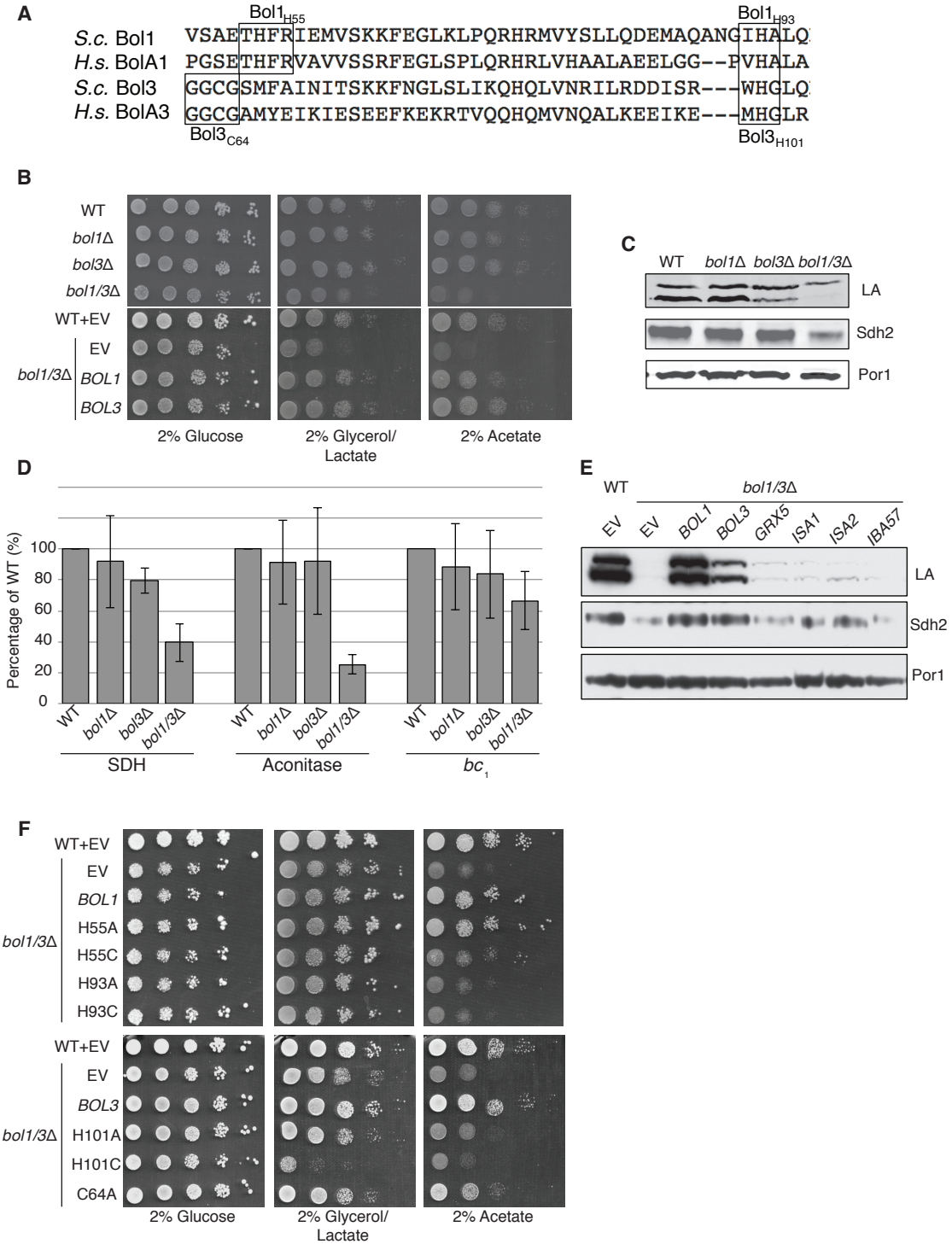
A
Bol1H55
Bol1H93
S.c. Bol1 VSAETHFRIEMVSKKFEGLKLPQRHRMVYSLLQDEMAQANGIHALQ
H.s. BolA1 PGSETHFRVAVVSSRFEGLSPLQRHRLVHAALAEELGG--PVHALA
S.c. Bol3 GGCGSMFAINITSKKFNGLSLIKQHQLVNRILRDDISR---WHGLQ
H.s. BolA3 GGCGAMYEIKIESEEFKEKRTVQQHQMVNQALKEEIKE---MHGLR
Bol3C64
Bol3H101
B
WT
bol1Δ
bol3Δ
bol1/3Δ
WT+EV
bol1/3Δ
EV
BOL1
BOL3
2% Glucose
2% Glycerol/ Lactate
2% Acetate
C
WT
bol1Δ
bol3Δ
bol1/3Δ
LA
Sdh2
Por1
D
Percentage of WT (%)
100
80
60
40
20
0
WT
bol1Δ
bol3Δ
bol1/3Δ
SDH
Aconitase
bc1
E
WT
bol1/3Δ
EV
EV
BOL1
BOL3
GRX5
ISA1
ISA2
IBA57
LA
Sdh2
Por1
F
WT+EV
bol1/3Δ
EV
BOL1
H55A
H55C
H93A
H93C
WT+EV
bol1/3Δ
EV
BOL3
H101A
H101C
C64A
2% Glucose
2% Glycerol/ Lactate
2% Acetate

defect on acetate medium, but to a lesser extent on glycerol/lactate medium (Fig. 5.5B). Mitochondria isolated from single mutants and the double null was used for biochemical characterization studies. As with *nfu1*Δ cells, protein lipolyation was partially impaired in PDH in the *bol3*Δ null, but markedly in the *bol1*Δ*bol3*Δ null strain (Fig. 5.5C). SDH and aconitase activities were depressed in the double null strain and partially done in the individual single mutants (Fig. 5.5D). The attenuation of aconitase activity in both *bol3*Δ and *nfu1*Δ cells is in contrast to BOLA3 and NFU1 patient mutant cells. A modest attenuation was seen in bc_1 activity in the *bol1*Δ*bol3*Δ null strain and this was not observed in *nfu1*Δ cells.

Since the respiratory growth defect of *nfu1*Δ cells was partially suppressed by overexpression of Isa2, we tested whether overexpression of a series of late mitochondrial Fe-S cluster assembly genes would likewise rescue the respiratory defect of *bol1*Δ *bol3*Δ cells. As can be seen in Fig. 5.5E, only a marginal restoration of LA and Sdh2 levels was observed with overexpression of Grx5, Isa1 and Isa2.

BolA proteins, like Nfu1, are implicated in binding Fe-S clusters. Whereas Nfu1 is known to bind a [4Fe-4S] cluster at the homodimer interface, BolA proteins have been shown to bind [2Fe-2S] clusters in association with glutaredoxins as heterodimer (*31-33*). We evaluated the roles of potential Fe-S cluster ligands in Bol1 and Bol3. Bol1 has conserved His56 and His93 residues, which in the case of an *Arabidopsis thaliana* BolA1 are apparent ligands to a [2Fe-2S] cluster in association with a monothiol glutaredoxin (*32*). Bol3 has conserved Cys64 and His101 residues in corresponding loops to that of Bol1 and are expected to serve as ligands for a Fe-S cluster. We converted the conserved histidyl residues to alanines or cysteines to test for phenotypic effects. We observed that

the C-terminal His in each BolA protein was important for the respiratory growth of cells (Fig. 5.5F). Whereas the $H^{101}A$ Bol3 mutant was nonfunctional, the variant containing a $H^{101}C$ substitution exhibited a dominant negative phenotype in that the respiratory defect was more pronounced than the starting *bol1*Δ *bol3*Δ null strain (Fig. 5.5F). The Bol3 $C^{64}A$ mutant was only a partial loss-of-function allele. The Bol1 $H^{93}A$ or $H^{93}C$ mutants exhibited similar loss-of-function phenotypes without any observed dominant negative effects. The upstream Bol1 $H^{56}A$ mutant retains function, but the $H^{56}C$ allele was a partial loss-of-function mutant (Fig. 5.5F). These data show a functional importance of Bol1 and Bol3 in mitochondrial Fe-S cluster biogenesis and highlights the need for one of the two putative Fe-S ligands for physiological function. The BolA proteins, like Nfu1, are not essential for mitochondrial Fe-S biogenesis, as a bypass exists enabling limited respiratory growth on glycerol/lactate medium.

Nfu1 and Bol3 physically interact with [4Fe-4S] client mitochondrial proteins

To glean further insights into the function of Nfu1, Bol1 and Bol3 in mitochondrial Fe-S cluster biogenesis, we performed proteomic analyses on affinity purified Nfu1, Bol1 and Bol3 proteins each expressed as C-terminal Strep fusions. Purification of each protein was accomplished on Strep-Tactin resin and protein eluates were analyzed by mass spectrometry. Multiple independent proteomic analyses were conducted on WT proteins as well as mutant proteins of each (a double G/T>C Nfu1, $H^{93}C$ Bol1 and $H^{101}C$ Bol3) (Fig. 5.6, A and B). Of the mutant proteins, both the Nfu1 and BolA3 were dominant negative mutants, whereas the Bol1 $H^{93}C$ variant was a loss-

Fig. 5.6. Proteomic analyses reveal Nfu1 and BolA proteins interacting partners. **(A and B)** Percentages of peptides identified by MS proteomics. Percentages were calculated by the number of peptides identified for a denoted protein in an individual Strep-tagged protein divided by the total number of peptides for that protein identified from all seven samples. Strep-tagged proteins were expressed from low-copy plasmids in corresponding single deletion mutants. Samples were Strep-affinity purified as in Fig. 5.3. Bol1m is the H93C variant. Bol3m is the H101C variant. Nfu1m is the G/T>H variant. All were fused with a C-terminal Strep-tag. WT is BY4741 wild-type harboring a low-copy empty plasmid. **(C)** Strep-tag affinity purification of Nfu1-Strep in the presence of ectopically expressed Ilv3-FLAG.

A

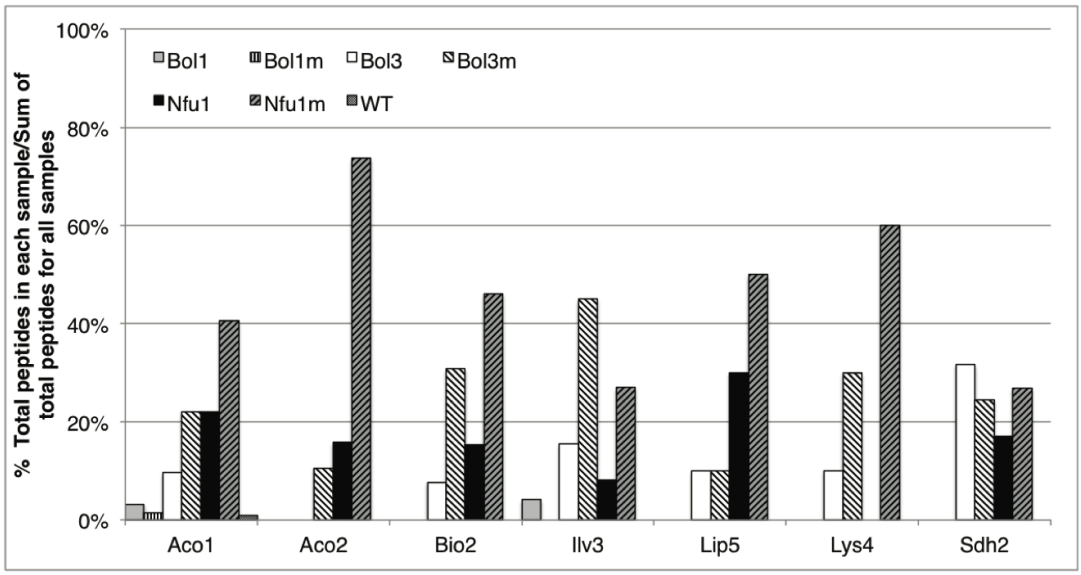
100%
80%
60%
40%
20%
0%
% Total peptides in each sample/Sum of total peptides for all samples
Bol1
Bol1m
Bol3
Bol3m
Nfu1
Nfu1m
WT
Aco1
Aco2
Bio2
Ilv3
Lip5
Lys4
Sdh2

B

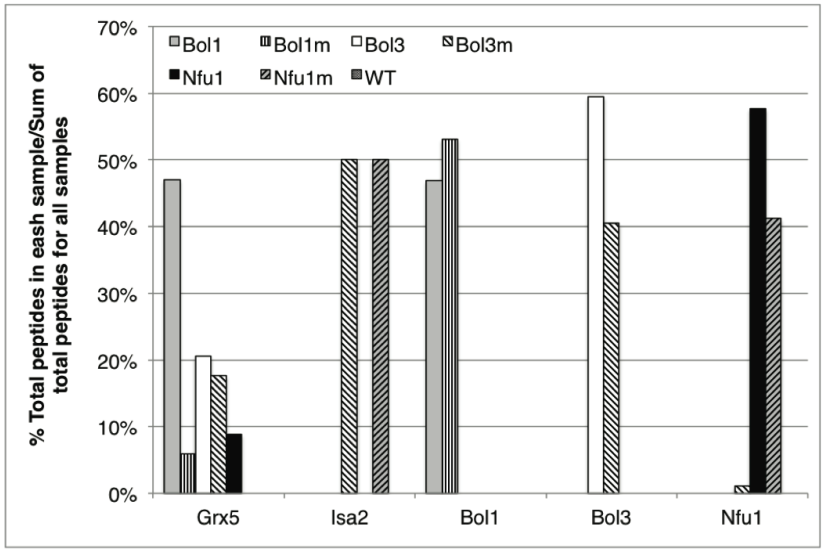
70%
60%
50%
40%
30%
20%
10%
0%
% Total peptides in eash sample/Sum of total peptides for all samples
Bol1
Bol1m
Bol3
Bol3m
Nfu1
Nfu1m
WT
Grx5
Isa2
Bol1
Bol3
Nfu1

C

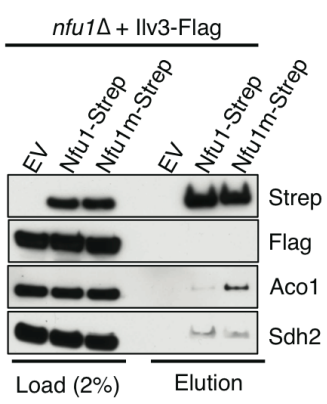
nfu1Δ + Ilv3-Flag
EV
Nfu1-Strep
Nfu1m-Strep
EV
Nfu1-Strep
Nfu1m-Strep
Strep
Flag
Aco1
Sdh2
Load (2%)
Elution

of-function mutant without a dominant negative characteristic. Inspection of datasets of protein interactors revealed a common set of [4Fe-4S] client proteins associating with both Nfu1 and Bol3. These include Aco1, Aco2, Lys4, Sdh2, Lip5 and Bio2 (Fig. 5.6A). For all client proteins except Sdh2, the observed peptide count was markedly higher for clients purified with mutant Nfu1 and Bol3 variants. The lack of stalling of Sdh2 with mutant proteins may arise from depressed levels of Sdh2 in cells with the mutants as shown in Fig. 5.4F for $G^{194}C$ Nfu1. Additionally, the mutant forms of Bol3 and Nfu1 both co-purified the ISA complex component, Isa2 (Fig. 5.6B). The physical interactions of Nfu1 with the clients, Aco1, Lys4, Aco2 and Sdh2, and with the ISA complex are consistent with the results shown by affinity purification experiments followed by SDS-PAGE and immunoblotting (Fig. 5.3, A, B and C). We observed the co-purification of Nfu1 and Bol3 in cells containing Bol3-Strep (Fig. 5.6B).

The Nfu1 and Bol3 proteomics experiments did not identify any novel mitochondrial [4Fe-4S] cluster client proteins. However, the [2Fe-2S] enzyme dihydroxyacid dehydratase (Ilv3) was recovered in multiple independent mass spectrometry analyses in Nfu1 and Bol3 samples. However, we were unable to verify that interaction when using a FLAG-tagged Ilv3 chimera in Nfu1-Strep affinity capture (Fig. 5.6C). In addition, we were unable to observe a defect in Ilv3 function in *nfu1*Δ cells (data not shown).

Unlike Bol3, Bol1 purification did not lead to appreciable co-purification of [4Fe-4S] client proteins, but Grx5 was isolated as a reproducible interactor with WT but not the loss-of-function $H^{93}C$ Bol1 mutant (Fig. 5.6B). Grx5 was a significantly less abundant interactor with Bol3 or Nfu1. Human BOLA1 was previously shown to

associate with Grx5 in HEK293 cells (*12*), but a comparison with BOLA3 was not done.

Nfu1 and Bol3 function together in [4Fe-4S] cluster transfer from the ISA complex to apo-client proteins

The distinct overlap of [4Fe-4S] client protein interactors between Bol3 and Nfu1 suggested a potential overlap or partnership in the function of the two proteins in late step [4Fe-4S] cluster transfer. We tested whether a genetic linkage exists between the proteins by evaluating whether a synthetic phenotype exists in cells lacking Bol1, Bol3 and Nfu1. The triple deletion cell (*bol1*Δ*bol3*Δ*nfu1*Δ) exhibited a strong synergistic growth defect on glycerol/lactate medium (Fig. 5.7A). The synergistic defect can also be seen in protein lipolyation, Sdh2 steady-state levels and enzymatic activities of SDH and aconitase (Fig. 5.7, B and C). The growth defect of the triple mutant can be partially rescued by re-expression of *BOL1* or *NFU1*, but not by *BOL3* (Fig. 5.7D). This may suggest that Bol3 requires Nfu1 for its function.

Affinity purification of Nfu1-Strep expressed in the *bol1*Δ*bol3*Δ*nfu1*Δ triple null mutant was conducted to test the effect of loss of the two BolA proteins on the interaction of Nfu1 with [4Fe-4S] client proteins. As can be seen in Fig. 5.7E in the absence of Bol1 or Bol3, there was enhanced copurification of Aco1. Likewise, a similar enhanced interaction between client proteins and Nfu1 was apparent in cells lacking a functional ISA complex (Fig. 5.7F). These data are consistent with a role of Nfu1 in [4Fe-4S] cluster transfer from the ISA complex to client proteins.

Given the strong genetic interaction between the mitochondrial BOLA genes and *NFU1* (Fig. 5.7A), we attempted to substantiate the linkage. The proteomic results

Fig. 5.7. Nfu1 and Bol3 function together in [4Fe-4S] cluster transfer. **(A)** Exacerbated respiratory growth defects of *bol1*Δ*bol3*Δ*nfu1*Δ triple mutants compared to *nfu1*Δ single mutants and *bol1*Δ*bol3*Δ double mutants on nonfermentable carbon sources. **(B)** Steady-state levels of LA-conjugated proteins and Sdh2 in the absence of Bol1, Bol3 or Nfu1. **(C)** Relative activity of SDH and aconitase in the absence of Bol1, Bol3 or Nfu1. Data are shown as mean ± SE (n=3) **(D)** Respiratory growths of *bol1*Δ*bol3*Δ*nfu1*Δ triple mutants harboring plasmid-borne *BOL1*, *BOL3* and *NFU1*, respectively. **(E)** Strep-tag purification of Nfu1-Strep in the absence of Bol1 and Bol3. **(F)** Strep-tag purification of Nfu1-Strep in the absence of Isa2. **(G)** Steady-state levels of Bol1-Strep (upper panel) and Bol3-Strep (bottom panel) in response to overexpression of genes as indicated. **(H)** A working model of late stage mitochondrial iron-sulfur cluster biogenesis and delivery.

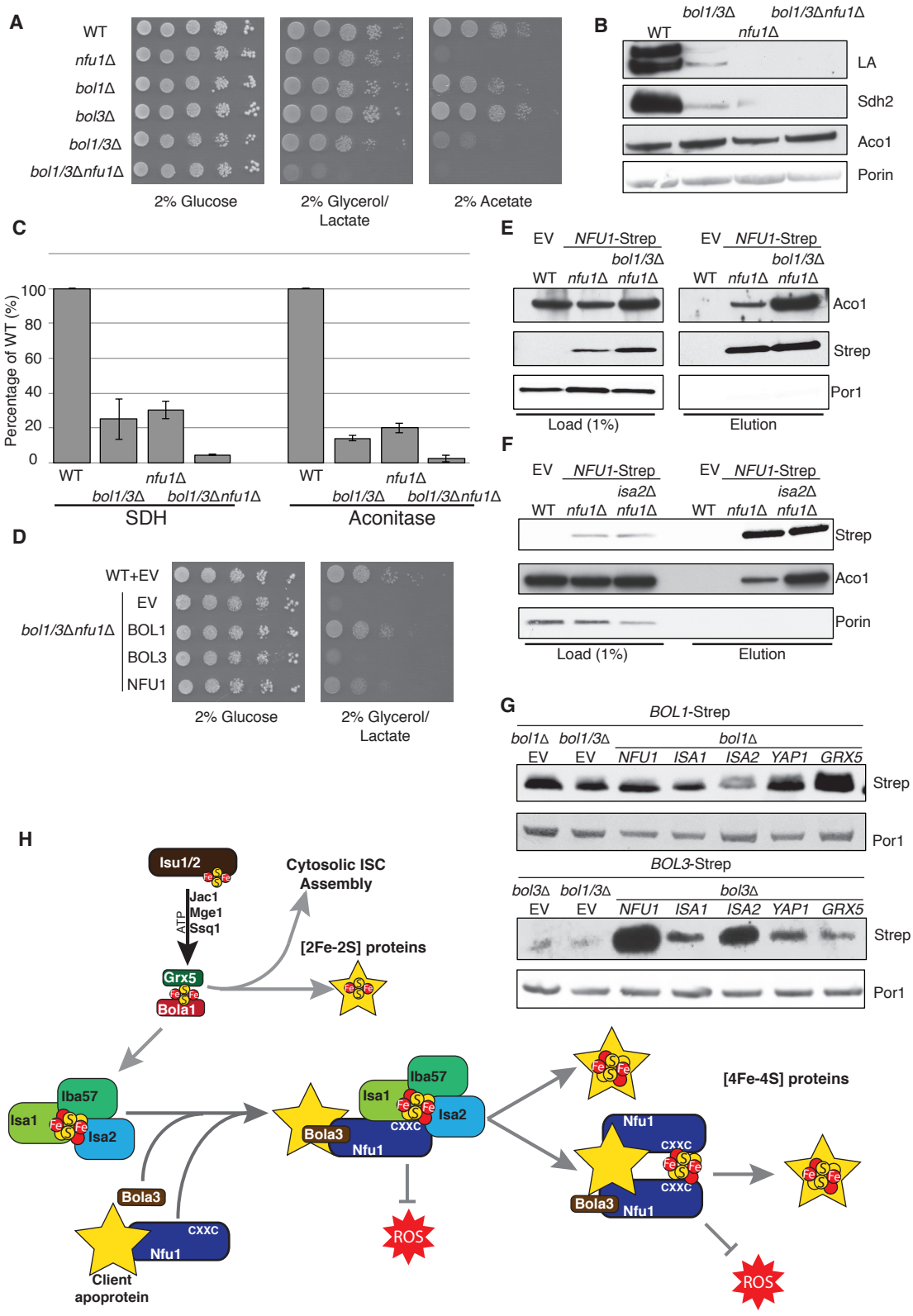
A
WT
nfu1Δ
bol1Δ
bol3Δ
bol1/3Δ
bol1/3Δnfu1Δ
2% Glucose
2% Glycerol/ Lactate
2% Acetate
B
bol1/3Δ
bol1/3Δnfu1Δ
WT
nfu1Δ
LA
Sdh2
Aco1
Porin
C
Percentage of WT (%)
100
80
60
40
20
0
WT
bol1/3Δ
nfu1Δ
bol1/3Δnfu1Δ
SDH
Aconitase
D
WT+EV
bol1/3Δnfu1Δ
EV
BOL1
BOL3
NFU1
2% Glucose
2% Glycerol/ Lactate
E
EV
NFU1-Strep
bol1/3Δ
WT
nfu1Δ
Aco1
Strep
Por1
Load (1%)
Elution
F
isa2Δ
G
BOL1-Strep
bol1Δ
bol1/3Δ
NFU1
ISA1
ISA2
YAP1
GRX5
BOL3-Strep
bol3Δ
H
Isu1/2
Jac1
Mge1
Ssq1
ATP
Grx5
Bola1
Cytosolic ISC Assembly
[2Fe-2S] proteins
Iba57
Isa1
Isa2
Bola3
Nfu1
CXXC
ROS
[4Fe-4S] proteins
Client apoprotein

suggested an association of Bol1 and Grx5, whereas Bol3 was associated with Nfu1 function. Mitochondrial BolA proteins are low abundance molecules making co-immuno-precipitation studies challenging (data not shown). Because of this, we tested whether increasing the levels of candidate interacting proteins would alter the abundance of Bol1 or Bol3. As can be seen in Fig. 5.7G, the steady-state levels of Bol3, but not Bol1, were dramatically increased in cells with elevated levels of Nfu1. Additionally, *ISA1* and *ISA2* overexpression resulted in a modest increase in Bol3, but not Bol1, protein levels. In contrast, Grx5 overexpression led to a marked enhancement in Bol1 levels without altering Bol3. In these studies, Strep-chimeras of Bol1 and Bol3 were expressed with heterologous promoters, so the change in protein level is likely occurring through post-transcriptional stabilization. These stabilization experiments corroborate the genetic and proteomic experiments, all of which suggest that Bol3 (BOLA3) functions with Nfu1 in [4Fe-4S] cluster transfer to client proteins and Bol1 functions with Grx5 for a yet to be determined purpose.

Discussion

A role of Nfu1 in Fe-S cluster biogenesis has long been implicated (*36, 37*); however, its molecular mechanism has not been definitely established. Patients harboring mutations in NFU1, as well as BOLA3, exhibit biochemical abnormalities in a set of 4Fe-4S enzymes leading to speculation that Nfu1, and BolA3, function as a late Fe-S maturation factor (*3, 27*) or that Nfu1 is an alternate Fe-S cluster synthesis scaffold protein used for a subset of specific Fe-S client proteins (*2, 28*). The phenotypic similarity between Nfu1 mutations and BolA3 mutations suggests the two proteins

function in a common pathway.

We demonstrate in studies using yeast as a model system that the yeast orthologs of human NFU1 and BOLA3 function in a late step of transfer of [4Fe-4S] clusters to client proteins. Yeast lacking Nfu1 are partially deficient in the [4Fe-4S] enzymes aconitase, succinate dehydrogenase and lipoic acid synthase. The defect in lipoic acid synthase is highlighted by the pronounced defect in protein lipolyation in mitochondria. The defect in yeast lacking Bol3 is modest, but is exacerbated in cells lacking both mitochondrial Bol3 and Bol1. The double null cells shows related partial defects in [4Fe-4S] enzymes aconitase, succinate dehydrogenase and lipoic acid synthase, although the defects are not as pronounced as in *nfu1*Δ cells. Yeast lacking all three proteins, Nfu1, Bol1 and Bol3, show an exaggerated phenotype approaching the defect seen in cells lacking the ISA complex required for [4Fe-4S] cluster synthesis. Clearly, *nfu1*Δ cells do not exhibit any defects in enzymes dependent on [2Fe-2S] centers, suggesting that Nfu1 functions in the [4Fe-4S] cluster transfer pathway.

Our systematic approach to identify endogenous binding partners of Nfu1, Bol1 and Bol3 revealed their molecular function. Affinity purification of Nful1 coupled with mass spectrometry led to the identification of [4Fe-4S] client proteins as physically associating proteins of Nfu1. It is of interest that the $G^{194}C$ Nfu1 variant exhibiting a partial dominant negative effect showed enhanced interaction with the same client proteins. This yeast mutant mimics the known $G^{208}C$ patient mutation in human NFU1 that causes the severe infantile encephalopathy. Nfu1 is implicated in Fe-S cluster binding. Recombinant Nfu1 has been shown competent to associate with a [4Fe-4S] cluster and ^{55}Fe in vivo labeling studies showed iron binding by Nfu1, with enhanced

^{55}Fe binding by the patient mimic G^{194}C Nfu1 yeast variant (*3*). Moreover, It is also noteworthy that Gly194 is in juxtaposition to the CxxC motif, which has been proposed to bind Fe-S clusters. Therefore, it is plausible that the dominant negative effect of the G^{194}C Nfu1 variant may result from the inefficient release of [4Fe-4S] clusters from the Nfu1 variant to client proteins.

The dramatic phenotype of cells harboring G^{194}C Nfu1 is likely due to secondary effects of impaired lipoic acid formation. As mentioned, yeast lacking enzymes involved in octanoic acid formation or the Lip5 lipoic acid synthase are deficient in tRNA processing by RNase P, leading to attenuation in mitochondrial translation (*38, 39*).

The physical interactions of Nfu1 with Isa1 and Isa2 corroborate our model that Nfu1 is implicated in [4Fe-4S] cluster transfer to client proteins. Interestingly, we isolated Isa2 as a suppressor of the respiratory defect of *nfu1*Δ cells. Whereas the condensation of two [2Fe-2S] to form a single [4Fe-4S] cluster requires the participation of Isa1, Isa2 and Iba57, Isa2 is capable of forming homo-dimers that may exert a transfer function as proposed for Nfu1.

The same 4Fe-4S client proteins were pulled down in affinity purification of Bol3, but not Bol1, compared to proteins interacting with Nfu1. In the case of Bol3, the dominant negative H^{101}C Bol3 variant also showed enhanced interactions with [4Fe-4S] client proteins. BolA proteins are known to bind [2Fe-2S] clusters in association with monothiol glutaredoxins (*31*). Current results are consistent with both proteins participating in Fe-S cluster binding in vivo. The double C>A variant in the conserved Nfu1 C-terminal domain is a loss-of-function allele that is impaired in binding Aco1. The dominant negative phenotype of the H^{101}C Bol3 mutant (putative Fe-S ligand) but only

loss-of-function phenotype for the $H^{101}A$ mutant is consistent with a model that a Fe-S cluster may associate with Bol3. Thus, both Nfu1 and Bol3 may function in the context of Fe-S cluster binding.

The partial deficiency of [4Fe-4S] enzyme activity suggests that function of Nfu1 may be conditionally important in [4Fe-4S] cluster transfer and that a bypass mechanism exists in yeast. We demonstrate that Nfu1 in yeast has a heightened importance in cells undergoing oxidative metabolism as opposed to anoxic metabolism. In addition, the protein lipolyation defect in *nfu1*Δ cells is partially suppressed in mutant cells with elevated expression of either Yap1 or Yap2, which are paralogous transcriptional activators of antioxidant genes, or supplemental GSH in the growth medium. Yap1- or Yap2-containing *nfu1*Δ cells do not recover significant levels of SDH, suggesting that elevated redox capacity is limited in its restoration of function in the mutant cells.

One curiosity is that human patients with mutations in NFU1 or BOLA3 lack defects in mitochondrial aconitase, whereas the yeast mutants, *nfu1*Δ and the double *bol1*Δ *bol3*Δ, exhibit a partial aconitase defect. There are two implications of this result. First, since partial respiratory function persists in *nfu1*Δ cells, Nfu1 may facilitate cluster transfer in oxidative growth conditions. Second, Nfu1 may exhibit client selectivity in the actual transfer of [4Fe-4S] clusters. Although Nfu1 binds all [4Fe-4S] client proteins, it may facilitate cluster transfer to select clients and this may differ between human and yeast cells as in the case of aconitase. This postulate is supported by selectively enhanced interaction of the Nfu1 HxxC mutant with Aco1, Aco2 and Lys4, but not with Sdh2, compared to WT Nfu1. The binding of [4Fe-4S] client proteins by Nfu1 is analogous to the function of Mms19 in the cytosolic Fe-S cluster transfer step in which Mms19

associates with apo-client proteins prior to Fe-S cluster transfer (*40*).

One dramatic phenotype in human and yeast Nfu1 mutant cells is impaired protein lipoylation. Yeast and human cells require lipoylation on E2 subunits of pyruvate dehydrogenase, 2-oxoglutarate dehydrogenase and the glycine cleavage enzyme complex. In addition, the human branched chain 2-oxoacid dehydrogenase require lipolyation for function. The enzyme catalyzing formation of the lipoate coenzyme lipoic acid synthase binds two [4Fe-4S] clusters, one of which serves as the sulfur donor for lipoic acid formation in a radical S-adenosylmethionine dependent reaction (*41, 42*). Two sulfide ions from this auxiliary cluster are used for formation of lipoate resulting in disassembly of the cluster. Each catalytic cycle of the enzyme requires repair of the auxiliary cluster (*43*). Nfu1 may have a specialized role in cluster repair in lipoic acid synthase. Each catalytic cycle of the synthase liberates Fe(II) ions that may catalyze deleterious ROS species in oxidative cells, so Nfu1 may have evolved to shield its [4Fe-4S] prior to transfer. In addition, endogenous oxidants are generated by the 2-oxoacid dehydrogenases including 2-oxoglutarate dehydrogenase and pyruvate dehydrogenase as well as the respiratory complexes (*44*). Nfu1 may exert its facilitatory role in shielding its bound cluster from endogenous oxidants as well as being a reservoir of [4Fe-4S] clusters for lipoic acid synthase function.

Bol3 but not Bol1 was found to associate with [4Fe-4S] client proteins, whereas Bol1 reproducibly associated with Grx5. These binding studies suggest that Bol1 and Bol3 have specialized functions, yet yeast mutants lacking only one of these proteins have only modest respiratory phenotypes. Since the double *bol1*Δ *bol3*Δ mutant has a respiratory defect with similarities to *nfu1*Δ cells but more modest, some redundancy

must exist between Bol1 and Bol3. It remains unclear if the role of Bol3 in late [4Fe-4S] transfer requires the participation of Grx5. However, the known BolA:glutaredoxin complexes that have been studied only bind [2Fe-2S] clusters (*31*).

In summary, the present work suggests that Nfu1 has a significant role in a late step transfer of [4Fe-4S] clusters to select client proteins. Nfu1 binds the client proteins independent of the ISA complex and its association with the ISA complex may serve to recruit apo-clients to the ISA complex where [4Fe-4S] clusters are formed. Some [4Fe-4S] client proteins may get their [4Fe-4S] cluster directly from the ISA complex, whereas others may derive their clusters after prior transfer of a [4Fe-4S] cluster to Nfu1. In these cases, Nfu1 facilitates the process as an adapter protein in oxidatively grown cells. Additional work is required to discern the client selectivity in [4Fe-4S] cluster transfer by Nfu1. This model of eukaryotic Nfu1 function resembles the role of *E. coli* Nfu1 ortholog NfuA, which binds a subset of Fe-S apo-client proteins and facilitates cluster transfer especially under oxidative stress conditions (*27, 29*). Likewise, the *Azobacter* NfuA is reported to be critical under oxidative growth conditions (*30*). In the case of *E. coli*, NfuA cluster transfer is likely mediated directly by NfuA (*27*). Bol3 may function at a similar step in cluster transfer, but its role is more nebulous considering some apparent redundancy with Bol1. Clearly, interaction studies separate Bol1 and Bol3 into two separate classes, with Bol3 working with Nfu1 in [4Fe-4S] client binding and Bol1 working with Grx5, which has its known function upstream of the ISA complex (*24, 45, 46*). However, Bol1 appears to have a compensatory redundancy with Bol3, since a phenotype is exposed only in the absence of both proteins. The BolA proteins may have a role in [4Fe-4S] cluster dissociation from either the ISA complex or Nfu1 in [4Fe-4S]

cluster transfer. Additional work will be required to discern their mechanisms.

Materials and methods

Yeast strains and plasmids

BY4741 Strains were used unless indicated otherwise. Deletion strains were generated by homologous recombination and confirmed by PCR analyses of loci as described earlier (*47*). Plasmids used in this study were constructed using general subcloning techniques. For mutagenesis or adding epitope tags, Phusion DNA Polymerases (Thermo Fisher Scientific) were used. All plasmid-borne genes were expressed under the *MET25* promoter and the *CYC1* terminator unless indicated otherwise.

Enzymatic activity assay

Activity assays for aconitase, succinate dehydrogenase (SDH), cytochrome bc_1 complex and cytochrome *c* oxidase were performed as described previously (*48, 49*). Aconitase activity was determined by measuring the initial rate of conversion of 100 mM *cis*-aconitate to isocitrate in 50 mM Tris (pH 7.4) at 240 nm. Soluble fractions of mitochondria were obtained by repetitive freeze-thaw. SDH activity was measured by quinone-mediated reduction of dichlorophenolindophenol (DCPIP) upon succinate oxidation at 600 nm. For cytochrome bc_1 complex activity, the reduction rate of cytochrome *c* was measured upon the oxidation of reduced decylubiquinol at 550 nm. Cytochrome *c* oxidase activity was determined by measuring the initial rate of oxidation of cytochrome *c* oxidation (*50*).

Miscellaneous procedures

Yeast mitochondria isolation was performed using the method of Glick and Pon (*51*). Standard procedures were performed for SDS-PAGE and immunoblotting. Anti-Sdh2 was from the previous study (*52*). Anti-Strep was purchased from Qiagen. Antibodies against LA-conjugated proteins were from Calbiochem. Anti-Myc and anti-HA were from Santa Cruz Biotechnology. Anti-Por1 was purchased from Molecular Probes and anti-FLAG was from Sigma-Aldrich. Each polyclonal antibody against Aco1, Isa1, Isa2 and Nfu1 was a generous gift from Dr. Roland Lill. Protein concentration was determined by the Bradford assay.

Strep-tag affinity purification

Affinity purifications of Strep-tagged proteins were conducted using Strep-Tactin superflow beads (Qiagen) following the manufacturer's instruction with slight changes. Briefly, isolated mitochondria were solubilized with 0.1 % n-dodecyl maltoside (DDM) in the lysis buffer, 50 mM NaH_2PO_4 (pH 8.0), 300 mM NaCl and 1x protease inhibitor (*c*Omplete mini, Roche), for 30 min on ice. After clarification of solubilized mitochondria by high-speed centrifugation, supernatants were incubated with Strep-Tactin superflow beads for 16 hours at 4°C. The beads were washed five times with the lysis buffer. Strep-tagged proteins bound to the beads were eluted with 2.5 mM dethiobiotin in the lysis buffer, which were subjected to mass spectrometry analyses or immunoblotting.

Acknowledgments

We thank James Cox and the University of Utah Metabolomics Core facility for the metabolomic analyses. We acknowledge support of funds in conjunction with grant P30 CA042014 awarded to Huntsman Cancer Institute. A.M. was supported by training grant T32 DK007115 from the National Institutes of Health. This research was supported by a grant from the National Institutes of Health (RO1 GM110755) awarded to D.R.W.

References

1. A. Seyda *et al.*, A novel syndrome affecting multiple mitochondrial functions, located by microcell-mediated transfer to chromosome 2p14-2p13. *Am. J. Hum. Genet.* **68**, 386-396 (2001).

2. J. M. Cameron *et al.*, Mutations in iron-sulfur cluster scaffold genes NFU1 and BOLA3 cause a fatal deficiency of multiple respiratory chain and 2-oxoacid dehydrogenase enzymes. *Am. J. Hum. Genet.* **89**, 486-495 (2011).

3. A. Navarro-Sastre *et al.*, A fatal mitochondrial disease is associated with defective NFU1 function in the maturation of a subset of mitochondrial Fe-S proteins. *Am. J. Hum. Genet.* **89**, 656-667 (2011).

4. X. Ferrer-Cortes *et al.*, Protein expression profiles in patients carrying NFU1 mutations. Contribution to the pathophysiology of the disease. *J. Inherit. Metab. Dis.* **36**, 841-847 (2013).

5. M. Nizon *et al.*, Leukoencephalopathy with cysts and hyperglycinemia may result from NFU1 deficiency. *Mitochondrion* **15**, 59-64 (2014).

6. P. R. Baker, 2nd *et al.*, Variant non ketotic hyperglycinemia is caused by mutations in LIAS, BOLA3 and the novel gene GLRX5. *Brain* **137**, 366-379 (2014).

7. F. G. Debray *et al.*, Mutation of the iron-sulfur cluster assembly gene IBA57 causes fatal infantile leukodystrophy. *J. Inherit. Metab. Dis.* (2015). doi:10.1007/s10545-015-9857-1.

8. J. K. Hiltunen *et al.*, Mitochondrial fatty acid synthesis and respiration. *Biochim. Biophys. Acta* **1797**, 1195-1202 (2010).

9. C. Gelling, I. W. Dawes, N. Richhardt, R. Lill, U. Muhlenhoff, Mitochondrial Iba57p is required for Fe/S cluster formation on aconitase and activation of

radical SAM enzymes. *Mol. Cell. Biol.* **28**, 1851-1861 (2008).

10. A. D. Sheftel *et al.*, The human mitochondrial ISCA1, ISCA2, and IBA57 proteins are required for [4Fe-4S] protein maturation. *Mol. Biol. Cell* **23**, 1157-1166 (2012).

11. B. Schilke, C. Voisine, H. Beinert, E. Craig, Evidence for a conserved system for iron metabolism in the mitochondria of *Saccharomyces cerevisiae*. *Proc. Natl. Acad. Sci. U.S.A* **96**, 10206-10211 (1999).

12. P. Willems *et al.*, BOLA1 is an aerobic protein that prevents mitochondrial morphology changes induced by glutathione depletion. *Antioxid. Redox Signal* **18**, 129-138 (2013).

13. R. Lill *et al.*, The role of mitochondria in cellular iron-sulfur protein biogenesis and iron metabolism. *Biochim. Biophys. Acta* **1823**, 1491-1508 (2012).

14. S. Schmucker *et al.*, Mammalian frataxin: an essential function for cellular viability through an interaction with a preformed ISCU/NFS1/ISD11 iron-sulfur assembly complex. *PLoS ONE* **6**, e16199 (2011).

15. C. L. Tsai, D. P. Barondeau, Human frataxin is an allosteric switch that activates the Fe-S cluster biosynthetic complex. *Biochemistry* **49**, 9132-9139 (2010).

16. R. Lill, U. Muhlenhoff, Maturation of iron-sulfur proteins in eukaryotes: mechanisms, connected processes, and diseases. *Annu. Rev. Biochem.* **77**, 669-700 (2008).

17. J. Gerber, U. Muhlenhoff, R. Lill, An interaction between frataxin and Isu1/Nfs1 that is crucial for Fe/S cluster synthesis on Isu1. *EMBO Rep.* **4**, 906-911 (2003).

18. A. Biederbick *et al.*, Role of human mitochondrial Nfs1 in cytosolic iron-sulfur protein biogenesis and iron regulation. *Mol. Cell Biol.* **26**, 5675-5687 (2006).

19. J. Bridwell-Rabb, N. G. Fox, C. L. Tsai, A. M. Winn, D. P. Barondeau, Human frataxin activates Fe-S cluster biosynthesis by facilitating sulfur transfer chemistry. *Biochemistry* **53**, 4904-4913 (2014).

20. A. Parent *et al.*, Mammalian frataxin directly enhances sulfur transfer of NFS1 persulfide to both ISCU and free thiols. *Nat. Commun.* **6**, 5686 (2015).

21. N. G. Fox, D. Das, M. Chakrabarti, P. A. Lindahl, D. P. Barondeau, Frataxin Accelerates [2Fe-2S] Cluster Formation on the Human Fe-S Assembly Complex. *Biochemistry* **54**, 3880-3889 (2015).

22. S. J. Ciesielski *et al.*, Interaction of J-protein co-chaperone Jac1 with Fe-S scaffold Isu is indispensable in vivo and conserved in evolution. *J. Mol. Biol.* **417**, 1-12 (2012).

23. J. Majewska *et al.*, Binding of the chaperone Jac1 protein and cysteine desulfurase Nfs1 to the iron-sulfur cluster scaffold Isu protein is mutually exclusive. *J. Biol. Chem.* **288**, 29134-29142 (2013).

24. M. A. Uzarska, R. Dutkiewicz, S. A. Freibert, R. Lill, U. Muhlenhoff, The mitochondrial Hsp70 chaperone Ssq1 facilitates Fe/S cluster transfer from Isu1 to Grx5 by complex formation. *Mol. Biol. Cell* **24**, 1830-1841 (2013).

25. U. Muhlenhoff, N. Richter, O. Pines, A. J. Pierik, R. Lill, Specialized function of yeast Isa1 and Isa2 proteins in the maturation of mitochondrial [4Fe-4S] proteins. *J. Biol. Chem.* **286**, 41205-41216 (2011).

26. D. Brancaccio *et al.*, Formation of [4Fe-4S] clusters in the mitochondrial iron-sulfur cluster assembly machinery. *J. Am. Chem. Soc.* **136**, 16240-16250 (2014).

27. B. Py *et al.*, Molecular organization, biochemical function, cellular role and evolution of NfuA, an atypical Fe-S carrier. *Mol. Microbiol.* **86**, 155-171 (2012).

28. W. H. Tong, G. N. Jameson, B. H. Huynh, T. A. Rouault, Subcellular compartmentalization of human Nfu, an iron-sulfur cluster scaffold protein, and its ability to assemble a [4Fe-4S] cluster. *Proc. Natl. Acad. Sci. U.S.A.* **100**, 9762-9767 (2003).

29. S. Angelini *et al.*, NfuA, a new factor required for maturing Fe/S proteins in Escherichia coli under oxidative stress and iron starvation conditions. *J. Biol. Chem.* **283**, 14084-14091 (2008).

30. S. Bandyopadhyay *et al.*, A proposed role for the Azotobacter vinelandii NfuA protein as an intermediate iron-sulfur cluster carrier. *J. Biol. Chem.* **283**, 14092-14099 (2008).

31. H. Li, C. E. Outten, Monothiol CGFS glutaredoxins and BolA-like proteins: [2Fe-2S] binding partners in iron homeostasis. *Biochemistry* **51**, 4377-4389 (2012).

32. T. Roret *et al.*, Structural and spectroscopic insights into BolA-glutaredoxin complexes. *J. Biol. Chem.* **289**, 24588-24598 (2014).

33. H. Li, D. T. Mapolelo, S. Randeniya, M. K. Johnson, C. E. Outten, Human glutaredoxin 3 forms [2Fe-2S]-bridged complexes with human BolA2. *Biochemistry* **51**, 1687-1696 (2012).

34. F. Fazius, E. Shelest, P. Gebhardt, M. Brock, The fungal alpha-aminoadipate pathway for lysine biosynthesis requires two enzymes of the aconitase family for the isomerization of homocitrate to homoisocitrate. *Mol. Microbiol.* **86**, 1508-1530 (2012).

35. L. Fernandes, C. Rodrigues-Pousada, K. Struhl, Yap, a novel family of eight bZIP proteins in Saccharomyces cerevisiae with distinct biological functions. *Mol. Cell.*

Biol. **17**, 6982-6993 (1997).

36. M. R. Jacobson *et al.*, Biochemical and genetic analysis of the nifUSVWZM cluster from Azotobacter vinelandii. *Mol. Gen. Genet.* **219**, 49-57 (1989).

37. B. Schilke, C. Voisine, H. Beinert, E. Craig, Evidence for a conserved system for iron metabolism in the mitochondria of Saccharomyces cerevisiae. *Proc. Natl. Acad. Sci. U.S.A.* **96**, 10206-10211 (1999).

38. M. S. Schonauer, A. J. Kastaniotis, J. K. Hiltunen, C. L. Dieckmann, Intersection of RNA processing and the type II fatty acid synthesis pathway in yeast mitochondria. *Mol. Cell. Biol.* **28**, 6646-6657 (2008).

39. J. K. Hiltunen *et al.*, Mitochondrial fatty acid synthesis type II: more than just fatty acids. *J. Biol. Chem.* **284**, 9011-9015 (2009).

40. O. Stehling *et al.*, MMS19 assembles iron-sulfur proteins required for DNA metabolism and genomic integrity. *Science* **337**, 195-199 (2012).

41. R. M. Cicchillo *et al.*, Escherichia coli lipoyl synthase binds two distinct [4Fe-4S] clusters per polypeptide. *Biochemistry* **43**, 11770-11781 (2004).

42. R. M. Cicchillo, S. J. Booker, Mechanistic investigations of lipoic acid biosynthesis in Escherichia coli: both sulfur atoms in lipoic acid are contributed by the same lipoyl synthase polypeptide. *J. Am. Chem. Soc.* **127**, 2860-2861 (2005).

43. J. E. Cronan, The structure of lipoyl synthase, a remarkable enzyme that performs the last step of an extraordinary biosynthetic pathway. *Biochem. J.* **464**, e1-3 (2014).

44. C. L. Quinlan *et al.*, The 2-oxoacid dehydrogenase complexes in mitochondria can produce superoxide/hydrogen peroxide at much higher rates than complex I. *J. Biol. Chem.* **289**, 8312-8325 (2014).

45. K. D. Kim, W. H. Chung, H. J. Kim, K. C. Lee, J. H. Roe, Monothiol glutaredoxin Grx5 interacts with Fe-S scaffold proteins Isa1 and Isa2 and supports Fe-S assembly and DNA integrity in mitochondria of fission yeast. *Biochem. Biophys. Res. Commun.* **392**, 467-472 (2010).

46. L. Banci *et al.*, [2Fe-2S] cluster transfer in iron-sulfur protein biogenesis. *Proc. Natl. Acad. Sci. U.S.A.* **111**, 6203-6208 (2014).

47. M. S. Longtine *et al.*, Additional modules for versatile and economical PCR-based gene deletion and modification in Saccharomyces cerevisiae. *Yeast* **14**, 953-961 (1998).

48. A. Atkinson *et al.*, The LYR Protein Mzm1 Functions in the Insertion of the

Rieske Fe/S Protein in Yeast Mitochondria. *Mol. Cell. Biol.* **31**, 3988-3996 (2011).

49. U. Na *et al.*, The LYR factors SDHAF1 and SDHAF3 mediate maturation of the iron-sulfur subunit of succinate dehydrogenase. *Cell Metab.* **20**, 253-266 (2014).

50. F. Pierrel *et al.*, Coa1 links the Mss51 post-translational function to Cox1 cofactor insertion in cytochrome c oxidase assembly. *EMBO J.* **26**, 4335-4346 (2007).

51. B. S. Glick, L. A. Pon, Isolation of highly purified mitochondria from *Saccharomyces cerevisiae*. *Meth. Enzymol.* **260**, 213-223 (1995).

52. H. J. Kim, M. Y. Jeong, U. Na, D. R. Winge, Flavinylation and assembly of succinate dehydrogenase are dependent on the C-terminal tail of the flavoprotein subunit. *J. Biol. Chem.* **287**, 40670-40679 (2012).

CHAPTER 6

CONCLUSION

One of the major challenges during the assembly of electron transport chain (ETC) complexes is handling redox-labile cofactors such as copper centers, iron-sulfur clusters and hemes. These redox-labile cofactors are deleterious for cells as pro-oxidants and/or susceptible for oxidative damage in forms exposed to solvent. Therefore, in order to transfer intact redox cofactors under the oxidative environment, one can expect that biology has evolved with means to minimize the possibility of cofactors to contact oxygen species in the process of cofactor delivery and insertion to target proteins. In the case of cofactor delivery to target proteins, one can expect machinery that ensures fast and efficient delivery of cargos to correct positions in recipients. A specialized protein would also play a role in protecting cofactors that are incorporated in assembly intermediates. In addition, unprotected assembly intermediates may result in generation of reactive oxygen species (ROS) as they can catalyze incomplete redox reactions. Therefore, a chaperone might be required to block unwanted incomplete reactions by assembly intermediates with redox cofactors.

In the field of ETC complex biogenesis, we define assembly factors as proteins that mediate and facilitate assembly of ETC complexes. These assembly factors are different from auxiliary subunits of ETC complexes as they are not normally seen in the mature forms of ETC complexes. In the last decade, numerous assembly factors for ubiquinol-cytochrome *c* reductase (complex III) and cytochrome *c* oxidase (complex IV) have been identified: Mzm1 for maturation of Rip1 (the [2Fe-2S] Rieske subunit of complex III) (*1*), Cyc2 and Cyc3 heme lyases for hemylation of Cyt1 (the heme *c* subunit of complex III) (*2*, *3*), Coa1, Coa2 and Shy1 for hemylation of Cox1 (a complex IV core subunit) (*3*), Cox11, Cox17 and Sco1 metallochaperones for Cox1 and Cox2 (another

complex IV core subunit) maturation with copper centers (*4*), etc. However, the mechanism for SDH biogenesis, which involves an assembly process of four subunits and five redox cofactors, was poorly understood until the recent years when two novel SDH assembly factors were identified. SDHAF1 (Sdh6 in yeast) mutants were identified in leukoencephalopathy patients that presented with SDH deficiency (*5*). However, the molecular function of SDHAF1 remained undefined. Another SDH assembly factor, SDHAF2 (Sdh5 in yeast), was shown to mediate insertion of FAD cofactor into SDHA (*6*). The same study also revealed that mutations in *SDHAF2* were associated with paraganglioma.

In Chapter 2, we expanded our understanding of SDH assembly that FAD binding, but not covalent attachment of FAD to Sdh1, is sufficient for SDH assembly. Interestingly, the study provided additional information on pre-stalled SDH assembly intermediates. We showed that Sdh2 (the Fe-S subunit of SDH) was quickly degraded in the absence of Sdh1 (the FAD subunit), but not in the absence of Sdh3 and Sdh4 that form the membrane anchor domain of SDH. Moreover, Sdh2 appeared to form a hydrophilic intermediate with Sdh1 in the absence of the membrane anchor domain. This result led us to a proteomic study to discover novel SDH assembly factors during the assembly of an Sdh1/Sdh2 subcomplex.

Chapter 3 treats the main objective of this dissertation: defining the mechanism by which the Fe-S cluster subunit, Sdh2, is matured. Although a significant amount of information on Sdh2 structure with three different Fe-S clusters ([2Fe-2S], [4Fe-4S] and [3Fe-4S]) has been collected in the last decade, the entire process of Sdh2 maturation, especially the process of Fe-S cluster incorporation, remained elusive. In order to

understand the mechanism for Sdh2 maturation with Fe-S clusters, we initiated a study to elucidate the molecular function of Sdh6, which belongs to the LYR motif protein family. Previously, it has been shown that function of most LYR proteins is related to Fe-S cluster proteins. In the meantime, we identified another functionally uncharacterized LYR protein, Acn9 (now designated Sdh7), using an *in silico* method. Genetic studies and biochemical characterizations led to relating the molecular function of Sdh7 as well as Sdh6 to Sdh2 maturation. Metabolite profiling revealed that as in *sdh6*Δ deletion mutants, succinate accumulates in *sdh7*Δ mutants compared to WT, indicating impaired SDH in cells lacking Sdh7. Overexpression of Sdh6 in *sdh7*Δ mutants suppressed the respiratory growth defect, suggesting that Sdh7 might be a novel SDH assembly factor exerting a similar function to Sdh6. The physical interaction of Sdh6 and Sdh7 with Sdh2, as well as a specific attenuation of Sdh2 levels in *sdh6*Δ mutants and *sdh7*Δ mutants among SDH subunits, indicates that Sdh6 and Sdh7 are assembly factors required for Sdh2 maturation.

To understand the exact biochemical mechanism by which Sdh6 and Sdh7 facilitate Sdh2 maturation, we exploited high-copy genomic suppressor screening, resulting in the identification of Yap1, a transcription activator that induces expression of antioxidant genes. Antioxidant supplementation as well as Yap1 overexpression restored SDH activity in cells lacking Sdh6 or Sdh7. ROS levels were not increased in *sdh6*Δ cells and *sdh7*Δ cells. Therefore, the identification of Yap1 suppressor suggests that Sdh6 and Sdh7 are required for protecting the Fe-S subunit of SDH from oxidative damage during SDH assembly.

Several studies have suggested that some metabolic enzymes would be tumor suppressors. It has been shown that gain-of-function mutations in isocitrate dehydrogenase and loss-of-function mutations in fumarate hydratase and succinate dehydrogenase are associated with a subset of tumors (*7*). Mutations in these metabolic enzymes result in abnormal accumulation of succinate in cells. Subsequently, accumulation of succinate leads to inhibition of proteins that belong to the dioxygenase family, including proline hydroxylase responsible for degradation of hypoxia inducible factor 1 (HIF1) and DNA and histone demethylases regulating chromatin remodeling (*7-9*). Up-regulation of HIF1 levels and dysregulation of chromatin remodeling are well-known features of tumor progression. In the case of SDH, loss-of-function mutations in SDH structural subunits have been linked to paraganglioma, pheochromocytoma, renal cell carcinoma, neuroblastoma and gastrointestinal stromal tumor (*10*). Pathogenic mutations in *SDHAF1* and *SDHAF2* have also been exhibited in the context of neurodegenerative diseases and endocrine-related tumors. However, there has been a subset of SDH-deficient tumors reported without any mutation in genes encoding SDH subunits and two SDH assembly factors. Therefore, it has been thought that the study on SDH assembly could help to discover tumorigenic alleles of novel SDH assembly factors. Indeed, the genetic study using massively parallel sequencing in Chapter 4 revealed a higher rate of occurrence of sequence variation (c.157T>C, p.Phe53Leu) in SDHAF3 (a human ortholog of Sdh7) in patients presenting familial and sporadic paraganglioma or pheochromocytoma, compared to a normal population. We confirmed that SDHAF3 F53L is less competent to bind SDHB (a human ortholog of Sdh2) in mammalian cells compared to WT and is a loss-of-function mutant leading to SDH deficiency when

expressed in yeast. However, the impact of heterozygote alleles of SDHAF3 F53L on tumorigenesis via SDH deficiency remains unclear, considering the coexistence of SDHAF3 WT alleles. We are currently testing whether SDHAF3 F53L is a dominant negative allele.

The aforementioned study to discover putative SDH assembly factors interacting with an Sdh1/Sdh2 subcomplex led to a study to understand Fe-S cluster delivery pathways, especially [4Fe-4S] cluster delivery to target proteins. Using a proteomics approach coupled with affinity purification of Sdh2 in cells lacking Sdh3 and Sdh4, we identified several components in Fe-S cluster biosynthesis including Isa2 and Nfu1. In Chapter 5, we revealed that Nfu1 plays a role in [4Fe-4S] cluster transfer to mitochondrial [4Fe-4S] cluster proteins by pursuing our previous observation on the interaction between Nfu1 and Sdh2. The fact that importance of Nfu1 function was pronounced under oxidative stress conditions implies that adequate means of protection need to be provided during transfer of Fe-S clusters from Fe-S cluster synthesis machineries to recipient proteins. In this case, Nfu1 facilitates delivery of [4Fe-4S] clusters from the ISA complex to target proteins such as Aco1, Aco2, Lys4 and Sdh2. Interestingly, it has been proposed that Grx5 could play a role in [2Fe-2S] cluster transfer, implying that biology might have evolved with dedicated factors for each type of Fe-S cluster delivery as well as synthesis.

Although it has been shown that Sdh6 and Sdh7 are important for protecting Fe-S clusters from oxidative damage during Sdh2 maturation, the mechanism for initial Fe-S cluster insertion into Sdh2 remains elusive. Sdh2 is a small subunit with a complex ligand geometry to accommodate three different types of Fe-S clusters as it contains a total of 11

cysteines coordinating three Fe-S clusters. Thus, there are several key aspects to be interrogated among all details in order to establish a near complete model for initial Fe-S cluster insertion. One potential challenge for Fe-S cluster insertion is keeping 11 thiol groups from oxidation until they coordinate Fe-S clusters in the mitochondrial matrix. It is of interest whether a reductase is required to keep thiol groups reduced during Sdh2 maturation.

Another aspect of Fe-S cluster insertion into Sdh2 is whether Fe-S cluster insertion is a step-wise process. Recently, Maio *et al.* have shown that a human ortholog of Sdh2, SDHB, has two domains that can be expressed separately in mammalian cells (*11*). The N-terminal domain contains a [2Fe-2S] cluster, and the C-terminal domain has a [4Fe-4S] cluster and a [3Fe-4S] cluster. It is interesting whether maturation of one domain is a prerequisite for maturation of the other domain. Reflecting on the putative step-wise mechanism for Fe-S cluster insertion, it is also intriguing how many Sdh2 interacting proteins, such as Fe-S cluster biogenesis components as well as dedicated SDH assembly factors, are orchestrated during Sdh2 maturation. Despite well-defined function of each protein interacting with Sdh2, our understanding about the interplay among these proteins is still limited. We have recently initiated a study to understand a possible interplay among Sdh6, Sdh7 and Nfu1 during a [4Fe-4S] cluster insertion into Sdh2. Preliminary results suggest that Sdh7 may interact with Sdh2 prior to Nfu1, and Sdh7 could be important for the recruitment of Nfu1 to Sdh2, which is under examination.

It remains unclear how exactly the protection by Sdh6 and Sdh7 is accomplished although we have demonstrated that Sdh6 and Sdh7 impart protection for holo-Sdh2

during SDH assembly. A simple scenario is that Sdh6 and Sdh7 bind in the vicinity of an Fe-S cluster in Sdh2 to shield the cluster. Another possibility is that Sdh6 and Sdh7 may play roles in repairing damaged Fe-S clusters in Sdh2. It is also interesting whether Sdh6 and Sdh7 are important for a specific Fe-S cluster among three Fe-S clusters in Sdh2. Maio *et al.* have shown that SDHAF1 preferentially interacts with the C-terminal domain of SDHB, but not with the N-terminal domain (*11*). In addition, we have shown the loss of interaction between SDHAF3 and SDHB $R^{242}H$, compared to WT SDHB in Chapter 4. Arg242 is located in juxtaposition to [3Fe-4S] center in the C-terminal domain. Taken together, it is attractive to speculate that function of SDHAF1 and SDHAF3 might be related to Fe-S clusters in the C-terminal domain of Sdh2.

Previous studies about Fe-S cluster biogenesis have identified the ISU scaffold complex for [2Fe-2S] cluster synthesis and the ISA scaffold complex for [4Fe-4S] cluster synthesis. However, no dedicated machinery has been identified yet; thus, little is known about [3Fe-4S] cluster formation in Sdh2. The active site [4Fe-4S] cluster in aconitase is coordinated by three cysteine ligands. Interestingly, the release of the uncoordinated Fe atom from the [4Fe-4S] cluster by oxidative damages leaves the [3Fe-4S] cluster in inactivated aconitase (*12*). Since the [3Fe-4S] cluster in Sdh2 is also coordinated by three cysteine ligands, it is interesting whether a [4Fe-4S] cluster is initially incorporated into Sdh2 and subsequently transformed to the [3Fe-4S] cluster. If it is the case, it is also interesting whether any specialized factor would be in need of this conversion.

We have established a better model depicting the mechanism for the assembly of the hydrophilic domain of SDH with identification of novel SDH assembly factors and a good understanding of Fe-S cluster biogenesis. However, the assembly of the

hydrophobic domain containing a heme b remains barely studied. It is of interest whether there are novel SDH assembly factors required for the assembly of the hydrophobic domain, especially factors for hemylation and stabilization of this domain. A proteomic study will be of use for identification of these putative assembly factors. For this, it is required to establish a condition that ensures stable expression of nonaggregated Sdh3 and Sdh4 to some extent in the absence of Sdh1 and Sdh2. As we progress research to elucidate the mechanism for Sdh3 and Sdh4 maturation, we will have a better understanding of SDH biogenesis in great detail.

References

1. A. Atkinson *et al.*, Mzm1 influences a labile pool of mitochondrial zinc important for respiratory function. *J. Biol. Chem.* **285**, 19450-19459 (2010).

2. P. M. Smith, J. L. Fox, D. R. Winge, Biogenesis of the cytochrome bc(1) complex and role of assembly factors. *Biochim. Biophys. Acta* **1817**, 276-286 (2012).

3. H. J. Kim, O. Khalimonchuk, P. M. Smith, D. R. Winge, Structure, function, and assembly of heme centers in mitochondrial respiratory complexes. *Biochim. Biophys. Acta* **1823**, 1604-1616 (2012).

4. I. C. Soto, F. Fontanesi, J. Liu, A. Barrientos, Biogenesis and assembly of eukaryotic cytochrome c oxidase catalytic core. *Biochim. Biophys. Acta* **1817**, 883-897 (2012).

5. D. Ghezzi *et al.*, SDHAF1, encoding a LYR complex-II specific assembly factor, is mutated in SDH-defective infantile leukoencephalopathy. *Nat. Genet.* **41**, 654-656 (2009).

6. H. X. Hao *et al.*, SDH5, a gene required for flavination of succinate dehydrogenase, is mutated in paraganglioma. *Science* **325**, 1139-1142 (2009).

7. N. Raimundo, B. E. Baysal, G. S. Shadel, Revisiting the TCA cycle: signaling to tumor formation. *Trends Mol. Med.* **17**, 641-649 (2011).

8. M. Xiao *et al.*, Inhibition of α-KG-dependent histone and DNA demethylases by fumarate and succinate that are accumulated in mutations of FH and SDH tumor suppressors. *Genes Dev.* **26**, 1326-1338 (2012).

9. E. Letouzé *et al.*, SDH mutations establish a hypermethylator phenotype in paraganglioma. *Cancer Cell* **23**, 739-752 (2013).

10. A. S. Hoekstra, J.-P. Bayley, The role of complex II in disease. *Biochim. Biophys. Acta* **1827**, 543-551 (2013).

11. N. Maio *et al.*, Cochaperone binding to LYR motifs confers specificity of iron sulfur cluster delivery. *Cell Metab.* **19**, 445-457 (2014).

12. P. R. Gardner, I. Fridovich, Inactivation-reactivation of aconitase in Escherichia coli. A sensitive measure of superoxide radical. *J. Biol. Chem.* **267**, 8757-8763 (1992).